Interference Networks with Random User Activity and Heterogeneous Delay Constraints

Homa Nikbakht, *Member, IEEE,* Michèle Wigger, *Senior Member, IEEE*, Shlomo Shamai (Shitz), *Life Fellow, IEEE*, Jean-Marie Gorce, *Senior Member, IEEE*, and H. Vincent Poor, *Life Fellow, IEEE*

Abstract

This paper proposes coding schemes and information-theoretic converse results for the transmission of heterogeneous delay-constrained traffic over interference networks with random user activity and random data arrivals. The heterogeneous delay-constrained traffic is composed of delay-tolerant traffic and delay-sensitive traffic where only the former can benefit from transmitter and receiver cooperation since the latter is subject to stringent delay constraints. Even for the delay-tolerant traffic, the total number of cooperation rounds at transmitter and receiver sides is limited to D rounds. Each transmitter is assumed to be active with probability $\rho \in [0,1]$, and we study two different models for traffic arrival, each model reflecting a different application type. In Model 1, each active transmitter sends a delay-tolerant message, and with probability $\rho_f \in [0,1]$ also transmits an additional delay-sensitive message; in Model 2, each active transmitter sends either a delay-sensitive message with probability ρ_f or a delay-tolerant message with probability $1-\rho_f$. For both models, we derive inner and outer bounds on the fundamental per-user multiplexing gain (MG) region of the symmetric Wyner network as well as inner bounds on the fundamental MG region of the hexagonal model. The per-user MG of an interference network describes the logarithmic growth of the largest average per-user rate that can be achieved over the network at high signal-to-noise ratios (SNR). Our inner and outer bounds on the per-user MG are generally close and coincide in special cases. They also show that when both transmitters and receivers can cooperate, then under Model 1, transmitting delay-sensitive messages hardly causes any penalty on the sum per-user MG, and under Model 2, operating at large delay-sensitive per-user MGs incurs no penalty on the delay-tolerant per-user MG and thus even increases the sum per-user MG. However, when only receivers can cooperate, the maximum delay-tolerant per-user MG that our bounds achieve at maximum delay-sensitive per-user MG is significantly decreased.

I. Introduction

A massive Internet of Things (IoT) connectivity system consists of a large number of connected devices. At any given time, in order to save energy, a fraction of such devices might be in silence mode [3]–[6], while others send (or receive) delay-sensitive or delay-tolerant data to comply with the heterogeneous delay-requirements of modern wireless networks [7]–[10]. An example of such mixed-delay traffic is the coexistence of enhanced mobile broadband (eMBB) and ultra-reliable low-latency communication (URLLC), which are two notable services [11]–[14]. Data-intensive applications such as industrial video surveillance and augmented virtual reality are served by eMBB, whereas, URLLC serves time-sensitive and mission-critical IoT applications such as motion control and autonomous driving [15]–[17]. The heterogeneous nature (both in terms of delay constraints as well as of activity/silence modes) calls for a new theoretical framework that analyzes the performance limits and optimal coding schemes for networks that simultaneously accommodate random user activity and heterogeneous delay constraints. In this article, we formalize such a framework for cooperative interference networks and provide the first information-theoretic results for two specific network types. These two networks have previously been proposed to model cellular communication and due to their regular structures are amenable for rigorous information-theoretic analysis and thus to provide first insights for random user-activity networks with heterogeneous delay constraints. Before providing more details on the contributions of our work, we review relevant literature and motivate our model assumptions.

A. Heterogeneous Delay-Constrained Traffic, Cooperation, and Interference Mitigation

Modern communication systems, spanning from terahertz (THz) transmissions to vehicular communications [18]–[26], have to accommodate heterogeneous delay-constrained traffic composed of delay-sensitive and delay-tolerant data. In various scenarios, the two types of traffics can even arise at the same transmit or receive terminals. For example, autonomous vehicles have to exchange delay-sensitive control information related to accident prevention with other vehicles and at the same time send more delay-tolerant data for traffic control to nearby basestations or smart traffic lights [21]. Coding schemes for heterogeneous delay-constrained traffic types with different delay constraints are thus of notable importance and interest [27]–[29].

H. Nikbakht and H. V. Poor are with the Department of Electrical and Computer Engineering, Princeton University, NJ, USA (email: homa, poor@princeton.edu). M. Wigger is with LTCI, Télécom Paris, IP Paris, 91120 Palaiseau, France (e-mail: michele.wigger@telecom-paris.fr). S. Shamai, is with the Department of Electrical Engineering, Technion—Israel Institute of Technology, Technion City, 32000, Israel, (e-mail: sshlomo@ee.technion.ac.il). J-M. Gorce is with the INRIA and University of Lyon, CITI, INSA Lyon, 69100 Villeurbanne, France (e-mail: jean-marie.gorce@inria.fr). Part of this work has been presented at IEEE ITW 2020 [1] and IEEE ITW 2021 [2]. The work of H. Nikbakht and H. V. Poor has been supported by the U.S National Science Foundation under Grants CNS-2128448 and ECCS-2335876. The work of S. Shamai has been supported by the German Research Foundation (DFG) via the German-Israeli Project Cooperation (DIP), under Project SH 1937/1-1. The work of JM Gorce has been supported by the French National Agency for Research (ANR) via the project nANR-22-PEFT-0010 of the France 2030 program.

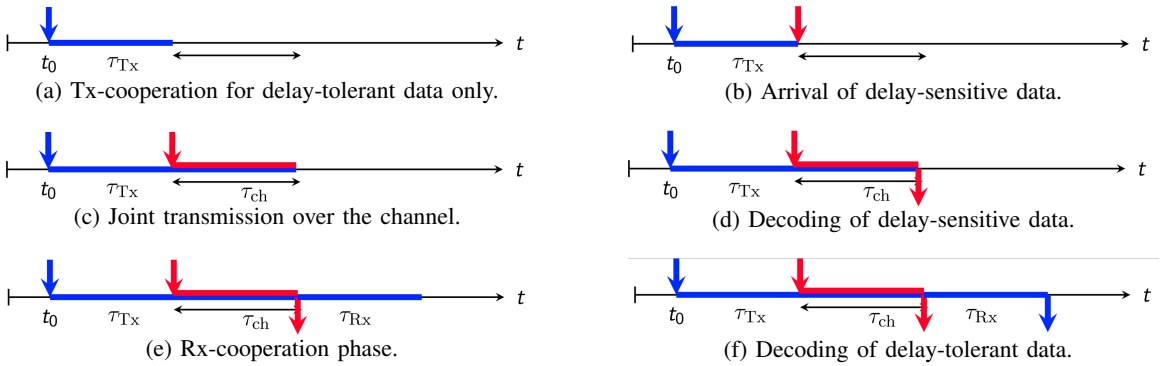

(a) Tx-cooperation for delay-tolerant data only.
(b) Arrival of delay-sensitive data.
(c) Joint transmission over the channel.
(d) Decoding of delay-sensitive data.
(e) Rx-cooperation phase.
(f) Decoding of delay-tolerant data.

Fig. 1: Chronological order of cooperation and transmissions over the channel and implications of the mixed data stream.

One way to deal with mixed-delay traffic is to puncture the delay-tolerant traffic (or bandwidth ressources associated to this traffic) in a way that accommodates the delay constraints for the delay-sensitive traffic. This approach has been investigated in various works, such as [18]–[21]. It has however been shown that improved performance can be achieved through a joint approach [22], [26], [27], [30] that jointly encodes and decodes delay-tolerant and delay-sensitive data. In particular, [22] showed for a simple point-to-point setup that the critical transmission of delay-sensitive data can be reinforced by mitigating the interference caused by delay-tolerant transmissions (e.g. example using dirty paper coding [31], [32]). The work in [26] instead suggests a superposition approach over a fading channel to communicate delay-sensitive messages within a single coherence blocks and delay-tolerant messages over multiple blocks.

Network scenarios are considered in [24], [25], [30]. Specifically, [30] considers a cooperative interference network where neighboring transmitters (Txs) can cooperate over dedicated links and also neighboring receivers (Rxs) cooperate over dedicated links. Cooperation over the links is assumed to be rate-limited and to take place over a maximum number of D rounds, so as to account for practical limitations on the processing delay. Similar models including both Tx- and Rx-cooperation have widely been considered in the literature, see for example [33]–[36]. Part of the motivation stems from cellular networks, where basestations (BSs) already cooperate over dedicated backhaul links, and in future communication standards mobile users could be allowed to communicate to each other over orthogonal links (separate frequencies). If one wishes to model the downlink of the cellular system, the Txs correspond to the single BSs of the various cells and the Rxs to the single mobiles in each cell. Multiple mobiles in a cell are typically served by replicating the scheme over multiple frequency slots or by accordingly extending the coding schemes to broadcast schemes. These extensions are however outside the scope of this article and left for future work.) Similar considerations hold when one wishes to model the uplink.

In the heterogeneous delay-constrained model of [30], each Tx has to send two data streams, a stream that is delay-tolerant, meaning that the data can profit from both Tx- and Rx-cooperation, and a delay-sensitive stream that has to be transmitted and decoded without further delay. The chronological order of the cooperations and transmissions as well as the implications of the different delay constraints on the two data streams are illustrated in Fig. 1. The work in [30] proposes a coding scheme for such a cooperative interference network with mixed delay constraints, and it analyzes its performance for specific network models [30]. For example, for Wyner's hexagonal model with interference only from neighboring cells, the scheme of [30] is depicted in Figure 2. The scheme is based on scheduling/multiplexing and on interference mitigation (dirty-paper coding, successive decoding) combined with Coordinated Multi-Point (CoMP) transmission and reception [33]. All these tools are required to deal with the four different types of interference that arise in networks mixing delay-sensitive and delay-tolerant traffic, because delay-sensitive data has to be transmitted and decoded without further delay. In fact, since delay-sensitive arrive only after the Tx-cooperation phase, interference *from* delay-sensitive transmissions cannot be canceled at the Tx-side. Similarly, since delay-sensitive transmissions have to be decoded prior to the Rx-cooperation phase, interference *to* delay-sensitive transmissions cannot be canceled at the Rx-side. Table I summarizes the interference mitigation possibilities for the four traffic types, and also describes which technique is used to mitigate each of the interference types.

Interference		**Interference Mitigation**		**Tool**
From	**To**	**Tx-Side**	**Rx-Side**	
Delay-Tolerant	Delay-Tolerant	YES	YES	Tx- or Rx-CoMP
	Delay-Sensitive	YES	NO	Dirty-Paper coding
Delay-Sensitive	Delay-Tolerant	NO	YES	Interference Cancelation
	Delay-Sensitive	NO	NO	Scheduling/Multiplexing

TABLE I: Interference mitigation techniques for the various streams.

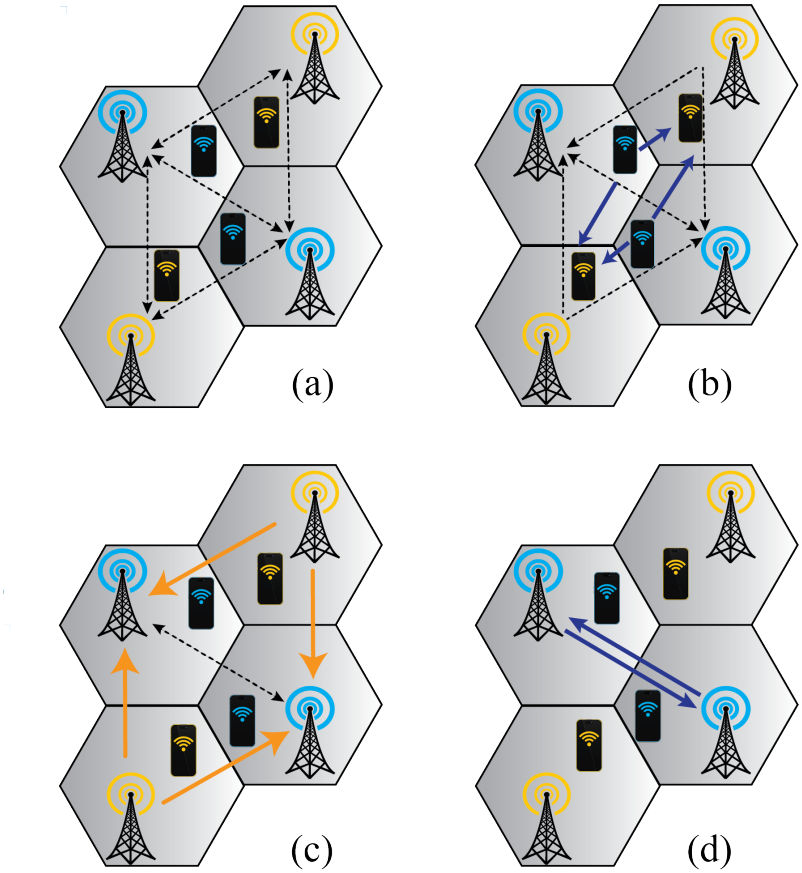

Fig. 2: Illustration of the coding scheme proposed in [30]. (a) illustrates the scheduling of the mixed-delay traffic; (b) the Tx-cooperation phase enabling the dirty-paper coding step; (c) the Rx-cooperation phase enabling successive interference cancelation; and (d) the subsequent Rx-cooperation enabling Rx-CoMP.

In fact, since interference between different delay-sensitive transmissions cannot be canceled neither at the Tx- nor the Rx-side, these interferences are managed by multiplexing (in time or frequency) different subschemes, where in each subscheme delay-sensitive transmissions are scheduled only on a non-interfering subset of users. Fig. 2 depicts such a scheduling protocol for Wyner's hexagonal model by colouring with yellow all mobile users that are allowed to transmit delay-sensitive data in a given subscheme. Other subsets of non-interfering users are scheduled in other subschemes. Interference from delay-tolerant transmissions to delay-sensitive transmissions can be eliminated at the Tx-side, and [30] proposes to use dirty-paper coding (or simply presubtracting the interference) for this interference mitigation. To this end, during the Tx-cooperation phase, Txs exchange information about their delay-tolerant data as we show in Fig. 2(b). Interference from delay-sensitive transmissions to delay-tolerant transmissions is eliminated at the Rx-side (BSs), by first decoding the delay-sensitive data and informing the terminals about this data to allow them to remove the interference; see Fig. 2(c). Finally, interference between delay-tolerant transmissions is mitigated through *Tx- or Rx-Coordinated Multi-Point (CoMP)* [33] (also known as network-multiple-input multiple-output (MIMO), virtual-MIMO, and multicell-MIMO). In Tx-CoMP, prior to the actual communication, Txs exchange information about their transmitted messages so as to be able to align their communications or mitigate mutual interference. In Rx-CoMP, Rxs exchange information about their observed receive signals and then decode their desired data using also this auxiliary information from other Rxs. The proposed scheme is shown to be almost optimal in the high-power regime for Wyner's symmetric network. Moreover, in this regime it operates close to sum-capacity even for large delay-sensitive rates, showing that the proposed sophisticated code designed manages to mitigate the degradation that the naive system would incurr due to the stringent delay constraint on part of the transmitted data.

The work in [37] also considered the setup where only Rxs can cooperate but not Txs, in which case even interference from delay-tolerant to delay-sensitive transmissions cannot be canceled, leading to a significantly degraded performance, which has been proved through information-theoretic converses. This is in sharp contrast to networks conveying only delay-tolerant data where duality holds between Tx- and Rx-cooperation and the capacity of the network depends only on the total cooperation rate but not on how it is distributed between the Tx- and the Rx-sides.

In this work we consider the same cooperative interference network as in [30] (Tx-and Rx-Cooperation) or as in [37] (Rx-Cooperation only). However, we combine it with a model for random user activity and data arrivals as we describe next. (In

[30] and [37] all users are always active and have both delay-sensitive and delay-tolerant traffic to send.) Moreover, since our model is considerably more complex than the model in [30], [37] due to the random user activity and data arrivals, we will not limit the capacity of the cooperation links. More specifically, to limit the capacity of the cooperative links, one should take into account that the utilized cooperation rate also depends on the realization of the random user activity and data arrival, and as such is random. In this case, it might be also necessary to reduce the cooperation rate beyond the rate that is used in the scheme that we propose in this paper. This can be done either by reducing the effectively used number of cooperation rounds or by time-sharing the proposed scheme with a non-cooperative scheme. Cooperation between Txs or Rxs is however still inherently limited, because as in [30], [37] we limit the number of cooperation rounds, i.e., to how many Txs or Rxs cooperation-information can be relayed, and as such the processing delay introduced by cooperation. Indeed the focus of this work is on delay constraints. Constraints on the capacity of the cooperation could easily be introduced to our model, and via time-sharing with non-cooperative schemes also to our schemes and results.

B. Random User Activity and Random Data Arrivals

In various modern communication applications, most prominently control applications, data is produced in a sporadic fashion, meaning that each terminal wishes to communicate data at certain times and remains silent otherwise. Whether users have data to transmit or not, typically depends on the status of higher-layer applications. For the communication layer on which we focus on this work, we shall thus simply assume that the user activity is determined by an external random process.

The impact of random user activity on the performance of communication networks has previously been treated in the literature. For example, in the context of a MIMO network with detection capabilities [38]–[40], or for cellular uplink networks with multicell processing capabilities [41]–[44]. These latter works are of a more information-theoretic nature, and model the random activity by assuming that each user is active with probability $\rho \in [0,1]$, irrespective of the other users. Due to the sparse network connectivities considered in these works, inactivation of users decomposes the networks into subnetworks, whose performance is then analyzed under single-cell processing or multi-cell processing (i.e., assuming that data can be decoded based on the signals observed at multiple BSs). The results in [43] confirm the intuition that multi-cell processing can strictly outperform single-cell processing also in the presence of random user activity.

In this work, we assume a similar *independent and identically distributed (i.i.d.)* model where each user is active with probability $\rho \in [0,1]$ independent of all other users. In addition, we assume a random arrival model, where given that a user is active it has a delay-sensitive message to transmit with probability $\rho_f \in [0,1]$. We consider two different models. In Model 1, each active transmitter has a delay-tolerant message to send, while in Model 2 it sends a delay-tolerant message only when it does not have a delay-sensitive message. Depending on the specific application, Model 1 or 2 might be more appropriate.

We combine both mixed-delay constraints and random user activity/data arrivals. To the best of our knowledge, this paper is the first to investigate the interplay between these two features in such a complex cooperative communication scenario and from an information-theoretic perspective.

C. Mixed-Delay Multiplexing Gain Region

Due to the complex nature of our network and its constraints, as a first approximation, this work will focus on the high signal-to-noise ratio (SNR) regime. In this regime, the capacity of a non-fading network is determined by the multiplexing gain (also known as degrees of freedom (DoF) or prelog factor). Or equivalently, by the per-user multiplexing gain (MG):

$$\mathsf{S} \triangleq \frac{\mathsf{C}}{\log \mathsf{P}} \tag{1}$$

where C denotes the "single-user capacity" of each message and P the symmetric average block-power constraint imposed on all inputs. The single-user capacity can be defined either as the highest *average* rate that can be transmitted in the system, or as the highest *worst-case* rate over all messages that can be sustained over the network. In this sense, for high powers P the per-user average or worst-case capacity scales as $\mathsf{C} \approx \mathsf{S} \cdot \log \mathsf{P}$, for S indicating the per-user MG.

Since we have two data streams, a delay-tolerant one and a delay-sensitive one, in our systems we have two per-user MGs with a possible tradeoff between them. Our goal will thus be to describe the *per-user MG region*, which characterizes all pairs of delay-sensitive and delay-tolerant per-user MGs that are simultaneously achievable over the network. We will consider the average capacity over all users to define the delay-tolerant per-user MG and the worst-case capacity to define the delay-sensitive per-user MG. Our motivation stems from the co-existence of eMBB and LLC data in 5G networks where the delay-sensitive LLC data is required to be highly reliable and thus a desired data rate needs to be guaranteed at all the users sending LLC data. eMBB transmissions generally require high rates with the throughput (sum-capacity) as the relevant quantity.

D. Contributions of this Work

In this paper, we analyze the coding scheme of [30] for cooperative interference networks with heterogeneous delay-sensitive and delay-tolerant traffic types in a setup with random user activity and random data arrivals, and we determine the corresponding

per-user MG region. We specialize our findings for two types of networks, Wyner's symmetric network and the hexagonal network. For these networks, we adapt the coding scheme to the specific realizations of the random activity and arrival patterns, which results in an improved performance. The per-user MG region achieved by our adaptive scheme significantly improves over the first generic non-adaptive scheme and moreover has performance close to the information-theoretic fundamental limits. Indeed, we also present information-theoretic converse results on the set of all achievable per-user MG pairs for Wyner's symmetric network and we show that for the setup with both Tx-and Rx-cooperation the adaptive scheme performs close to (and sometimes matches) our converse bound.

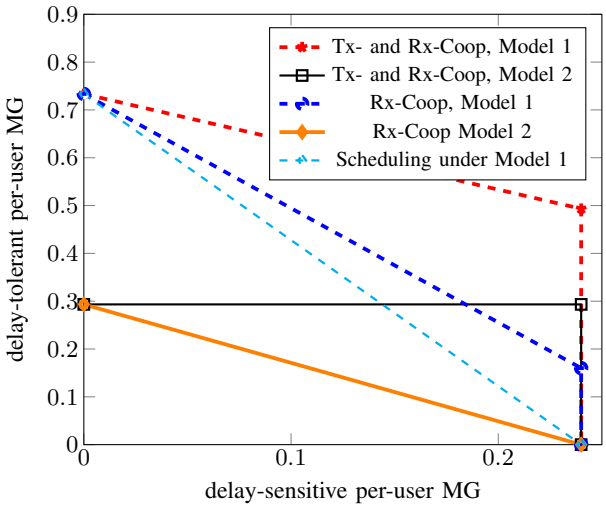

Fig. 3: Structure of the various per-user MG regions under the different models.

Our results allow us to derive tight approximations of the per-user MG regions for Wyner's symmetric network under mixed-delay traffic and with random user activity and data arrivals as functions of the allowed total number of cooperation rounds D. Numerical evaluation of our results show that, depending on the modelling assumptions, the per-user MG regions are of the forms sketched in Figure 3. Under Model 1 and when both Txs and Rxs can cooperate, the per-user MG region is mostly limited by a single constraint on the delay-sensitive MG and a sum constraint on the sum of the two MGs. There is thus no loss in overall performance (sum of per-user MGs) whether one sends at low or high delay-sensitive per-user MG. Under Model 2, the delay-tolerant MG is significantly decreased compared to Model 1, because delay-tolerant data is available only in the case where there is no delay-sensitive data. The shape of the per-user MG region differs in Model 2 (a rectangle) compared to Model 1, since the region is only constrained by two individual MG constraints. In particular, in this rectangular region the sum of the two MGs increases with increasing delay-sensitive per-user MGs. These observations should be put in contrast to the performance of scheduling systems that transmit delay-sensitive and delay-tolerant messages in orthogonal (e.g., time- or frequency) slices and for which the delay-tolerant per-user MG and the sum per-user MG decrease linearly by increasing delay-sensitive per-user MG.

The situation is different when only Rxs can cooperate, in which case the delay-tolerant and/or sum per-user MGs degrade when one transmits at high delay-sensitive per-user MG. In particular, our converse result proves that for large delay-sensitive per-user MGs the performance loss in delay-tolerant per-user MG that our schemes incur compared to the setup with both Tx- and Rx-cooperation is of a fundamental nature in the sense that any scheme will suffer from this degradation. In fact, if Txs cannot cooperate it does not seem to be possible to mitigate interference of delay-tolerant transmissions on delay-sensitive transmissions because Rx-cooperation cannot serve this purpose as delay-sensitive messages have to be decoded immediately without further delay.

Our numerical results for Wyner's symmetric network also indicate that for moderate activity parameters ρ a few cooperation rounds suffice to attain performance close to the limit as $D \to \infty$. The reason is that the random user activity decomposes the network into smaller subnets, for which the optimal performance can be attained with small or moderate number of cooperation rounds.

To summarize, the main contributions of this work are:

- We introduce an information-theoretic framework to study cooperative networks with mixed-delay traffic and random user activity and data arrivals. In particular we introduce the notion of mixed-delay MG region to analyze (in a first-order approximation) the performance of these networks in the high SNR and infinite blocklength regime.
- We propose and analyze a coding scheme for general cooperative interference networks with heterogeneous delay constraints on the traffics in situations with random user activity/data arrivals. We consider both Tx- and Rx-cooperation

as well as only Rx-cooperation, and data arrival Model 1 (only delay-sensitive messages arrive sporadically but not delay-tolerant messages) as well as Model 2 (all messages arrive only sporadically).

- For Wyner's symmetric network and the hexagonal network we propose improved coding schemes that better adapt to the random activity and data arrival patterns. For the symmetric Wyner network this improved scheme allows us to show that for moderate activity parameters the optimal performance can already be achieved with a small number of cooperation rounds D. In fact, when only a moderate number of users are active, the network can be decomposed into relatively small subnets, and a small number of cooperation rounds suffices to achieve optimal performance for delay-tolerant messages in each subnet.
- For Wyner's symmetric network we also present information-theoretic converse results. They are close to the performance of our improved schemes and match them in special cases.
- Our inner and outer bounds for the symmetric Wyner model allow us to conclude that when both Txs and Rxs can cooperate, then under Model 1, transmitting at a high delay-sensitive per-user MG does not impose any penalty on the overall performance of the system, i.e., the sum of delay-sensitive and delay-tolerant per-user MG. For Model 2, the sum per-user MG increases with the delay-sensitive per-user MG, and more specifically operating at large delay-sensitive per-user MG does not decrease the achievable delay-tolerant MG.
- Our converse result for the setups with only Rx-cooperation proves that the degradation in delay-tolerant per-user MG at large delay-sensitive MGs incurred by our schemes is inherent to any scheme and not an artifact of our proposition.
- For the hexagonal network, we derive inner bounds under the assumption that $\mathrm{D} \to \infty$. Under this assumption, when both Txs and Rxs can cooperate, the non-adaptive scheme performs as good as adaptive scheme. When only Rxs can cooperate, however, we propose improved coding schemes that better adapt to the random activity and data arrival patterns

The information-theoretic insights that can be taken from our work are thus three-fold. Under a moderate user activity parameter ρ, a small or moderate number of cooperation rounds D suffices for sparse network structures to achieve near-optimal performances. Moreover, simultaneously accommodating Tx- and Rx-cooperation and employing smart coding allows to mitigate the performance degradation that the system incurrs due to the stringent delay constraints on the delay-sensitive data, while only Rx-cooperation is not sufficient. Finally, our work also shows how to appropriately combine different interference mitigation strategies to cancel the four types of interference that can arise in mixed-delay networks in function of the activity and arrival patterns. In the following, for simplicity, we refer to delay-sensitive data as *low-latency communication (LLC)* data (inspired by the ultra-reliable low-latency communication of 5G systems which is subject to critical delay constraints) and to delay-tolerant data as *eMBB* data (inspired by the 5G enhanced Mobile Broad Band service which is less delay-limited).

E. Organization

The rest of this paper is organized as follows. We end this section with some remarks on notation. Section II describes the general problem setup. Sections III and IV present our coding schemes with both Tx and Rx- cooperation and with only Rx-cooperation, respectively. Sections V and VI discuss our main results for the symmetric Wyner and the hexagonal networks, respectively. Section VII concludes the paper. Technical proofs are deferred to appendices.

F. Notation

The set of all integers is denoted by $\mathbb{Z}$, the set of positive integers by $\mathbb{Z}^+$ and the set of real numbers by $\mathbb{R}$. For other sets we use calligraphic letters, e.g., $\mathcal{X}$. Random variables are denoted by uppercase letters, e.g., X, and their realizations by lowercase letters, e.g., x. For vectors we use boldface notation, i.e., upper case boldface letters such as $\mathbf{X}$ for random vectors and lower case boldface letters such as $\mathbf{x}$ for deterministic vectors. Matrices are depicted with sans serif font, e.g., H. We also write X^n for the tuple of random variables $(X_1, \ldots, X_n)$ and $\mathbf{X}^n$ for the tuple of random vectors $(\mathbf{X}_1, \ldots, \mathbf{X}_n)$.

II. Problem Setup: Data Arrival and Communication Model

Consider a cellular network with K transmitters (Tx) and K corresponding receivers (Rx). Define $\mathcal{K} \triangleq \{1, \ldots, K\}$. Various network interference structures will be considered and are described later.

Each Tx $k \in \mathcal{K}$ is *active* with probability $\rho \in [0, 1]$. Non-active Txs remain silent and do not participate in the communication. We consider two different models:

- *Model 1:* Each active Tx sends a so called eMBB message $M_k^{(\mathsf{e})}$ to its corresponding Rx k. With probability $\rho_f \in [0, 1]$, it also sends an additional LLC message $M_k^{(\mathsf{L})}$ to Rx k. These LLC messages are subject to stringent delay constraints, as we describe shortly.
- *Model 2:* Each active Tx sends with probability $(1-\rho_f)$ an eMBB message $M_k^{(\mathsf{e})}$ to its corresponding Rx k and otherwise (i.e., with probability ρ_f) it sends a LLC message $M_k^{(\mathsf{L})}$ to Rx k.

The only difference between the two models is that under Model 1 any active Tx sends an eMBB message whereas under Model 2 an active Tx only sends an eMBB message if it does not send a LLC message. In both models, the various transmitted eMBB messages in the network can be of different rates while the LLC messages are all of same rate $R^{(\mathsf{L})}$.

Let $A_k = 1$ if Tx k is active and $A_k = 0$ if Tx k is not active. Moreover, if Tx k is active and has a LLC message to send, set $B_k = 1$, and otherwise set $B_k = 0$. The random tuple $\mathbf{A} := (A_1, \ldots, A_K)$ is thus independent and identically distributed (i.i.d.) Bernoulli-ρ, and if they exist the random variables $B_1, \ldots, B_K$ are i.i.d. Bernoulli-ρ_f. Denote by $\mathbf{B}$ the tuple of B_k's that are defined. Further, define the *active set* and the *LLC set* as follows:

$$\mathcal{K}_{\text{active}} \triangleq \{k \in \mathcal{K} : A_k = 1\}, \tag{2}$$

$$\mathcal{K}_{\text{LLC}} \triangleq \{k \in \mathcal{K} \colon B_k = 1\}. \tag{3}$$

Under Model 1, the set $\mathcal{K}_{\text{eMBB}}$ of Txs transmitting an eMBB message is

$$\mathcal{K}_{\text{eMBB}} \triangleq \mathcal{K}_{\text{active}} \tag{4}$$

and under Model 2, it is

$$\mathcal{K}_{\text{eMBB}} \triangleq \mathcal{K}_{\text{active}} \backslash \mathcal{K}_{\text{LLC}}. \tag{5}$$

We shall assume that each eMBB message $M_k^{(\mathsf{e})}$ is uniformly distributed over a set $\mathcal{M}_k^{(\mathsf{e})} \triangleq \{1, \ldots, \lfloor 2^{nR_k^{(\mathsf{e})}} \rfloor\}$, with n denoting the blocklength and $R_k^{(\mathsf{e})}$ the rate of message $M_k^{(\mathsf{e})}$, which we allow to vary across users and can even depend on the random activity parameters $\mathbf{A}$ and $\mathbf{B}$. In contrast, each LLC message is uniformly distributed over the set $\mathcal{M}^{(\mathsf{L})} \triangleq \{1, \ldots, \lfloor 2^{nR^{(\mathsf{L})}} \rfloor\}$, where the constant rate $R^{(\mathsf{L})}$ can depend on the network structure but not on the realization of the random activity parameters. The motivation to consider these asymmetric rate constraints is that LLC messages have stringent delay constraint and have to be transmitted immediately in the next-following block. The rate $R^{(\mathsf{L})}$ needs to be guaranteed under any circumstances. In contrast, eMBB messages can be postponed to following blocks if required and in each transmission block the goal is to transmit as much eMBB rate as possible. In this sense, one can understand the setup as maximizing the expected eMBB message rate while ensuring a minimum rate for LLC messages.

We describe the encoding at the active Txs. The encoding starts with a first *Tx-cooperation phase* which consists of $\mathrm{D_{Tx}} > 0$ rounds and depends only on the eMBB messages in the system. The LLC messages, which are subject to stringent delay constraints, are only generated afterwards, at the beginning of the subsequent *channel transmission phase*. So, during the first Tx-cooperation phase, neighboring active Txs communicate with each other over dedicated noise-free links of unlimited capacity over $\mathrm{D_{Tx}} > 0$ rounds.

In each Tx-cooperation round $j \in \{1, \ldots, \mathrm{D_{Tx}}\}$, any active Tx $k \in \mathcal{K}_{\text{active}}$ sends a cooperation message to its active neighbors in the network $\ell \in \mathcal{N}_{k,\text{Tx,active}} \triangleq \mathcal{N}_k \cap \mathcal{K}_{\text{active}}$, where $\mathcal{N}_k$ indicates the set of neighboring Txs of Tx k. (The sets $\mathcal{N}_k$ depend on the specific network structure and will be specified latter for the various considered network models.)

Each cooperation message can depend on the Tx's eMBB message and the cooperation-information received during previous rounds. So, in round j, Tx $k \in \mathcal{K}_{\text{active}}$ sends a message

$$T_{k\to\ell}^{(j)} = \begin{cases} \psi_{k\to\ell}^{(j)}\Big(M_k^{(\mathsf{e})}, \big\{T_{\ell'\to k}^{(1)}, \ldots, T_{\ell'\to k}^{(j-1)}\big\}_{\ell' \in \mathcal{N}_{k,\text{Tx,active}}}, \mathbf{A}, \mathbf{B}\Big), & k \in \mathcal{K}_{\text{eMBB}} \\ \psi_{k\to\ell}^{(j)}\Big(\big\{T_{\ell'\to k}^{(1)}, \ldots, T_{\ell'\to k}^{(j-1)}\big\}_{\ell' \in \mathcal{N}_{k,\text{Tx,active}}}, \mathbf{A}, \mathbf{B}\Big), & k \notin \mathcal{K}_{\text{eMBB}} \end{cases}. \tag{6}$$

to each Tx $\ell \in \mathcal{N}_{k,\text{Tx,active}}$, for some functions $\psi_{k\to\ell}^{(j)}$ on appropriate domains.

At the beginning of the subsequent channel transmission phase, LLC messages are generated and each active Tx $k \in \mathcal{K}_{\text{active}}$ computes its channel inputs $X_k^n \triangleq (X_{k,1}, \ldots, X_{k,n}) \in \mathbb{R}^n$ as follows:

$$X_k^n = \begin{cases} f_k^{(B)}\big(M_k^{(\mathsf{L})}, M_k^{(\mathsf{e})}, \{T_{\ell'\to k}^{(j)}\}, \mathbf{A}, \mathbf{B}\big), & k \in \mathcal{K}_{\text{LLC}} \\ f_k^{(\mathsf{e})}\big(M_k^{(\mathsf{e})}, \{T_{\ell'\to k}^{(j)}\}, \mathbf{A}, \mathbf{B}\big), & k \in \mathcal{K}_{\text{eMBB}}. \end{cases}, \tag{7}$$

where the sets $\{T_{\ell'\to k}^{(j)}\}$ run over indices $j \in \{1, \ldots, \mathrm{D_{Tx}}\}$ and $\ell' \in \mathcal{N}_{k,\text{Tx,active}}$, and $f_k^{(B)}$ and $f_k^{(\mathsf{e})}$ are encoding functions on appropriate domains satisfying the average block-power constraint

$$\frac{1}{n}\sum_{t=1}^{n} X_{k,t}^2 \le \mathsf{P}, \quad \forall\ k \in \mathcal{K}_{\text{active}}, \qquad \text{almost surely.} \tag{8}$$

Inactive Txs simply send the all-zero sequence.

We shall assume a Gaussian communication network described as

$$Y_{k,t} = \sum_{\tilde{k} \in \{\mathcal{I}_k \cap \mathcal{K}_{\text{active}}\}} h_{\tilde{k},k} X_{\tilde{k},t} + Z_{k,t}, \tag{9}$$

where $\{Z_{k,t}\}$ are i.i.d. standard Gaussian random variables for all k and t and are independent of all messages; $h_{\tilde{k},k} \ge 0$ describes the channel coefficient between Tx $\tilde{k}$ and Rx k and is a fixed real number; and $X_{0,t} = 0$ for all t. In our model we assume that the received signal $Y_{k,t}$ is only interfered with by the signals from Txs in $\mathcal{I}_k$, if these neighboring Txs are active. We will assume short range interference, i.e., that only signals from Txs that are sufficiently close interfere because the

disturbance from further away Txs are below the noise level. This implies that any Tx k can cooperate with the Txs whose signals interfere at Rx k, i.e.,:

$$\mathcal{I}_k \subseteq \mathcal{N}_k. \tag{10}$$

Decoding also takes place in two phases. In the first *LLC-decoding phase*, any active Rx $k \in \mathcal{K}_{\text{LLC}}$ decodes the LLC message $M_k^{(\mathsf{L})}$ based on its own channel outputs $\boldsymbol{Y}_k^n$ by computing

$$\hat{M}_k^{(\mathsf{L})} = g_k^{(n)}\big(\boldsymbol{Y}_k^n, \mathbf{A}, \mathbf{B}\big), \tag{11}$$

for some decoding function $g_k^{(n)}$ on appropriate domains. In the subsequent *eMBB-decoding phase*, active Rxs first communicate with their active neighbors in the network $\ell \in \mathcal{N}_{k,\text{Rx,active}} \triangleq \mathcal{N}_k \cap \mathcal{K}_{\text{active}}$, during $\mathrm{D_{Rx}} \geq 0$ rounds over dedicated noise-free links with unlimited capacity, and then they decode their intended eMBB messages based on their outputs and based on this exchanged information. Specifically, in each cooperation round $j \in \{1, \ldots, \mathrm{D_{Rx}}\}$, each active Rx $k \in \mathcal{T}_{\text{active}}$ sends a cooperation message

$$Q_{k\to\ell}^{(j)} = \phi_{k\to\ell}^{(j)}\Big(\mathbf{Y}_k^n, \{Q_{\ell'\to k}^{(1)}, \ldots, Q_{\ell'\to k}^{(j-1)}\}_{\ell' \in \mathcal{N}_{k,\text{Rx,active}}}, \mathbf{A}, \mathbf{B}\Big) \tag{12}$$

to Rx ℓ if $\ell \in \mathcal{N}_{k,\text{Rx,active}}$ for some appropriate function $\phi_{k\to\ell}^{(j)}$.

After the last cooperation round, each active Rx $k \in \mathcal{K}_{\text{eMBB}}$ decodes its desired eMBB message as

$$\hat{M}_k^{(\mathsf{e})} = b_k^{(n)}\Big(\mathbf{Y}_k^n, \Big\{Q_{\ell'\to k}^{(1)}, \ldots, Q_{\ell'\to k}^{(\mathrm{D_{Rx}})}\Big\}_{\ell' \in \mathcal{N}_{k,\text{Rx,active}}}, \mathbf{A}, \mathbf{B}\Big), \tag{13}$$

where $b_k^{(n)}$ is a decoding function on appropriate domains.

Definition 1: Given $\mathsf{P} > 0$ and $K > 0$, a rate pair $(R^{(\mathsf{L})}(\mathsf{P}), \bar{R}_K^{(\mathsf{e})}(\mathsf{P}))$ is said to be D-*achievable* if there exist rates $\{R_k^{(\mathsf{e})}\}_{k=1}^K$ satisfying

$$\bar{R}_K^{(\mathsf{e})} \leq \mathbb{E}_{\mathbf{A},\mathbf{B}}\left[\sum_{k\in\mathcal{K}_{\text{eMBB}}} \frac{1}{K} R_k^{(\mathsf{e})}\right], \tag{14}$$

a pair of Tx- and Rx-cooperation rounds $\mathrm{D_{Tx}}, \mathrm{D_{Rx}}$ summing to $\mathrm{D_{Tx}} + \mathrm{D_{Rx}} = \mathrm{D}$ and encoding, cooperation, and decoding functions satisfying the power constraint (8) and so that the probability of error

$$\mathbb{P}\Big[\bigcup_{k\in\mathcal{K}_{\text{LLC}}} \big(\hat{M}_k^{(\mathsf{L})} \neq M_k^{(\mathsf{L})}\big) \text{ or } \bigcup_{k\in\mathcal{K}_{\text{eMBB}}} \big(\hat{M}_k^{(\mathsf{e})} \neq M_k^{(\mathsf{e})}\big)\Big] \tag{15}$$

tends to 0 as $n \to \infty$.

An expected average per-user MG pair $(\mathsf{S}^{(\mathsf{L})}, \mathsf{S}^{(\mathsf{e})})$ is called D-*achievable*, if for all powers $\mathsf{P} > 0$ there exist D-achievable rates $\big\{R^{(\mathsf{L})}(\mathsf{P}), \bar{R}_K^{(\mathsf{e})}(\mathsf{P})\big\}_{\mathsf{P}>0}$ satisfying

$$\mathsf{S}^{(\mathsf{L})} \triangleq \varlimsup_{K\to\infty} \varlimsup_{\mathsf{P}\to\infty} \frac{R^{(\mathsf{L})}(\mathsf{P})}{\frac{1}{2}\log(\mathsf{P})} \cdot \rho\rho_f, \tag{16}$$

and

$$\mathsf{S}^{(\mathsf{e})} \triangleq \varlimsup_{K\to\infty} \varlimsup_{\mathsf{P}\to\infty} \frac{\bar{R}_K^{(\mathsf{e})}(\mathsf{P})}{\frac{1}{2}\log(\mathsf{P})}. \tag{17}$$

The closure of the set of all D-achievable MG pairs $(\mathsf{S}^{(\mathsf{L})}, \mathsf{S}^{(\mathsf{e})})$ is called the (D-*cooperative*) *fundamental MG region* and is denoted by $\mathcal{S}_1^\star(\mathrm{D}, \rho, \rho_f)$ and $\mathcal{S}_2^\star(\mathrm{D}, \rho, \rho_f)$ for Models 1 and 2, respectively.

Remark 1: The MG in (17) measures the average expected eMBB MG on the network. Since the LLC rate is fixed to $R^{(\mathsf{L})}$ at all Txs in $\mathcal{K}_{\text{LLC}}$, we multiply the MG in (16) by $\rho\rho_f$ to obtain the average expected LLC MG of the network. By the definition in (14), the pair $(\mathsf{S}^{(\mathsf{L})}, \mathsf{S}^{(\mathsf{e})})$ thus corresponds to the expected per-user MG pair of the system. In particular, the expected total per-user MG of LLC *and* eMBB messages is given by the sum $\mathsf{S}^{(\mathsf{L})} + \mathsf{S}^{(\mathsf{e})}$.

Remark 2: In our model, we assume that neighboring Txs and neighboring Rxs can only cooperate if they lie in the active set $\mathcal{K}_{\text{active}}$. Txs and Rxs in the *inactive set* $\mathcal{K}\backslash\mathcal{K}_{\text{active}}$ do not participate in the cooperation phases. Notice that all our converse (infeasibility) results remain valid in a setup where inactive Txs and Rxs *do* participaLte in the cooperation phases. Since our inner and outer bounds are rather close in general (see the subsequent numerical discussion), this indicates that without essential loss in optimality Txs and Rxs in $\mathcal{K}\backslash\mathcal{K}_{\text{active}}$ can entirely be set to sleep mode to conserve their batteries.

For simplicity, throughout this manuscript we assume that D is even. In the following Section III, we propose a coding scheme with both Tx and Rx cooperation under the assumption that $\mathrm{D_{Tx}} = 1$ and $\mathrm{D_{Rx}} = \mathrm{D} - 1$. In Section IV, we propose a coding scheme with only Rx cooperation, i.e., when $\mathrm{D_{Tx}} = 0$ and $\mathrm{D_{Rx}} = \mathrm{D}$.

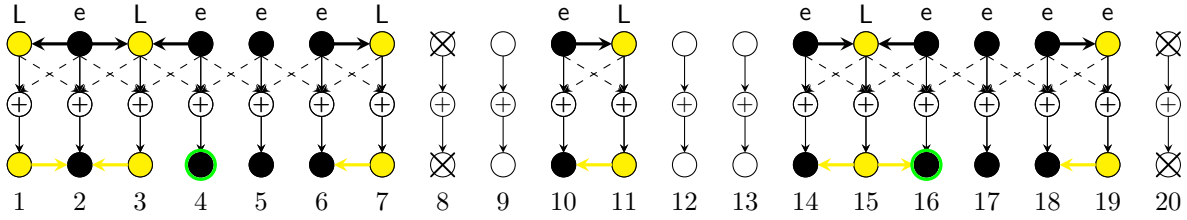

(a) The first Tx-cooperation round and the first Rx-cooperation round

(b) The last $\mathrm{D}-2$ Rx-cooperation rounds.

Fig. 4: Example for $\mathrm{D}=6$: Tx/Rx pairs in yellow have LLC messages to transmit, Tx/Rx pairs in black have eMBB messages to transmit, Tx/Rx pairs in white are deactivated. We deactivated Tx/Rx pairs 8 and 20 to satisfy the delay constraint D. Rx 4 and Rx 16 are master Rxs. Tx/Rx pair 19 employs the same coding scheme as the LLC transmissions.

III. Coding Scheme with both Tx- and Rx-Cooperation

We assume throughout this section that

$$\mathrm{D_{Tx}}=1 \quad \text{and} \quad \mathrm{D_{Rx}}=\mathrm{D}-1. \tag{18}$$

In Subsection III-A, we freely choose a message assignment and present an achievable total MG for this assignment. In the subsequent Subsection III-B we then build on these results to describe and analyze a scheme respecting the random message arrivals.

A. A Basic Scheme with Chosen Message Assignments

1) Creation of subnets and message assignment: Each network is decomposed into three subsets of Tx/Rx pairs, $\mathcal{T}_{\text{silent}}$, $\mathcal{T}_{\text{LLC}}$ and $\mathcal{T}_{\text{eMBB}}$, where

- Txs in $\mathcal{T}_{\text{silent}}$ are silenced and Rxs in $\mathcal{T}_{\text{silent}}$ do not take any action.
- Txs in $\mathcal{T}_{\text{LLC}}$ send only LLC messages. The corresponding Txs/Rxs are designated as LLC Txs/Rxs.
- Txs in $\mathcal{T}_{\text{eMBB}}$ send only eMBB messages. The corresponding Txs/Rxs are designated as eMBB Txs/Rxs.

We choose the sets $\mathcal{T}_{\text{silent}}$, $\mathcal{T}_{\text{LLC}}$, and $\mathcal{T}_{\text{eMBB}}$ in a way that:

C1: the signals sent by the LLC Txs do not interfere with one another; and

C2: silencing the Txs in $\mathcal{T}_{\text{silent}}$ decomposes the network into non-interfering subnets such that in each subnet there is a dedicated Rx, called the *master Rx*, that can send a cooperation message to any other eMBB Rx in the same subnet in at most $\frac{\mathrm{D}}{2}-1$ cooperation rounds.

For example, consider Wyner's symmetric network (described in detail in Section V) where Txs and Rxs are aligned on a grid and cooperation is possible only between subsequent Txs or Rxs. Interference at a given Rx is only from adjacent Txs. The network is illustrated in Fig. 4. The figure also shows a possible decomposition of the Tx/Rx pairs into the sets $\mathcal{T}_{\text{silent}}$ (in white), $\mathcal{T}_{\text{LLC}}$ (in yellow) and $\mathcal{T}_{\text{eMBB}}$ (in black) when $\mathrm{D}=6$. The proposed decomposition creates subnets with 7 active Tx/Rx pairs where the Rx in the center of any subnet (e.g. Rx 4 in the first subnet) can serve as a master Rx as it reaches any eMBB Rx in the same subnet in at most $\mathrm{D}/2-1=2$ cooperation rounds. As required, transmissions from LLC (yellow) Txs are only interfered with by transmissions from eMBB (black) Txs. Notice that in our example, Tx/Rx 19 has an eMBB message to send but still is depicted in yellow (LLC) because in our scheme it acts as if it had a LLC message to send. In general, any eMBB Tx/Rx can act as if it had a LLC message to send, because requirements for eMBB messages are less stringent than for LLC messages. This observation will play an important role in the following.

2) Precanceling of eMBB interference at LLC Txs: Any eMBB Tx k' quantizes its pre-computed input signal $\boldsymbol{X}_{k'}^n$ (how this signal is generated will be described under item 5)) and describes the quantized signal $\hat{\boldsymbol{X}}_{k'}^n$ during the single Tx-cooperation round to all its neighboring LLC Txs, which then precancel this interference in their transmit signals. Fig. 4 illustrates by black arrows the sharing of the described quantization information with neighboring LLC Txs for Wyner's symmetric network.

To describe this formally, for each $k\in\mathcal{K}$, we define the *eMBB interfering set*

$$\mathcal{I}_k^{(\mathrm{e})} \triangleq \mathcal{I}_k \cap \mathcal{T}_{\text{eMBB}}. \tag{19}$$

Also, we denote by $\boldsymbol{U}_k^n(M_k^{(\mathsf{L})})$ the non-precoded input signal precomputed at a given LLC Tx k, which we will see is of power P. (The following item 3) explains how to obtain $\boldsymbol{U}_k^n(M_k^{(\mathsf{L})})$.) Tx k sends the inputs

$$\boldsymbol{X}_k^n = \gamma_k \left(\boldsymbol{U}_k^n(M_k^{(\mathsf{L})}) - \sum_{k' \in \mathcal{I}_k^{(\mathsf{e})}} h_{k,k}^{-1} h_{k',k} \hat{\boldsymbol{X}}_{k'}^n \right) \tag{20}$$

over the channel, where γ_k is a factor that ensures that the transmit signal satisfies the power constraint in (8).[1] Since each LLC Rx k is not interfered by the signal sent at any other LLC Tx, the precoding in (20) ensures that a LLC Rx k observes the almost interference-free signal

$$\boldsymbol{Y}_k^n = \gamma_k \mathsf{h}_{k,k} \boldsymbol{U}_k^n + \underbrace{\sum_{k' \in \mathcal{I}_k^{(\mathsf{e})}} h_{k',k} (\boldsymbol{X}_{k'}^n - \gamma_k \hat{\boldsymbol{X}}_{k'}^n) + \boldsymbol{Z}_k^n}_{\text{disturbance}}, \tag{21}$$

where the variance of the above disturbance is around the noise level and does not grow with P. Notice that the simple pre-coding in (20) simply subtracts the interference signal. It is well known that dirty-paper coding (DPC) achieves higher rates at finite power values P. It is well-known that in terms of per-user MG the interference subtraction in (20) and dirty-paper coding are equivalent and achieve the same performance. In this article we use interference subtraction, at it is conceptually simpler.

3) Transmission of LLC messages: Each LLC Tx k encodes its desired message $M_k^{(\mathsf{L})}$ using a codeword $\mathbf{U}_k^{(n)}(M_k^{(\mathsf{L})})$ from a Gaussian point-to-point code of power P. The corresponding Rx k applies a standard point-to-point decoding rule to directly decode this LLC codeword without Rx-cooperation from its "almost" interference-free outputs $\mathbf{Y}_k$, see (21).

4) Canceling LLC interference at eMBB Rxs: According to the previous item 3), all LLC messages are decoded directly from the outputs without any Rx-cooperation. During the first Rx-cooperation round, all LLC Rxs share their decoded messages with all their neighboring eMBB Rxs, which can cancel the corresponding interference from their receive signals. More formally, we define the *LLC interference set*

$$\mathcal{I}_{\tilde{k}}^{(\mathsf{L})} \triangleq \mathcal{I}_{\tilde{k}} \cap \mathcal{T}_{\text{LLC}} \tag{22}$$

as the set of LLC Txs whose signals interfere at Rx $\tilde{k}$. Each eMBB Rx $\tilde{k}$ forms the new signal

$$\hat{\boldsymbol{Y}}_{\tilde{k}}^n := \boldsymbol{Y}_{\tilde{k}}^n - \sum_{\hat{k} \in \mathcal{I}_{\tilde{k}}^{(\mathsf{L})}} h_{\hat{k},\tilde{k}} \boldsymbol{U}_{\hat{k}}^n(\hat{M}_{\hat{k}}^{(\mathsf{L})}), \tag{23}$$

and decodes its desired eMBB message based on this new signal following the steps described in the following item 5). Fig. 4a illustrates by yellow arrows the sharing of decoded LLC messages with neighboring eMBB Rxs in Wyner's symmetric network. Recall again that for convenience in this example we treat Message $M_{19}^{(\mathsf{e})}$ as if it was LLC.

5) Transmission and reception of eMBB messages using CoMP *reception:* Each eMBB Tx k encodes its message $M_k^{(\mathsf{e})}$ using a codeword $\boldsymbol{X}_k^n(M_k^{(\mathsf{e})})$ from a Gaussian point-to-point code of power P. eMBB messages are decoded based on the new outputs $\hat{\boldsymbol{Y}}_{\tilde{k}}^n$ in (23). CoMP reception is employed to decode all eMBB messages in a given subnet. That means that each eMBB Rx $\tilde{k}$ applies a rate-$\frac{1}{2}\log(1+\mathsf{P})$ quantizer to the new output signal $\hat{\boldsymbol{Y}}_{\tilde{k}}^n$, and sends the quantization information over the cooperation links to the master Rx in its subnet. Each master Rx reconstructs all the quantized signals and jointly decodes the eMBB messages, before sending them back to their intended Rxs. By item 4) the influence of LLC transmissions has been canceled (up to the noise level) from the eMBB receive signals.

6) MG analysis: In the described scheme, all transmitted LLC and eMBB messages can be sent reliably at MG 1 because all interference is canceled (up to the noise level) either at the Tx or the Rx side and because the precoding factors γ_k do not vanish as $\mathsf{P} \to \infty$.

The presented coding scheme can sustain LLC rates

$$R_k^{(\mathsf{L})} = \frac{1}{2}\log(1+\mathsf{P}) + o(1), \quad k \in \mathcal{T}_{\text{LLC}}, \tag{24a}$$

and eMBB rates

$$R_k^{(\mathsf{e})} = \frac{1}{2}\log(1+\mathsf{P}) + o(1), \quad k \in \mathcal{T}_{\text{eMBB}}. \tag{24b}$$

[1]Since all channel coefficients $h_{k',k}$ are constant and both $\boldsymbol{U}_k^n(M_k^{(\mathsf{L})})$ and $\hat{\boldsymbol{X}}_{k'}^n$ are of power P, the prefactor γ_k does not grow with P.

7) Rate transfer for Model 1: In Model 1, any LLC Tx also has an eMBB message to send. Since LLC messages have more stringent requirements than eMBB messages, each Tx/Rx pair in $\mathcal{T}_{\text{LLC}}$ can use part of its rate to send an eMBB message instead of the LLC message. By this rate-transfer argument, our scheme can achieve any rate-tuple $(R_k^{(\mathsf{L})}, R_k^{(\mathsf{e})} \colon k \in \mathcal{K})$ satisfying

$$R_k^{(\mathsf{L})} + R_k^{(\mathsf{e})} \leq \frac{1}{2}\log(1+\mathsf{P}) + o(1), \quad k \in \mathcal{T}_{\text{LLC}}, \tag{25a}$$

$$R_k^{(\mathsf{e})} \leq \frac{1}{2}\log(1+\mathsf{P}) + o(1), \quad k \in \mathcal{T}_{\text{eMBB}}, \tag{25b}$$

$$R_k^{(\mathsf{L})} = 0, \quad k \in \mathcal{T}_{\text{eMBB}}, \tag{25c}$$

$$R_k^{(\mathsf{e})}, R_k^{(\mathsf{L})} = 0, \quad k \in \mathcal{T}_{\text{silent}}. \tag{25d}$$

B. Analysis under Random Arrivals

In our model, we can choose the sets $\mathcal{T}_{\text{silent}}$, $\mathcal{T}_{\text{LLC}}$, and $\mathcal{T}_{\text{eMBB}}$ depending on the realizations of the random sets $\mathcal{K}_{\text{LLC}}$ and $\mathcal{K}_{\text{eMBB}}$. An ideal choice would obviously be to set $\mathcal{T}_{\text{silent}} = \mathcal{K}\backslash\mathcal{K}_{\text{active}}$, $\mathcal{T}_{\text{LLC}} = \mathcal{K}_{\text{LLC}}$, and $\mathcal{T}_{\text{eMBB}} = \mathcal{K}_{\text{eMBB}}$. However, such a choice is not always possible because the sets $\mathcal{K}_{\text{active}}, \mathcal{K}_{\text{LLC}}, \mathcal{K}_{\text{eMBB}}$ are random while the sets $\mathcal{T}_{\text{silent}}$, $\mathcal{T}_{\text{LLC}}$, and $\mathcal{T}_{\text{eMBB}}$ have to satisfy specific requirements, e.g., users in $\mathcal{T}_{\text{LLC}}$ cannot be adjacent and users in $\mathcal{T}_{\text{silent}}$ cannot be too far away from each other so as to ensure that eMBB Rxs in a subnet can reach their master Rx within the required number of cooperation rounds.

As already mentioned, one remedy is to time-share different versions $i = 1, 2, \ldots$ of the scheme with different choices of the sets $\mathcal{T}_{\text{silent},i}$, $\mathcal{T}_{\text{LLC},i}$, and $\mathcal{T}_{\text{eMBB},i}$ in version i so that all LLC users $\mathcal{K}_{\text{LLC}}$ can transmit their LLC messages in at least one of the versions, i.e., so that each $k \in \mathcal{K}_{\text{LLC}}$ is present in at least one of the sets $\mathcal{T}_{\text{LLC},i}$.

Depending on the network structure, identifying the best choice of the time-shared schemes can be cumbersome. We therefore first propose a generic (non-adaptive) choice that works for all realizations of the activity parameters in the sense that the union of the sets $\bigcup_i \mathcal{T}_{\text{LLC},i}$ over all time-shared schemes covers each of the users in $\mathcal{K}$.

1) Non-adaptive scheme under random arrivals: The networks we consider in this paper have regular connectivity. It is thus possible to find a regular arrangement of the sets $\mathcal{T}_{\text{silent},1}$, $\mathcal{T}_{\text{LLC},1}$, and $\mathcal{T}_{\text{eMBB},1}$ satisfying the requirements in the scheme described in the previous section, and so that shifted arrangements $\mathcal{T}_{\text{silent},i}$, $\mathcal{T}_{\text{LLC},i}$, and $\mathcal{T}_{\text{eMBB},i}$ exist, for $i = 2, 3, \ldots, \kappa$ and $\kappa = \frac{K}{|\mathcal{T}_{\text{LLC},1}|}$, with each Tx/Rx pair k lying in exactly one set $\mathcal{T}_{\text{LLC},i}$. In such a regular arrangement, each LLC message is transmitted only during a fraction $\frac{1}{\kappa}$ of the time, and its rate is thus

$$R^{(\mathsf{L})} = \frac{|\mathcal{T}_{\text{LLC},1}|}{K} \cdot \frac{1}{2}\log(1+\mathsf{P}) + o(1). \tag{26}$$

This strategy can thus achieve a LLC per-user MG of

$$\mathsf{S}^{(\mathsf{L})} = \rho\rho_f \varlimsup_{K\to\infty} \frac{|\mathcal{T}_{\text{LLC},1}|}{K}, \tag{27}$$

where we recall that the factor $\rho\rho_f$ stems from the definition of $\mathsf{S}^{(\mathsf{L})}$.

In the i-th version of the scheme, the Tx/Rx pairs $k \in \mathcal{T}_{\text{eMBB},i}$ can transmit eMBB messages at a rate $\frac{1}{2}\log(1+\mathsf{P}) + o(1)$, if they have such eMBB messages. Moreover, as already explained, Tx/Rx pairs $k \in \mathcal{T}_{\text{LLC},i}$ that have an eMBB message but no LLC message can transmit these eMBB messages also at the same rate $\frac{1}{2}\log(1+\mathsf{P}) + o(1)$. Since by the regularity of the arrangements, each user lies a fraction $\frac{|\mathcal{T}_{\text{LLC},1}|}{K}$ of the time in the corresponding set $\mathcal{T}_{\text{LLC},i}$ and a fraction $\frac{|\mathcal{T}_{\text{eMBB},1}|}{K}$ of the time in the corresponding set $\mathcal{T}_{\text{eMBB},i}$, we have:

- If $k \in (\mathcal{K}_{\text{LLC}} \cap \mathcal{K}_{\text{eMBB}})$, then $R_k^{(\mathsf{e})} = \frac{|\mathcal{T}_{\text{eMBB},1}|}{K}\frac{1}{2}\log(1+\mathsf{P}) + o(1)$;
- If $k \in (\mathcal{K}_{\text{LLC}}\backslash\mathcal{K}_{\text{eMBB}})$, then $R_k^{(\mathsf{e})} = 0$;
- If $k \in (\mathcal{K}_{\text{eMBB}}\backslash\mathcal{K}_{\text{LLC}})$, then $R_k^{(\mathsf{e})} = \frac{|\mathcal{T}_{\text{eMBB},1}|+|\mathcal{T}_{\text{LLC},1}|}{K}\frac{1}{2}\log(1+\mathsf{P}) + o(1)$.

Under Model 1, any active user has an eMBB message to transmit and thus the set $\mathcal{K}_{\text{LLC}}\backslash\mathcal{K}_{\text{eMBB}}$ is empty. The expected per-user eMBB MG is therefore equal to

$$\mathsf{S}^{(\mathsf{e})} = \rho\rho_f \varlimsup_{K\to\infty} \frac{|\mathcal{T}_{\text{eMBB},1}|}{K} + \rho(1-\rho_f) \varlimsup_{K\to\infty} \frac{|\mathcal{T}_{\text{eMBB},1}| + |\mathcal{T}_{\text{LLC},1}|}{K} \tag{28}$$

$$= \rho \varlimsup_{K\to\infty} \frac{|\mathcal{T}_{\text{eMBB},1}|}{K} + \rho(1-\rho_f) \varlimsup_{K\to\infty} \frac{|\mathcal{T}_{\text{LLC},1}|}{K}. \tag{29}$$

By the rate-transfer arguments in Subsection III-A7, it follows that all pairs $(\mathsf{S}^{(\mathsf{L})}, \mathsf{S}^{(\mathsf{e})})$ satisfying the following two conditions are achievable:

$$\mathsf{S}^{(\mathsf{L})} \leq \rho\rho_f \varlimsup_{K\to\infty} \frac{|\mathcal{T}_{\text{LLC},1}|}{K} \tag{30}$$

$$\mathsf{S}^{(\mathsf{L})} + \mathsf{S}^{(\mathsf{e})} \leq \rho \varlimsup_{K\to\infty} \frac{|\mathcal{T}_{\text{LLC},1}| + |\mathcal{T}_{\text{eMBB},1}|}{K}. \tag{31}$$

Under Model 2 any active user that has a LLC message to send has no eMBB message and thus the set $\mathcal{K}_{\text{LLC}} \cap \mathcal{K}_{\text{eMBB}}$ is empty. The expected per-user eMBB MG is therefore equal to

$$\mathsf{S}^{(\mathsf{e})} = \rho(1-\rho_f) \varlimsup_{K\to\infty} \frac{|\mathcal{T}_{\text{eMBB},1}| + |\mathcal{T}_{\text{LLC},1}|}{K}. \tag{32}$$

The LLC MG is as in (27).

2) Non-adaptive scheme under random arrivals transmitting at $\mathsf{S}^{(\mathsf{L})} = 0$*:* If we are interested in transmitting at the largest possible total eMBB MG, we can set $\mathcal{T}_{\text{LLC}} = \emptyset$ and simply choose a set $\mathcal{T}_{\text{eMBB}}$ satisfying Condition C2 in the previous section. Under Model 1, the expected per-user eMBB MG is then equal to

$$\mathsf{S}^{(\mathsf{e})} = \rho \varlimsup_{K\to\infty} \frac{|\mathcal{T}_{\text{eMBB}}|}{K} \tag{33}$$

and under Model 2 it is

$$\mathsf{S}^{(\mathsf{e})} = \rho(1-\rho_f) \varlimsup_{K\to\infty} \frac{|\mathcal{T}_{\text{eMBB}}|}{K}. \tag{34}$$

3) Fully-adaptive schemes under random arrivals: Here, the idea is to adapt the choice of the sets $\{\mathcal{T}_{\text{eMBB},i}\}$ and $\{\mathcal{T}_{\text{LLC},i}\}$ to the realizations of the user activity and data arrival patterns, so as to optimize the per-user MGs achieved by the assignment. Finding an optimal choice for general networks seems very challenging. In this work, we shall present good choices for Wyner's symmetric network, see Subsections V-B2 (Model 1) and V-B4 (Model 2). For the hexagonal network we only focus on $\mathrm{D} \to \infty$, in which case one obviously wishes to choose $\mathcal{T}_{\text{eMBB},i}$ as the complement of $\mathcal{T}_{\text{LLC},i}$ in $\mathcal{K}_{\text{eMBB}}$. That means, any Tx that can (i.e., is active and has eMBB data to transmit) should send an eMBB message. For large networks it is clear that three subschemes $i = 1, 2, 3$ are required for the hexagonal network (and two $i = 1, 2$ for Wyner's symmetric network) if one wishes to accomodate all LLC transmissions in $\mathcal{K}_{\text{LLC}}$ in at least one of the subschemes. There is thus no advantage in adapting the sets $\{\mathcal{T}_{\text{LLC},i}\}$ to the realizatios of the random data arrivals.

IV. Coding Scheme with only Rx-Cooperation

We assume throughout this section that

$$\mathrm{D}_{\text{Tx}} = 0 \quad \text{and} \quad \mathrm{D}_{\text{Rx}} = \mathrm{D}. \tag{35}$$

A. The Basic Scheme with Chosen Message Assignment

The only difference between this scheme and the one proposed in Section III-A is that without Tx-cooperation, item 2) cannot be executed. More specifically, in this scheme, precanceling of eMBB interference at LLC Txs is not allowed. Therefore, Txs in $\mathcal{T}_{\text{eMBB}}$ whose transmissions interfere with LLC transmissions are deactivated.

With Rx-cooperation only, we therefore choose sets $\mathcal{T}_{\text{silent}}$, $\mathcal{T}_{\text{LLC}}$, and $\mathcal{T}_{\text{eMBB}}$ that satisfy the two conditions C1 and C2 in Subsection III-A and the additional condition

C3: eMBB transmit signals do not interfere at LLC Rxs:

$$k \notin \mathcal{I}_{k'}, \quad \forall k \in \mathcal{T}_{\text{eMBB}},\ k' \in \mathcal{T}_{\text{LLC}}, \tag{36}$$

where we recall that $\mathcal{I}_{k'}$ denotes the set of Txs whose signals interfere at Rx k'.

The coding scheme in Section III (without item 2) then again achieves the rates in (24). Moreover, with an appropriate rate-transfer argument from LLC to eMBB messages, under Model 1 it even achieves the rates in (25). Notice that in our schemes, the penalty from having only Rx-cooperation but no Tx-cooperation thus only stems from the additional requirement C3, compared to the case with Tx- and Rx-cooperation.

B. Analysis under Random Arrivals

1) Non-adaptive scheme under random arrivals: Unlike with Tx- and Rx-cooperation, when only Rxs can cooperate there does not seem to be any interesting non-adaptive scheme that is not degrading, i.e., that includes a non-trivial combination of LLC and eMBB Tx/Rx pairs. The reason is that Requirement C3 is very stringent and for many networks does not seem to allow for meaningful choices where both $\mathcal{T}_{\text{LLC}}$ and $\mathcal{T}_{\text{eMBB}}$ are non-empty. In these networks the best option seems to time-share schemes with either only LLC or only eMBB Txs. The scheme with only LLC Txs should time-share different schemes with different choices of $\mathcal{T}_{\text{LLC},i}$ so that each Tx lies in $\mathcal{T}_{\text{LLC},i}$ for at least one phase i. Each of the sets $\mathcal{T}_{\text{LLC},i}$ has to satisfy Condition C1, and we set $\mathcal{T}_{\text{silent},i} = \mathcal{K} \backslash \mathcal{T}_{\text{LLC},i}$ so that $\mathcal{T}_{\text{eMBB},i} = \emptyset$. The scheme with only eMBB Txs sets $\mathcal{T}_{\text{LLC}} = \emptyset$ and then chooses $\mathcal{T}_{\text{silent}}$ so as to decompose the network in an appropriate way so that the remaining set $\mathcal{T}_{\text{eMBB}} = \mathcal{K} \backslash \mathcal{T}_{\text{silent}}$ satisfies Condition C2.

After time-sharing, the overall scheme then achieves the expected per-user MG pair

$$\mathsf{S}^{(\mathsf{L})} = \alpha \cdot \rho\rho_f \varlimsup_{K\to\infty} \frac{|\mathcal{T}'_{\text{LLC}}|}{K} \tag{37}$$

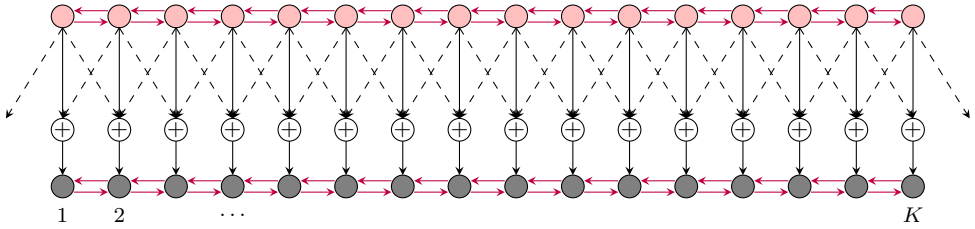

Fig. 5: Wyner's symmetric network. Black dashed arrows show interference links and purple arrows show cooperation links.

$$\mathsf{S}^{(\mathsf{e})} = \alpha\rho(1-\rho_f)\,\overline{\lim_{K\to\infty}}\,\frac{|\mathcal{T}'_{\text{LLC}}|}{K} + (1-\alpha)\cdot\rho(1-\rho_f)\,\overline{\lim_{K\to\infty}}\,\frac{|\mathcal{T}'_{\text{eMBB}}|}{K}, \tag{38}$$

where $\alpha \in [0,1]$ is the time-sharing parameter and the set $\mathcal{T}'_{\text{LLC}} \subseteq \mathcal{K}$ has to satisfy Condition C1 while the set $\mathcal{T}'_{\text{eMBB}} \subseteq \mathcal{K}$ has to satisfy Condition C2. (Notice that here the sets $\mathcal{T}'_{\text{LLC}}$ and $\mathcal{T}'_{\text{eMBB}}$ do not need to be disjoint; for this reason we use the prime-notation.)

Under Model 1 each Tx has an eMBB message to send with probability ρ, and moreover we can apply a rate-transfer argument from LLC to eMBB messages. The scheme can then achieve any expected per-user MG pair satisfying

$$\mathsf{S}^{(\mathsf{L})} \le \alpha\cdot\rho\rho_f\,\overline{\lim_{K\to\infty}}\,\frac{|\mathcal{T}'_{\text{LLC}}|}{K} \tag{39}$$

$$\mathsf{S}^{(\mathsf{L})} + \mathsf{S}^{(\mathsf{e})} \le \alpha\cdot\rho\,\overline{\lim_{K\to\infty}}\,\frac{|\mathcal{T}'_{\text{LLC}}|}{K} + (1-\alpha)\cdot\rho\,\overline{\lim_{K\to\infty}}\,\frac{|\mathcal{T}'_{\text{eMBB}}|}{K}, \tag{40}$$

where $\alpha \in [0,1]$, and the sets $\mathcal{T}'_{\text{LLC}}$ and $\mathcal{T}'_{\text{eMBB}}$ satisfy Conditions C1 and C2, respectively.

Under Model 2 any active user that has a LLC message to send has no eMBB message and thus the set $\mathcal{K}_{\text{LLC}} \cap \mathcal{K}_{\text{eMBB}}$ is empty. The expected per-user eMBB MG is therefore equal to

$$\mathsf{S}^{(\mathsf{e})} = \rho(1-\rho_f)\,\overline{\lim_{K\to\infty}}\,\frac{(1-\alpha)|\mathcal{T}'_{\text{eMBB}}| + \alpha|\mathcal{T}'_{\text{LLC}}|}{K}. \tag{41}$$

2) Adaptive schemes under random arrivals: We again describe fully-adaptive schemes for Wyner's symmetric network in Subsections V-C2 and V-C4 and for the hexagonal network in Subsections VI-C2 and VI-C4. Notice that under Rx-Cooperation only, adaptive schemes are also interesting when $\mathsf{D} \to \infty$, because even in this extreme case we cannot simply schedule all active eMBB users that do not send LLC messages. The reason is that without Tx-Cooperation, interference from eMBB transmissions cannot be canceled on LLC transmissions. The trivial choice $\mathcal{T}_{\text{eMBB},i} = \mathcal{K}_{\text{eMBB}} \backslash \mathcal{T}_{\text{LLC},i}$ is thus not always possible.

V. The Symmetric Wyner Network

A. Network and Cooperation Model

Consider Wyner's symmetric linear cellular model where cells are aligned in a single dimension and signals of users that lie in a given cell interfere only with signals sent in the two adjacent cells. See Fig. 5 where the interference pattern is illustrated by black dashed lines. We assume that the various mobile users in a cell are scheduled on different frequency bands, and focus on a single mobile user per cell (i.e., on a single frequency band).

The input-output relation of the network is

$$\boldsymbol{Y}_{k,t} = h_{k,k}\boldsymbol{X}_{k,t} + \sum_{\tilde{k}\in\{k-1,k+1\}} h_{\tilde{k},k}\boldsymbol{X}_{\tilde{k},t} + \boldsymbol{Z}_{k,t}, \tag{42}$$

where $\boldsymbol{X}_{0,t} = \boldsymbol{0}$ for all t, and the interference set at a given user k is

$$\mathcal{I}_k = \{k-1, k+1\}, \tag{43}$$

where indices out of the range $\mathcal{K}$ should be ignored. In this model, Rxs and Txs can cooperate with the two Rxs and Txs in the adjacent cells, so

$$\mathcal{N}_k = \{k-1, k+1\} \tag{44}$$

Fig. 5 illustrates the interference pattern of the network and the available cooperation links.

B. Results with Both Tx- and Rx-Cooperation

We first present our results for Model 1.

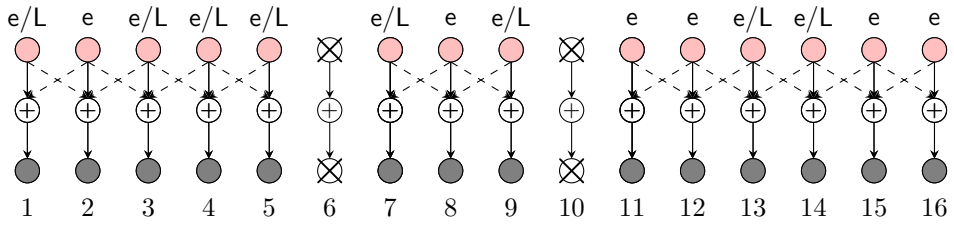

(a) User activity pattern

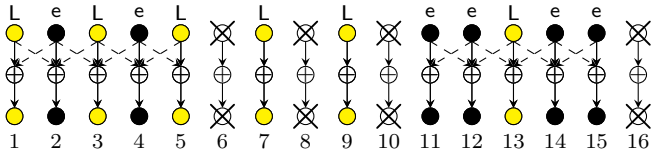

(b) Non-adaptive, Phase 1

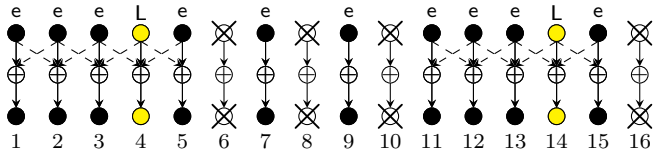

(c) Non-adaptive, Phase 2

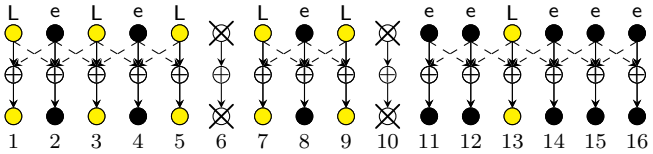

(d) Adaptive, Phase 1

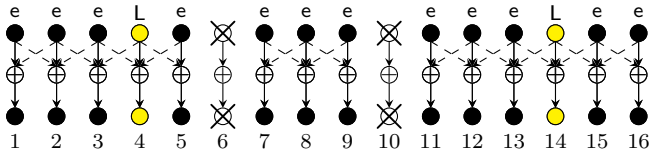

(e) Adaptive, Phase 2

Fig. 6: An illustration of the network and user activity pattern in Model 1 with both Tx- and Rx-cooperation for $\mathrm{D} = 6$.

1) Non-Adaptive Scheme under Model 1*:*

Proposition 1 (Non-Adaptive Scheme, Model 1): For $\rho \in (0, 1]$, the fundamental per-user MG region $\mathcal{S}_1^\star(\mathrm{D}, \rho, \rho_f)$ includes all nonnegative pairs $(\mathsf{S}^{(\mathsf{L})}, \mathsf{S}^{(\mathsf{e})})$ satisfying

$$\mathsf{S}^{(\mathsf{L})} \le \frac{\rho\rho_f}{2}, \tag{45}$$

$$\mathsf{S}^{(\mathsf{e})} + \mathsf{S}^{(\mathsf{L})} \le \rho\frac{\mathrm{D}+1}{\mathrm{D}+2}. \tag{46}$$

Proof: Achievability of the rate-pair $\mathsf{S}^{(\mathsf{L})} = \frac{\rho\rho_f}{2}$ and $\mathsf{S}^{(\mathsf{e})} = \rho\frac{\mathrm{D}+1}{\mathrm{D}+2} - \frac{\rho\rho_f}{2}$ holds by (30) and (31) and the choice of the sets

$$\mathcal{T}_{\text{silent},1} = \left\{\ell\,(\mathrm{D}+2) : \ell = 1, \ldots, \left\lfloor \frac{K}{\mathrm{D}+2} \right\rfloor\right\}, \tag{47a}$$

$$\mathcal{T}_{\text{LLC},1} = \{1, 3, \ldots, K-1\}, \tag{47b}$$

$$\mathcal{T}_{\text{eMBB},1} = \mathcal{K}\backslash(\mathcal{T}_{\text{silent},1} \cup \mathcal{T}_{\text{LLC},1}). \tag{47c}$$

■

2) Adaptive Scheme Under Model 1*:* In Wyner's symmetric network, the random user activity pattern $\mathbf{A}$ splits the network into different subnets. Our adaptive scheme acts on each of these subnets independently. Since these subnets have full user activity, we simply choose the transmit sets in the same way as in the non-adaptive scheme. In particular, for each subnet the two LLC transmit sets with even or odd integers are chosen and LLC transmissions are only scheduled in the corresponding phase.

The advantage of the proposed adaptive choice of transmit set is that it silences fewer transmitters than in the generic non-adaptive scheme. For example, consider the network and user activity pattern in Fig. 6(a) under data arrival Model 1. The generic non-adaptive scheme schedules eMBB and LLC transmissions as indicated in Fig. 6(b) and Fig. 6(c), and achieves the per-user MG pair $(\mathsf{S}^{(\mathsf{L})} = 1/4, \mathsf{S}^{(\mathsf{e})} = 1/2)$. In contrast, our adaptive scheme schedules them as in Fig 6(d) and Fig. 6(e), and achieves the improved per-user MG pair $(\mathsf{S}^{(\mathsf{L})} = 1/4, \mathsf{S}^{(\mathsf{e})} = 5/8)$.

Theorem 1 (Adaptive Scheme, Model 1): For $\rho \in (0, 1)$, the fundamental per-user MG region $\mathcal{S}_1^\star(\mathrm{D}, \rho, \rho_f)$ includes all nonnegative pairs $(\mathsf{S}^{(\mathsf{L})}, \mathsf{S}^{(\mathsf{e})})$ satisfying

$$\mathsf{S}^{(\mathsf{L})} \le \frac{\rho\rho_f}{2}, \tag{48}$$

$$\mathsf{S}^{(\mathsf{e})} + M_{\text{both},1}^{(\mathrm{A})} \cdot \mathsf{S}^{(\mathsf{L})} \le \rho - \frac{(1-\rho)\rho^{\mathrm{D}+2}}{1-\rho^{\mathrm{D}+2}}, \tag{49}$$

where

$$M_{\text{both},1}^{(\mathrm{A})} \triangleq 1+\frac{(1-\rho)^2\rho^{\mathrm{D}}}{\rho_f(1-\rho^{\mathrm{D}+2})}-\frac{(1-\rho)^2\rho^{\mathrm{D}}(1-\rho_f)^2}{\rho_f(1-\rho^{\mathrm{D}+2}(1-\rho_f)^2)}. \tag{50}$$

Proof: The result follows by rate- and time-sharing arguments and the achievability of the pairs $(\mathsf{S}^{(\mathsf{L})},\mathsf{S}^{(\mathsf{e})})$, with $\mathsf{S}^{(\mathsf{e})}$ given in (165) and the pair $(\mathsf{S}^{(\mathsf{L})},\mathsf{S}^{(\mathsf{e})})$ as given in (173) and (186). See Appendix B for the proof. ■

We also have the following outer bound.

Theorem 2 (Outer Bound, Model 1): For $\rho\in(0,1)$, all achievable MG pairs $(\mathsf{S}^{(\mathsf{L})},\ \mathsf{S}^{(\mathsf{e})})$ of Model 1 satisfy (45) and

$$\mathsf{S}^{(\mathsf{e})}+\mathsf{S}^{(\mathsf{L})}\leq\rho-\frac{(1-\rho)\rho^{\mathrm{D}+2}}{1-\rho^{\mathrm{D}+2}}. \tag{51}$$

For $\rho=1$ they satisfy (45) and (46).

Proof: See Appendix B-C. ■

Inner and outer bounds are generally very close. In particular, they determine the largest achievable LLC per-user MG, which is $\mathsf{S}_{\max}^{(\mathsf{L})}=\frac{\rho\rho_f}{2}$, and the largest eMBB per-user MG, which is

$$S_{\max}^{(\mathsf{e})}=\rho-\frac{(1-\rho)\rho^{\mathrm{D}+2}}{1-\rho^{\mathrm{D}+2}}. \tag{52}$$

Our inner and outer bounds completely coincide in the extreme cases $\rho=1$ and $\mathrm{D}\to\infty$.

Corollary 1: For $\rho=1$ or when $\mathrm{D}\to\infty$, Theorem 2 is exact. For $\rho=1$, the fundamental per-user MG region $\mathcal{S}_1^\star(\mathrm{D},\rho,\rho_f)$ *is* the set of all nonnegative MG pairs $(\mathsf{S}^{(\mathsf{L})},\ \mathsf{S}^{(\mathsf{e})})$ satisfying (45) and (46), and for $\rho\in(0,1)$ and $\mathrm{D}\to\infty$ it *is* the set of all MG pairs $(\mathsf{S}^{(\mathsf{L})},\ \mathsf{S}^{(\mathsf{e})})$ satisfying (45) and

$$\mathsf{S}^{(\mathsf{e})}+\mathsf{S}^{(\mathsf{L})}\leq\rho. \tag{53}$$

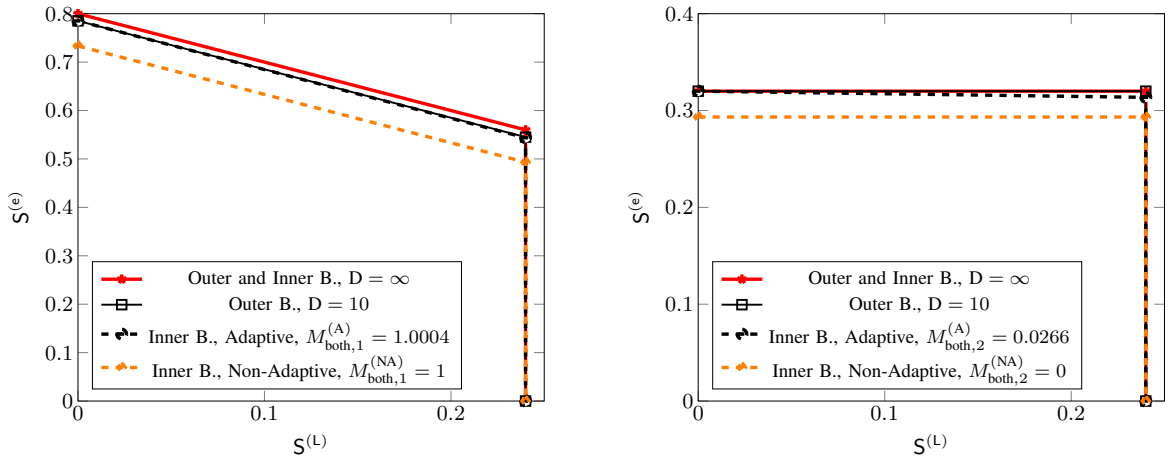

(a) Tx- and Rx-Cooperation, Model 1

(b) Tx- and Rx-Cooperation, Model 2

Fig. 7: Inner and outer bounds on the fundamental per-user MG regions $\mathcal{S}_1^\star(\mathrm{D},\rho,\rho_f)$ and $\mathcal{S}_2^\star(\mathrm{D},\rho,\rho_f)$ for $\rho=0.8$, $\rho_f=0.6$ and $\mathrm{D}=10$ for Tx- and Rx-Cooperation.

For Model 2 we have the following results.

3) Non-Adaptive Scheme under Model 2:

Proposition 2 (Non-Adaptive Scheme, Model 2): For $\rho\in(0,1]$, the fundamental per-user MG region $\mathcal{S}_2^\star(\mathrm{D},\rho,\rho_f)$ includes all nonnegative pairs $(\mathsf{S}^{(\mathsf{L})},\ \mathsf{S}^{(\mathsf{e})})$ satisfying

$$\mathsf{S}^{(\mathsf{L})}\leq\frac{\rho\rho_f}{2}, \tag{54}$$

$$\mathsf{S}^{(\mathsf{e})}\leq\rho(1-\rho_f)\frac{\mathrm{D}+1}{\mathrm{D}+2}. \tag{55}$$

Proof: The pair $\mathsf{S}^{(\mathsf{L})}=\frac{\rho\rho_f}{2}$ and $\mathsf{S}^{(\mathsf{e})}=\rho(1-\rho_f)\frac{\mathrm{D}+1}{\mathrm{D}+2}$ is achievable by (26) and (32) and the choice of the sets in (47). On the other hand, the pair $\mathsf{S}^{(\mathsf{L})}=0$ and $\mathsf{S}^{(\mathsf{e})}=\rho(1-\rho_f)\frac{\mathrm{D}+1}{\mathrm{D}+2}$ is achievable by (34) and the choice $\mathcal{T}_{\text{eMBB}}=\mathcal{K}\backslash\mathcal{T}_{\text{silent},1}$ for $\mathcal{T}_{\text{silent},1}$ as in (47a). The proposition then follows by time-sharing arguments. ■

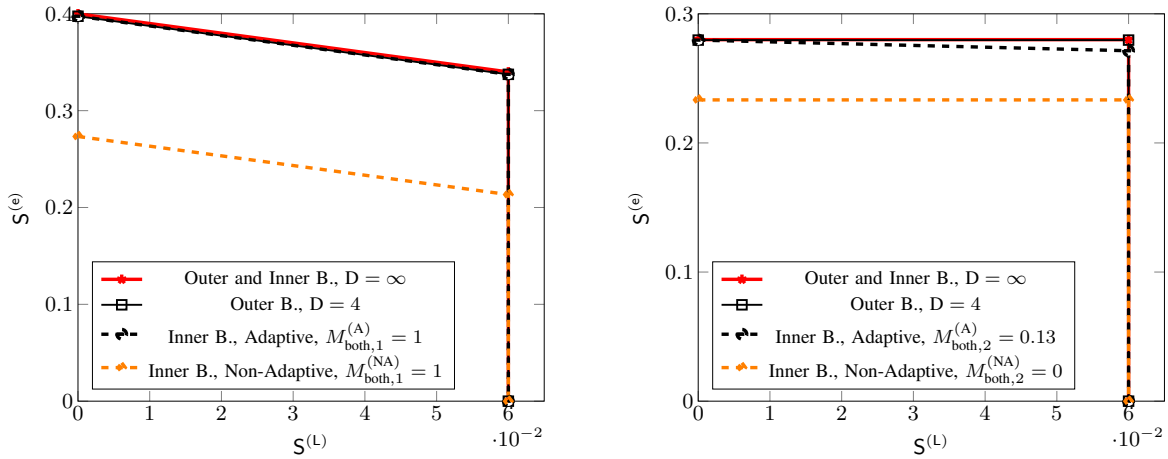

(a) Tx- and Rx-Cooperation, Model 1

(b) Tx- and Rx-Cooperation, Model 2

Fig. 8: Inner and outer bounds on the fundamental per-user MG regions $\mathcal{S}_1^\star(\mathrm{D}, \rho, \rho_f)$ and $\mathcal{S}_2^\star(\mathrm{D}, \rho, \rho_f)$ for $\rho = 0.4$, $\rho_f = 0.3$ and $\mathrm{D} = 4$ for Tx- and Rx-Cooperation.

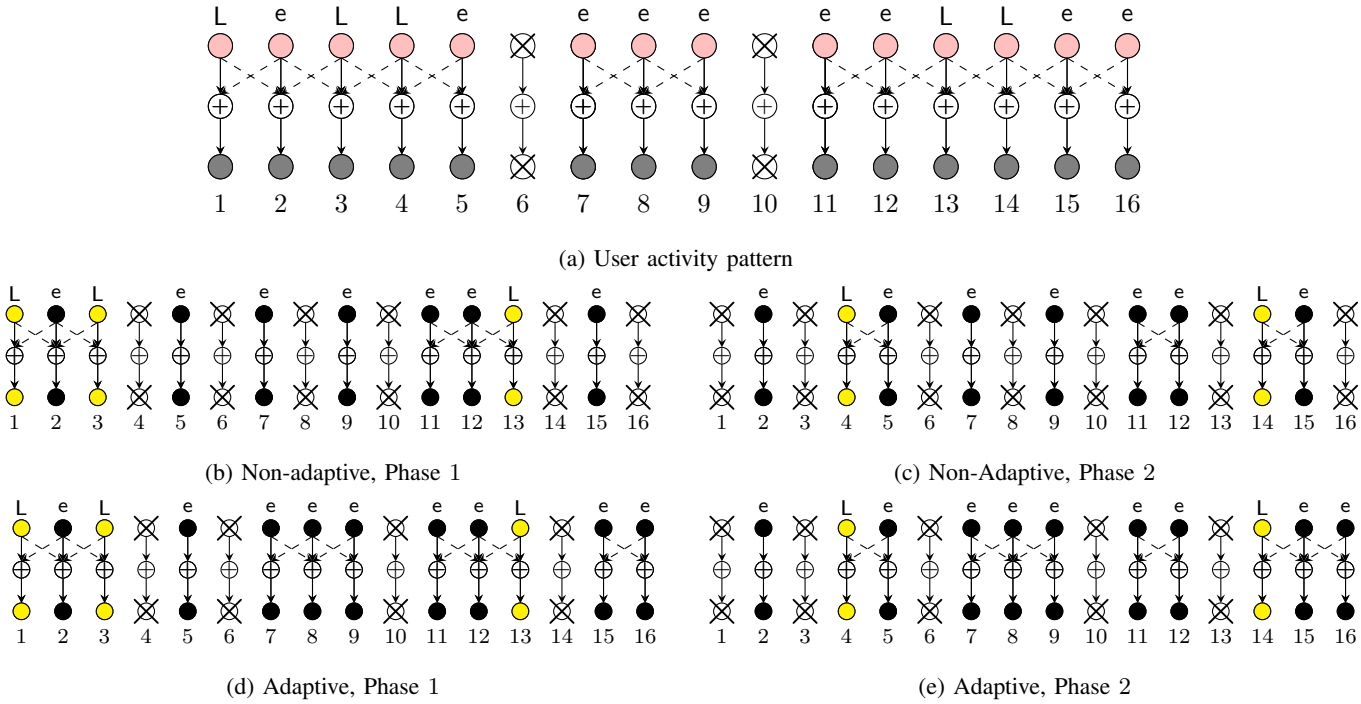

(a) User activity pattern

(b) Non-adaptive, Phase 1

(c) Non-Adaptive, Phase 2

(d) Adaptive, Phase 1

(e) Adaptive, Phase 2

Fig. 9: An illustration of the network and user activity pattern in Model 2 with both Tx- and Rx-cooperation for $\mathrm{D} = 6$.

4) Adaptive Scheme under Model 2: We reuse the two LLC Tx sets $\mathcal{T}_{\mathrm{LLC},1}$ and $\mathcal{T}_{\mathrm{LLC},2}$ consisting of the odd and even indices from 1 and K, and in Phase i we schedule LLC transmissions only on the LLC Tx set $\mathcal{T}_{\mathrm{LLC},i}$ but not on the other transmitters. With this assignment of LLC messages, under Model 2 and in each Phase i, the network is split into even smaller subnets than under Model 1, because not only inactive Txs are silenced but also Txs that have LLC messages to send but do not belong to $\mathcal{T}_{\mathrm{LLC},i}$. (Under Model 1 these Txs still participated in the communication because besides their LLC messages they also have eMBB messages to send.) On each of these small subnets, we then schedule eMBB transmissions as in the generic-non-adaptive scheme. In Fig. 9 we show the scheduling of LLC transmissions for the user activity and data arrival patterns in Fig. 9(a) under the generic (Fig. 9(b) and Fig. 9(c)) and adaptive (Fig. 9(d) and Fig. 9(e)) schemes. We see that while the generic scheme only achieves a per-user MG pair of $(\mathsf{S}^{(\mathsf{L})} = 5/32, \mathsf{S}^{(\mathsf{e})} = 14/32)$, the adaptive scheme can achieve $(\mathsf{S}^{(\mathsf{L})} = 5/32, \mathsf{S}^{(\mathsf{e})} = 18/32)$.

Theorem 3 (Adaptive Scheme, Model 2): For $\rho \in (0, 1)$ and $\rho_f \in (0, 1]$, the fundamental per-user MG region $\mathcal{S}_2^\star(\mathrm{D}, \rho, \rho_f)$

includes all nonnegative pairs $(\mathsf{S}^{(\mathsf{L})},\ \mathsf{S}^{(\mathsf{e})})$ satisfying

$$\mathsf{S}^{(\mathsf{L})} \leq \frac{\rho\rho_f}{2}, \tag{56}$$

$$\mathsf{S}^{(\mathsf{e})} + M^{(\mathrm{A})}_{\mathrm{both},2} \cdot \mathsf{S}^{(\mathsf{L})} \leq \rho(1-\rho_f) - \frac{(1-\rho(1-\rho_f))\rho^{\mathrm{D}+2}(1-\rho_f)^{\mathrm{D}+2}}{1-\rho^{\mathrm{D}+2}(1-\rho_f)^{\mathrm{D}+2}}, \tag{57}$$

where

$$\begin{aligned} M^{(\mathrm{A})}_{\mathrm{both},2} \triangleq\ & 1 + \frac{2(1-\rho_f)}{\rho_f} - \frac{2(1-\rho(1-\rho_f))\rho^{\mathrm{D}+1}(1-\rho_f)^{\mathrm{D}+2}}{\rho_f(1-\rho^{\mathrm{D}+2}(1-\rho_f)^{\mathrm{D}+2})} \\ & - \frac{2(1-\rho_f)}{\rho_f(1-\rho^2(1-\rho_f))^2}\left((1+\rho)(1-\rho(1-\rho_f))^2 - \rho^3\rho_f^2\right) \\ & - \frac{\left((1-\rho(1-\rho_f))^2 + (1-\rho)^2(1-\rho_f)(2\rho+2\rho^2(1-\rho_f)+1)\right)}{\rho_f(1-\rho^2(1-\rho_f))} - \frac{(1-\rho)^2\rho^{\mathrm{D}+1}(1-\rho_f)^{\frac{\mathrm{D}+6}{2}}}{2(1-\rho^{\mathrm{D}+2}(1-\rho_f)^{\frac{\mathrm{D}+6}{2}})} \\ & + \frac{\rho^{\mathrm{D}+2}(1-\rho_f)^{\frac{\mathrm{D}+2}{2}}}{2(1-\rho^2(1-\rho_f))(1-\rho^{\mathrm{D}+2}(1-\rho_f)^{\frac{\mathrm{D}+2}{2}})}\left((1+\rho)\left((1-\rho(1-\rho_f))^2 + \frac{(1-\rho)^2}{\rho}\right)\right). \end{aligned} \tag{58a}$$

For $\rho_f = 0$, the left-hand side of (57) has to be replaced by $\mathsf{S}^{(\mathsf{e})}$ only.

Proof: The results hold by time-sharing arguments and the achievability of the pairs $(\mathsf{S}^{(\mathsf{L})}, \mathsf{S}^{(\mathsf{e})})$, with $\mathsf{S}^{(\mathsf{e})}$ given in (194) and the pair $(\mathsf{S}^{(\mathsf{L})}, \mathsf{S}^{(\mathsf{e})})$ as given in (173) and (218); see Appendix C for the proof. ∎

We also have the following outer bound.

Theorem 4 (Outer Bound, Model 2): For $\rho \in (0,1]$, all achievable MG pairs $(\mathsf{S}^{(\mathsf{L})},\ \mathsf{S}^{(\mathsf{e})})$ of Model 2 satisfy (56) and

$$\mathsf{S}^{(\mathsf{e})} \leq \rho(1-\rho_f) - \frac{(1-\rho(1-\rho_f))\rho^{\mathrm{D}+2}(1-\rho_f)^{\mathrm{D}+2}}{1-\rho^{\mathrm{D}+2}(1-\rho_f)^{\mathrm{D}+2}}. \tag{59}$$

Proof: See Appendix C-B. ∎

Inner and outer bounds are generally very close also for this Model 2. As under Model 1, they also determine the largest achievable LLC per-user MG, which is again $\mathsf{S}^{(\mathsf{L})}_{\max} = \frac{\rho\rho_f}{2}$, and the largest eMBB per-user MG, which now under Model 2 is

$$S^{(\mathsf{e})}_{\max} = \rho(1-\rho_f) - \frac{(1-\rho(1-\rho_f))\rho^{\mathrm{D}+2}(1-\rho_f)^{\mathrm{D}+2}}{1-\rho^{\mathrm{D}+2}(1-\rho_f)^{\mathrm{D}+2}}. \tag{60}$$

Notice that Expression (60) can be obtained from (52), which determines the largest eMBB per-user under Model 1, by replacing ρ by $\rho(1-\rho_f)$. The reason is that when only eMBB messages are to be transmitted, then only the probability of each user having an eMBB message matters, and this probability equals ρ under Model 1 and it equals $\rho(1-\rho_f)$ under Model 2.

Corollary 2: For $\mathrm{D} \to \infty$, Theorem 4 is exact. In this case, the fundamental MG region $\mathcal{S}_2^\star(\mathrm{D}=\infty, \rho, \rho_f)$ *is* the set of all non-negative MG pairs $(\mathsf{S}^{(\mathsf{L})},\ \mathsf{S}^{(\mathsf{e})})$ satisfying (56) and

$$\mathsf{S}^{(\mathsf{e})} \leq \rho(1-\rho_f). \tag{61}$$

Proof: The results follow from Proposition 2 and Theorem 4. ∎

Fig. 7 illustrates the outer and inner bounds on the MG region for Models 1 and 2 under both Tx- and Rx-Cooperation for $\rho = 0.8, \rho_f = 0.6$ and $\mathrm{D} = 10$. We generally notice that the best inner bound is quite close to the best outer bound, thus providing a good approximation of the fundamental per-user MG regions. Comparing the different inner bounds, we further remark that the adaptive scheme significantly improves over the non-adaptive scheme, and for the presented set of parameters and for $\mathrm{D} = 10$ the fundamental per-user MG is already close to the one for an unlimited number of cooperation rounds $\mathrm{D} \to \infty$. Fig. 8, which shows similar plots but for $\rho = 0.4, \rho_f = 0.3$ and $\mathrm{D} = 4$, allows for the same conclusions, and moreover shows that for a small user activity parameter $\rho = 0.4$ even $\mathrm{D} = 4$ cooperation rounds suffice to well approximate the asymptotic fundamental per-user MG region for $\mathrm{D} \to \infty$. The reason is that a large number of cooperation rounds is only useful in subnets with a large number of consecutive Txs that are active, and such subnets are extraordinarily rare when ρ is small. In our achievability and converse results this phenomenon can be observed by noting that the influence of D in the exponent decreases with the value of ρ (for Model 1) and with $\rho(1-\rho_f)$ for Model 2.

In Model 1, the bounds all have the shapes of right-angled trapezoids with parallel sides at $\mathsf{S}^{(\mathsf{L})} = 0$ and at the maximum LLC MG $\mathsf{S}^{(\mathsf{L})} = \frac{\rho\rho_f}{2}$. The most interesting part of the bounds is the upper side of the trapezoids, which lies opposite the two right angles. In particular, the slope of this side is -1 for the outer bounds which indicates that sum per-user MG along this line stays constant for all values of the LLC per-user MG $\mathsf{S}^{(\mathsf{L})} \leq \frac{\rho\rho_f}{2}$. For the inner bounds the slope is $-M^{(i)}_{\mathrm{both},1}$ with $i \in \{\mathrm{A}, \mathrm{NA}\}$ indicating that their sum per-user MG is reduced by $(M^{(i)}_{\mathrm{both},1} - 1)\beta$ when the LLC per-user MG $\mathsf{S}^{(\mathsf{L})}$ is increased by β.

In Model 2, the outer bounds have rectangular shapes and the inner bounds are nearly-rectangular. These shapes indicate that the sum per-user MG increases with the LLC per-user MG, and thus operating at large LLC per-user MG $\mathsf{S}^{(\mathsf{L})}$ does not penalize the achievable eMBB per-user MG $\mathsf{S}^{(\mathsf{e})}$. In fact, under Model 2 one cannot trade LLC messages for eMBB messages because each Tx only has one of the two to send.

The shapes of the per-user MG regions in the two models should also be compared to a triangular shape which corresponds to a scheme that schedules the eMBB and LLC transmissions into orthogonal slices (e.g., frequency bands or time-slots). Under both models, our schemes significantly outperform such simple scheduling schemes.

C. Results with only Rx-Cooperation

1) Non-Adaptive Scheme under Model 1*:*

Proposition 3 (Non-Adaptive Scheme, Model 1): For $\rho \in (0,1]$ and $\rho_f \in (0,1]$, the fundamental MG region $\mathcal{S}_1^\star(\mathrm{D},\rho,\rho_f)$ for Model 1 includes all nonnegative pairs $(\mathsf{S}^{(\mathsf{L})},\ \mathsf{S}^{(\mathsf{e})})$ satisfying

$$\mathsf{S}^{(\mathsf{L})} \le \frac{\rho\rho_f}{2}, \tag{62}$$

$$\mathsf{S}^{(\mathsf{e})} + M_{\text{Rx},1}^{(\text{NA})}\mathsf{S}^{(\mathsf{L})} \le \rho\frac{\mathrm{D}+1}{\mathrm{D}+2}, \tag{63}$$

where

$$M_{\text{Rx},1}^{(\text{NA})} \triangleq \frac{\mathrm{D}+1}{\mathrm{D}+2}\frac{2}{\rho_f} - \frac{1-\rho_f}{\rho_f}. \tag{64}$$

For $\rho \in (0,1]$ and $\rho_f = 0$, above result continues to hold if the left-hand side of (63) is replaced by the single term $\mathsf{S}^{(\mathsf{e})}$.

Proof: Choose

$$\mathcal{T}'_{\text{LLC}} = \{1,3,\ldots,K-1\} \tag{65a}$$

$$\mathcal{T}'_{\text{silent}} = \{c(\mathrm{D}+2)\}_{c=1}^{\lceil \frac{\ell}{\mathrm{D}+2}\rceil} \tag{65b}$$

$$\mathcal{T}'_{\text{eMBB}} = \mathcal{K}\backslash\mathcal{T}'_{\text{silent}}. \tag{65c}$$

Substituting this choice into (39) and (40) proves achievability of the pair $\mathsf{S}^{(\mathsf{L})} = \alpha\frac{\rho_f\rho}{2}$ and $\mathsf{S}^{(\mathsf{e})} = \alpha\frac{(1-\rho_f)\rho}{2} + (1-\alpha)\rho\frac{\mathrm{D}+1}{\mathrm{D}+2}$ for any $\alpha \in [0,1]$. The proposition is obtained by time-sharing the schemes for $\alpha = 0$ and $\alpha = 1$. ∎

2) Adaptive Scheme under Model 1*:* We again reuse the two LLC Tx sets $\mathcal{T}_{\text{LLC},1}$ and $\mathcal{T}_{\text{LLC},2}$ consisting of the odd and even indices from 1 and K, and in Phase i we schedule LLC transmissions only on the LLC Tx set $\mathcal{T}_{\text{LLC},i}$ but not on the other Txs. As in Subsection V-B4, we again have to silence all Txs that interfere on LLC transmissions because in our model Txs cannot cooperate. We then schedule in each of the resulting small subnets eMBB transmissions as in the generic, non-adaptive scheme. In Fig. 10 we show our proposed schedulings for the user activity and data arrival patterns in Fig. 10.a under the generic (Fig. 10.b and Fig. 10.c) and adaptive (Fig. 10.d and Fig. 10.e) schemes. We see that while the generic scheme only achieves a per-user MG pair of $(\mathsf{S}^{(\mathsf{L})} = 8/32, \mathsf{S}^{(\mathsf{e})} = 8/32)$, the adaptive scheme can achieve $(\mathsf{S}^{(\mathsf{L})} = 8/32, \mathsf{S}^{(\mathsf{e})} = 11/32)$.

Theorem 5 (Adaptive Scheme, Model 1): For $\rho \in (0,1)$ and $\rho_f \in (0,1]$, the fundamental MG region $\mathcal{S}_1^\star(\mathrm{D},\rho,\rho_f)$ of Model 1 includes all nonnegative pairs $(\mathsf{S}^{(\mathsf{L})},\ \mathsf{S}^{(\mathsf{e})})$ satisfying

$$\mathsf{S}^{(\mathsf{L})} \le \frac{\rho\rho_f}{2}, \tag{66}$$

$$\mathsf{S}^{(\mathsf{e})} + M_{\text{Rx},1}^{(\text{A})} \cdot \mathsf{S}^{(\mathsf{L})} \le \rho - \frac{(1-\rho)\rho^{\mathrm{D}+2}}{1-\rho^{\mathrm{D}+2}}, \tag{67}$$

where

$$\begin{aligned} M_{\text{Rx},1}^{(\text{A})} \triangleq\ & \frac{2}{\rho_f} - \frac{2(1-\rho)\rho^{\mathrm{D}+1}}{\rho_f(1-\rho^{\mathrm{D}+2})} + \frac{\rho^3\rho_f(1-\rho_f)}{(1-\rho^2(1-\rho_f)))}\left(\frac{2}{(1-\rho^2(1-\rho_f))} - \frac{\rho^{\mathrm{D}}(1-\rho_f)^{\frac{\mathrm{D}}{2}}}{1-\rho^{\mathrm{D}+2}(1-\rho_f)^{\frac{\mathrm{D}+2}{2}}}\right) \\ & - \frac{(1-\rho_f)(1-\rho(1-\rho_f))^2}{\rho_f(1-\rho^2(1-\rho_f))}\left(2\rho + 2\rho^2(1-\rho_f) + 1 - \frac{\rho^{\mathrm{D}+1}(1-\rho_f)^{\frac{\mathrm{D}}{2}}(1+\rho(1-\rho_f))}{(1-\rho^{\mathrm{D}+2}(1-\rho_f)^{\frac{\mathrm{D}+2}{2}})}\right) \\ & - \frac{(1-\rho)^2}{\rho_f(1-\rho^2(1-\rho_f))}\left(\frac{2\rho(1-\rho_f)}{(1-\rho^2(1-\rho_f))} + 1 - \frac{\rho^{\mathrm{D}+1}(1-\rho_f)^{\frac{\mathrm{D}+2}{2}}(1+\rho)}{(1-\rho^{\mathrm{D}+2}(1-\rho_f)^{\frac{\mathrm{D}+2}{2}})}\right). \end{aligned} \tag{68}$$

For $\rho \in (0,1)$ and $\rho_f = 0$, above result holds if the left-hand side of (67) is replaced by $\mathsf{S}^{(\mathsf{e})}$.

Proof: See Appendix D. ∎

Theorem 6 (Outer Bound, Model 1): For $\rho \in (0,1)$, all achievable MG pairs $(\mathsf{S}^{(\mathsf{L})},\ \mathsf{S}^{(\mathsf{e})})$ of Model 1 satisfy (66)

$$\mathsf{S}^{(\mathsf{e})} + \mathsf{S}^{(\mathsf{L})} \le \rho - \frac{(1-\rho)\rho^{\mathrm{D}+2}}{1-\rho^{\mathrm{D}+2}}. \tag{69}$$

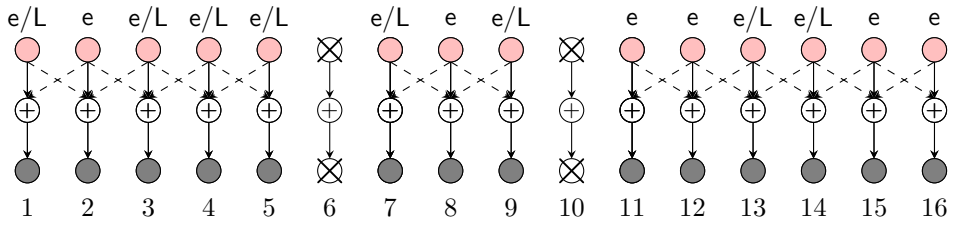

(a) User activity pattern

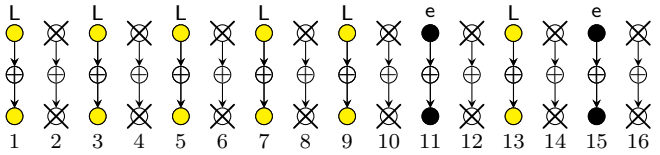

(b) Non-adaptive, Phase 1

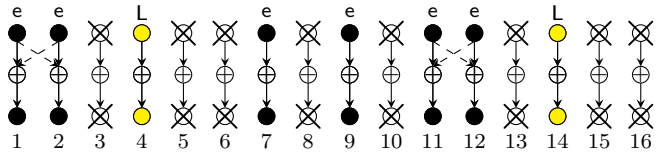

(c) Non-adaptive, Phase 2

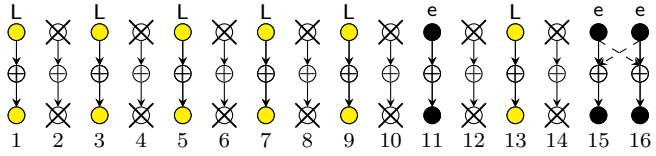

(d) Adaptive, Phase 1

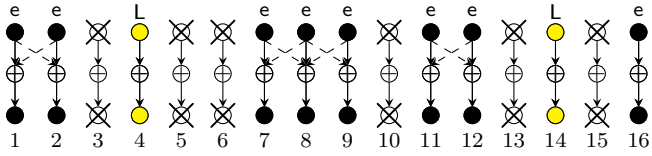

(e) Adaptive, Phase 2

Fig. 10: An illustration of the network and user activity pattern in Model 1 with only Rx-cooperation for $\mathrm{D} = 6$.

$$\mathsf{S}^{(\mathsf{e})} + (1+\rho)\mathsf{S}^{(\mathsf{L})} \leq \rho. \tag{70}$$

Proof: The bounds in (66) and (69) coincide with the bounds for Tx- and Rx-cooperation in Theorem 2 and can be proved in the same way. The bound in (69) is proved in Appendix D-C. ■

Our inner and outer bounds determine again the largest LLC and the largest eMBB per-user MGs. They are the same as under both Tx- and Rx-cooperation. Having only Rx-cooperation thus does not harm the individual largest per-user MGs. In contrast, the largest eMBB per-user MG that is achievable for $\mathsf{S}^{(\mathsf{L})} = \frac{\rho\rho_f}{2}$ is significantly deteriorated when only Rxs can cooperate. For example, in the extreme case $\mathrm{D} \to \infty$, with Tx- and Rx-cooperation $\mathsf{S}^{(\mathsf{e})} = \rho\left(1 - \frac{\rho\rho_f}{2}\right)$ is achievable when $\mathsf{S}^{(\mathsf{L})} = \frac{\rho\rho_f}{2}$. Our converse result in Theorem 6 indicates that in this case no eMBB per-user MG above $\rho\left(1 - (1+\rho)\frac{\rho\rho_f}{2}\right)$ is achievable. The reason for this degradation is that cancelling interference of eMBB transmissions on LLC transmissions requires Tx-cooperation and seems unfeasible otherwise. As a consequence, when Txs cannot cooperate, eMBB transmissions that would interfere LLC transmissions cannot be scheduled.

We next present our results under Model 2.

3) Non-Adaptive Scheme under Model 2: We have the following proposition on Non-Adaptive scheme under Model 2.

Proposition 4 (Non-Adaptive Scheme, Model 2): For $\rho \in (0,1]$ and $\rho_f \in (0,1]$, the fundamental MG region $\mathsf{S}_2^*(\mathrm{D}, \rho, \rho_f)$ includes all nonnegative pairs $(\mathsf{S}^{(\mathsf{L})}, \mathsf{S}^{(\mathsf{e})})$ satisfying

$$\mathsf{S}^{(\mathsf{L})} \leq \frac{\rho\rho_f}{2}, \tag{71}$$

$$\mathsf{S}^{(\mathsf{e})} + M_{\mathrm{Rx},2}^{(\mathrm{NA})} \cdot \mathsf{S}^{(\mathsf{L})} \leq \rho(1-\rho_f)\frac{\mathrm{D}+1}{\mathrm{D}+2}., \tag{72}$$

where

$$M_{\mathrm{Rx},2}^{(\mathrm{NA})} \triangleq \frac{1-\rho_f}{\rho_f} \cdot \frac{2(\mathrm{D}+1)}{\mathrm{D}+2}. \tag{73}$$

For $\rho \in (0,1]$ and $\rho_f = 1$ the same result holds if the left-hand side of (71) is replaced by the single term $\mathsf{S}^{(\mathsf{e})}$.

Proof: This result follows by substituting the choice (65) into (37) and (38). For $\alpha = 0$ this proves achievability of the pair $\mathsf{S}^{(\mathsf{L})} = 0$ and $\mathsf{S}^{(\mathsf{e})} = \rho(1-\rho_f)\frac{\mathrm{D}+1}{\mathrm{D}+2}$ and for $\alpha = 1$ achievability of the pair $\mathsf{S}^{(\mathsf{L})} = \frac{\rho\rho_f}{2}$ and $\mathsf{S}^{(\mathsf{e})} = \frac{\rho(1-\rho_f)}{2}$. The proposition then holds by time-sharing arguments. ■

4) Adaptive Scheme under Model 2: As under Model 1, but taking into account that users in $\mathcal{K}_{\mathrm{LLC}}$ cannot send eMBB messages, see also the adaptive scheme in Section V-B4. In Figs. 11(b) and 11(c) we show our proposed scheduling for the adaptive scheme under the user activity and data arrival patterns in Fig. 11(a). We see that the adaptive scheme can achieve $(\mathsf{S}^{(\mathsf{L})} = 5/32, \mathsf{S}^{(\mathsf{e})} = 14/32)$. Note that, in this case, the non-adaptive scheme is equivalent to the time-sharing scheme.

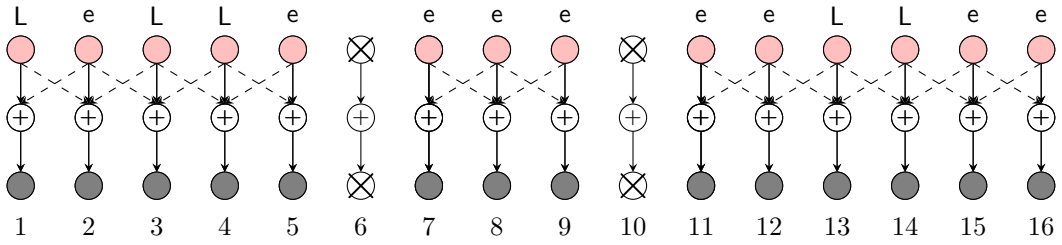

(a) User activity pattern

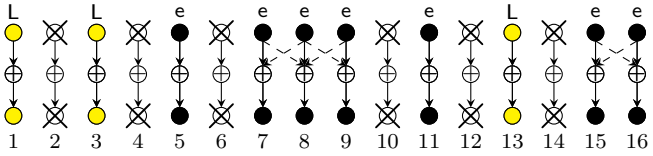

(b) Adaptive, Phase 1

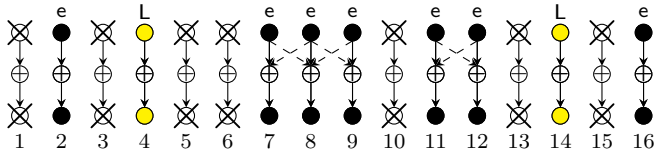

(c) Adaptive, Phase 2

Fig. 11: An illustration of the network and user activity pattern in Model 2 with only Rx-cooperation for $\mathrm{D}=6$.

Theorem 7 (Adaptive Scheme, Model 2): For $\rho \in (0,1)$ and $\rho_f \in (0,1]$, the fundamental MG region $\mathcal{S}_2^\star(\mathrm{D},\rho,\rho_f)$ includes all nonnegative pairs $(\mathsf{S}^{(\mathsf{L})},\ \mathsf{S}^{(\mathsf{e})})$ satisfying

$$\mathsf{S}^{(\mathsf{L})} \le \frac{\rho\rho_f}{2}, \tag{74}$$

$$\mathsf{S}^{(\mathsf{e})} + M_{\mathrm{Rx},2}^{(\mathrm{A})} \cdot \mathsf{S}^{(\mathsf{L})} \le \rho(1-\rho_f) - \frac{(1-\rho(1-\rho_f))\rho^{\mathrm{D}+2}(1-\rho_f)^{\mathrm{D}+2}}{1-\rho^{\mathrm{D}+2}(1-\rho_f)^{\mathrm{D}+2}}, \tag{75}$$

where

$$\begin{aligned} M_{\mathrm{Rx},2}^{(\mathrm{A})} \triangleq\ & \frac{2(1-\rho_f)}{\rho_f} - \frac{2(1-\rho(1-\rho_f))\rho^{\mathrm{D}+1}(1-\rho_f)^{\mathrm{D}+2}}{\rho_f(1-\rho^{\mathrm{D}+2}(1-\rho_f)^{\mathrm{D}+2})} \\ & + \frac{\rho^3\rho_f(1-\rho_f)^2}{(1-\rho^2(1-\rho_f)^2)}\left(\frac{2}{1-\rho^2(1-\rho_f)^2} - \frac{\rho^{\mathrm{D}}(1-\rho_f)^{\mathrm{D}}}{1-\rho^{\mathrm{D}+2}(1-\rho_f)^{\mathrm{D}+2}}\right) \\ & - \frac{(1-\rho_f)\left((1-\rho(1-\rho_f))^2+(1-\rho)^2\right)}{\rho_f(1-\rho(1-\rho_f))}\left(\frac{1}{1-\rho(1-\rho_f)} - \frac{\rho^{\mathrm{D}+1}(1-\rho_f)^{\mathrm{D}+1}}{1-\rho^{\mathrm{D}+2}(1-\rho_f)^{\mathrm{D}+2}}\right). \end{aligned} \tag{76}$$

For $\rho \in (0,1)$ and $\rho_f = 1$ the same result holds if the left-hand side of (75) is replaced by the single term $\mathsf{S}^{(\mathsf{e})}$.

Proof: See Appendix D. ∎

Theorem 8 (Outer Bound, Model 2): For $\rho \in (0,1)$, all achievable MG pairs $(\mathsf{S}^{(\mathsf{L})},\ \mathsf{S}^{(\mathsf{e})})$ of Model 2 satisfy (66) and the two bounds

$$\mathsf{S}^{(\mathsf{e})} \le \rho(1-\rho_f) - \frac{(1-\rho(1-\rho_f))\rho^{\mathrm{D}+2}(1-\rho_f)^{\mathrm{D}+2}}{1-\rho^{\mathrm{D}+2}(1-\rho_f)^{\mathrm{D}+2}}. \tag{77}$$

and

$$\mathsf{S}^{(\mathsf{e})} + \rho(1-\rho_f)\cdot\mathsf{S}^{(\mathsf{L})} \le \rho(1-\rho_f). \tag{78}$$

Proof: The bounds in (66) and (77) coincide with the bounds for Tx- and Rx-cooperation in Theorem 4 and can be proved in the same way. The bound in (78) is proved in Appendix D-F. ∎

Fig. 12 plots our inner and outer bounds on the fundamental per-user MG regions $\mathcal{S}_1^\star(\mathrm{D},\rho,\rho_f)$ and $\mathcal{S}_2^\star(\mathrm{D},\rho,\rho_f)$ for Rx-cooperation under both models and for $\rho=0.8$, $\rho_f=0.6$ and $\mathrm{D}=10$. As discussed above, the bounds show a significant degradation of the largest eMBB per-user MG that is simultaneously achievable as the LLC per-user MG $\mathsf{S}^{(\mathsf{L})} = \frac{\rho\rho_f}{2}$ compared to the case with both Tx- and Rx- cooperation.

VI. Hexagonal Network

A. Network Model and Cooperation

Consider a network with K hexagonal cells, where each cell consists of one single mobile user (MU) and one BS. The signals of users that lie in a given cell interfere with the signals sent in the 6 adjacent cells. The interference pattern of our

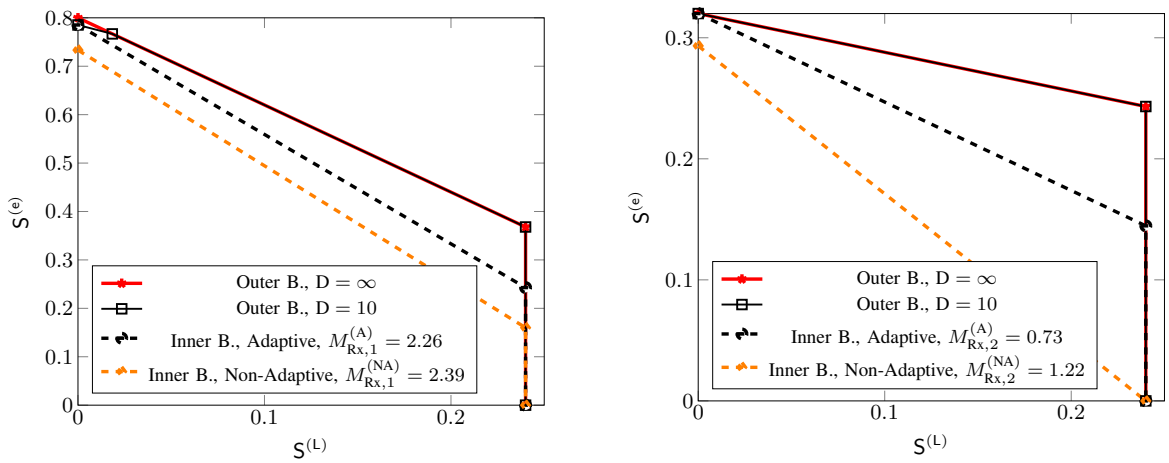

(a) Only Rx-cooperation, Model 1

(b) Only Rx-cooperation, Model 2

Fig. 12: Inner and outer bounds on the fundamental per-user MG regions $\mathcal{S}_1^\star(\mathrm{D},\rho,\rho_f)$ and $\mathcal{S}_2^\star(\mathrm{D},\rho,\rho_f)$ for $\rho = 0.8$ and $\rho_f = 0.6$, $\mathrm{D} = 10$ for Rx-cooperation only.

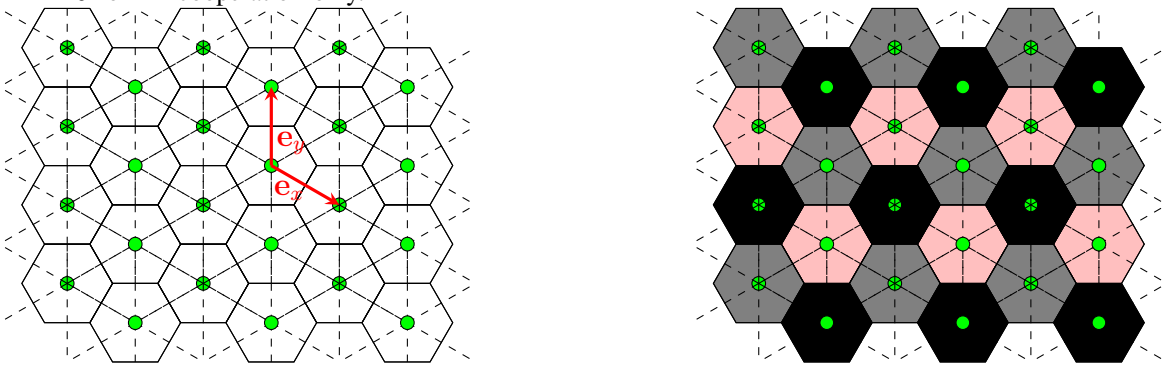

(a)

(b)

Fig. 13: An illustration of the hexagonal a) Small circles indicate Txs and Rxs, black solid lines the cell borders, and black dashed lines interference between cells. b) the Tx/Rx pairs in $\mathcal{K}_1$ are colored in gray, the Tx/Rx pairs in $\mathcal{K}_2$ in black and the Tx/Rxs in $\mathcal{K}_3$ in pink.

network is depicted by the black dashed lines in Fig. 13a, i.e., the interference set $\mathcal{I}_k$ contains the indices of the 6 neighboring cells whose signals interfere with cell k. Each Tx k and each Rx k can cooperate with the six Txs or Rxs in the adjacent cells, i.e., $|\mathcal{N}_k| = 6$.

To describe the setup and our schemes in detail, we parametrize the locations of the Tx/Rx pair in the k-th cell by a number o_k in the complex plane $\mathbb{C}$. Introducing the coordinate vectors

$$\mathbf{e}_x = \frac{\sqrt{3}}{2} - \frac{1}{2}i \quad \text{and} \quad \mathbf{e}_y = i, \tag{79}$$

as in Fig. 13a, the position o_k of Tx/Rx pair k is than associated with a pair of integers (a_k, b_k) satisfying

$$o_k \triangleq a_k \cdot \mathbf{e}_x + b_k \cdot \mathbf{e}_y. \tag{80}$$

The interference set $\mathcal{I}_k$ and the neighbour set $\mathcal{N}_k$ of Tx/Rx pair k can then be expressed as

$$\mathcal{N}_k = \mathcal{I}_k = \{k' : \quad |a_k - a_{k'}| = 1 \quad \text{and} \quad |b_k - b_{k'}| = 1 \quad \text{and} \quad |a_k - a_{k'} - b_k + b_{k'}| = 1\}. \tag{81}$$

For simplicity, in this section we assume

$$\mathrm{D} = \infty. \tag{82}$$

Similar results can be derived for finite number of cooperation round $\mathrm{D} < \infty$.

B. Results with both Tx- and Rx-Cooperation

Notice that when $\mathrm{D} \to \infty$ there is no difference between the adaptive and non-adaptive schemes we proposed in the previous section. In this section therefore we only propose a single achievability result under Tx- and Rx-cooperation based on a non-adaptive scheme.

Proposition 5 (Achievability Result, Model 1): For $\rho \in (0,1]$, the fundamental MG region $\mathcal{S}_1^\star(\mathrm{D}=\infty,\rho,\rho_f)$ for Model 1 includes all non-negative pairs $(\mathsf{S}^{(\mathsf{L})},\ \mathsf{S}^{(\mathsf{e})})$ satisfying

$$\mathsf{S}^{(\mathsf{L})} \le \frac{\rho\rho_f}{3}, \tag{83}$$

$$\mathsf{S}^{(\mathsf{e})} + \mathsf{S}^{(\mathsf{L})} \le \rho. \tag{84}$$

Proof: We partition $\mathcal{K}$ into three subsets $\mathcal{K}_1,\mathcal{K}_2,\mathcal{K}_3$ as in Figure 13b so that all the signals sent by Txs in a given subset $\mathcal{K}_i$ do not interfere with one another, i.e., for each $i\in\{1,2,3\}$:

$$k' \notin \mathcal{I}_{k''} \quad \text{and} \quad k'' \notin \mathcal{I}_{k'}, \quad \forall k',k'' \in \mathcal{K}_i. \tag{85}$$

Substituting for $i\in\{1,2,3\}$ the choice $\mathcal{T}_{\text{silent},i}=\emptyset$ and

$$\mathcal{T}_{\text{LLC},i} = \mathcal{K}_i \tag{86a}$$

$$\mathcal{T}_{\text{eMBB},i} = \mathcal{K}\backslash\mathcal{T}_{\text{LLC},i} \tag{86b}$$

into (30) and (31) proves the proposition. ∎

Proposition 6 (Achievability Result, Model 2): For $\rho \in (0,1]$, the fundamental MG region $\mathcal{S}_2^\star(\mathrm{D}=\infty,\rho,\rho_f)$ for Model 2 includes all nonnegative pairs $(\mathsf{S}^{(\mathsf{L})},\ \mathsf{S}^{(\mathsf{e})})$ satisfying

$$\mathsf{S}^{(\mathsf{L})} \le \frac{\rho\rho_f}{3}, \tag{87}$$

$$\mathsf{S}^{(\mathsf{e})} \le \rho(1-\rho_f). \tag{88}$$

Proof: We partition $\mathcal{K}$ into three subsets $\mathcal{K}_1,\mathcal{K}_2,\mathcal{K}_3$ as in Figure 13b so that all the signals sent by Txs in a given subset $\mathcal{K}_i$ do not interfere with one another, i.e., for each $i\in\{1,2,3\}$:

$$k' \notin \mathcal{I}_{k''} \quad \text{and} \quad k'' \notin \mathcal{I}_{k'}, \quad \forall k',k'' \in \mathcal{K}_i. \tag{89}$$

Substituting the choice (86) into (30) and (32) proves the proposition. ∎

C. Results with Only Rx-Cooperation

1) Non-Adaptive Scheme under Model 1: We have the following proposition on Non-Adaptive scheme under Model 1.

Proposition 7 (Non-Adaptive Scheme, Model 1): For $\rho \in (0,1]$, the fundamental MG region $\mathcal{S}_1^\star(\mathrm{D}=\infty,\rho,\rho_f)$ under Model 1 includes all nonnegative pairs $(\mathsf{S}^{(\mathsf{L})},\ \mathsf{S}^{(\mathsf{e})})$ satisfying

$$\mathsf{S}^{(\mathsf{L})} \le \frac{\rho\rho_f}{3}, \tag{90}$$

$$\mathsf{S}^{(\mathsf{e})} + L_{\text{Rx},1}^{(\text{NA})}\mathsf{S}^{(\mathsf{L})} \le \rho, \tag{91}$$

where

$$L_{\text{Rx},1}^{(\text{NA})} \triangleq \frac{2+\rho_f}{\rho_f}. \tag{92}$$

Proof: Substitute (86) into (39) and (40). ∎

2) Adaptive Scheme under Model 1: We reuse the sets $\mathcal{K}_1,\mathcal{K}_2$ and $\mathcal{K}_3$ as in Figure 13b and in phase i only assign LLC transmissions to users in $\mathcal{K}_i$. Then, we silence all interfering users, because in this setup without Tx-cooperation, interference on LLC messages cannot be canceled. In contrast to Wyner's symmetric network, here typically the network is not split into subnets, but still consist of a large network with an irregular shape. We then schedule eMBB messages on all active users because with Rx-cooperation over an infinite number of rounds we can cancel all interference on eMBB transmissions.

Theorem 9 (Adaptive Scheme, Model 1): For $\rho \in (0,1)$, the fundamental MG region $\mathcal{S}_1^\star(\mathrm{D}=\infty,\rho,\rho_f)$ of Model 1 includes all nonnegative pairs $(\mathsf{S}^{(\mathsf{L})},\ \mathsf{S}^{(\mathsf{e})})$ satisfying

$$\mathsf{S}^{(\mathsf{L})} \ \le \ \frac{\rho\rho_f}{3}, \tag{93}$$

$$\mathsf{S}^{(\mathsf{e})} + L_{\text{Rx},1}^{(\text{A})}\mathsf{S}^{(\mathsf{L})} \le \rho. \tag{94}$$

where

$$L_{\text{Rx},1}^{(\text{A})} \triangleq \frac{2+\rho_f-2(1-\rho\rho_f)^3}{\rho_f}. \tag{95}$$

Proof: See Appendix E-A and Appendix E-B. ∎

For Model 2 we have the following results.

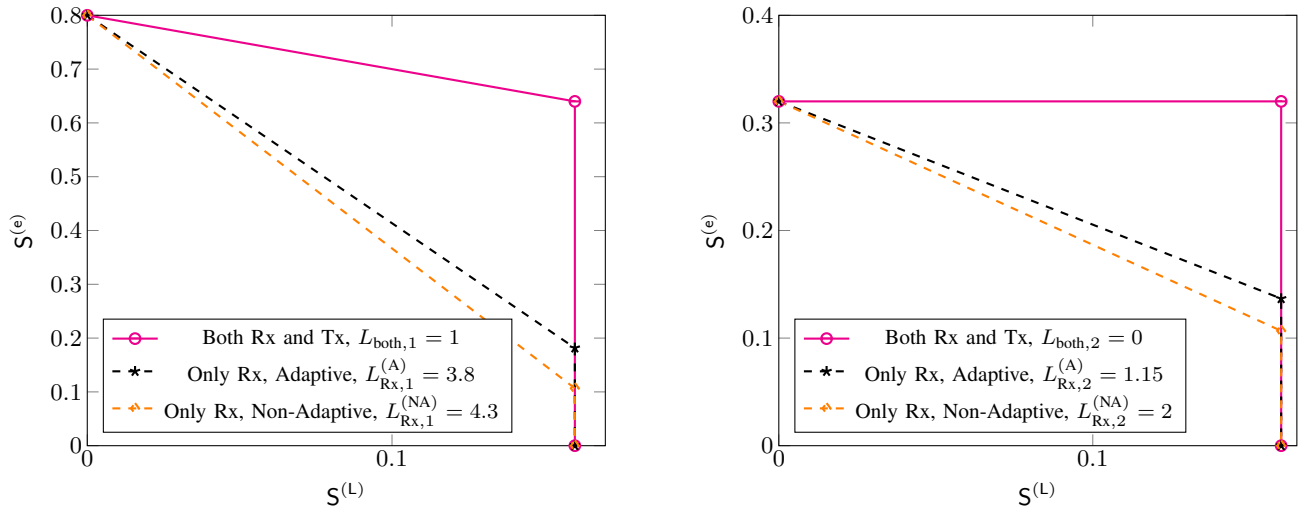

(a) Model 1

(b) Model 2

Fig. 14: Inner bounds on the fundamental per-user MG regions $\mathcal{S}_1^\star(\mathrm{D}=\infty,\rho,\rho_f)$ and $\mathcal{S}_2^\star(\mathrm{D}=\infty,\rho,\rho_f)$ under the two models for the hexagonal network with $\rho = 0.8$ and $\rho_f = 0.6$.

3) Non-Adaptive Scheme under Model 2: We have the following proposition on Non-Adaptive scheme under Model 2.

Proposition 8 (Non-Adaptive Scheme, Model 2): For $\rho \in (0,1]$, the fundamental MG region $\mathcal{S}_2^\star(\mathrm{D}=\infty,\rho,\rho_f)$ for Model 2 includes all nonnegative pairs $(\mathsf{S}^{(\mathsf{L})},\ \mathsf{S}^{(\mathsf{e})})$ satisfying

$$\mathsf{S}^{(\mathsf{L})} \le \frac{\rho\rho_f}{3}, \tag{96}$$

$$\mathsf{S}^{(\mathsf{e})} + L^{(\text{NA})}_{\text{Rx},2}\mathsf{S}^{(\mathsf{L})} \le \rho(1-\rho_f), \tag{97}$$

where

$$L^{(\text{NA})}_{\text{Rx},2} \triangleq \frac{2(1-\rho_f)}{\rho_f}. \tag{98}$$

Proof: Substitute (86) into (37) and (38). ■

4) Adaptive Scheme under Model 2: As under Model 1, we reuse the sets $\mathcal{K}_1, \mathcal{K}_2$ and $\mathcal{K}_3$ as in Figure 13b and in phase i only assign LLC transmissions to users in $\mathcal{K}_i$. Then, we silence all interfering users, because in this setup without Tx-cooperation, interference on LLC messages cannot be canceled. We then schedule eMBB messages only on active users that have eMBB messages.

Theorem 10 (Adaptive Scheme, Model 2): For $\rho \in (0,1)$, the fundamental MG region $\mathcal{S}_2^\star(\mathrm{D}=\infty,\rho,\rho_f)$ of Model 2 includes all nonnegative pairs $(\mathsf{S}^{(\mathsf{L})},\ \mathsf{S}^{(\mathsf{e})})$ satisfying

$$\mathsf{S}^{(\mathsf{L})} \le \frac{\rho\rho_f}{3}, \tag{99}$$

$$\mathsf{S}^{(\mathsf{e})} + L^{(\text{A})}_{\text{Rx},2}\mathsf{S}^{(\mathsf{L})} \le \rho(1-\rho_f). \tag{100}$$

where

$$L^{(\text{A})}_{\text{Rx},2} \triangleq \frac{2(1-\rho_f)(1-(1-\rho\rho_f)^3)}{\rho_f}. \tag{101}$$

Proof: See Appendix E-C and Appendix E-D. ■

Figures 14 and 15 illustrate the inner bounds on the MG region $\mathcal{S}_1^\star(\mathrm{D}=\infty,\rho,\rho_f)$ and $\mathcal{S}_2^\star(\mathrm{D}=\infty,\rho,\rho_f)$ for $\rho = 0.8$, $\rho_f = 0.6$ and $\rho_f = 0.1$. As can be seen from this figures, when both Txs and Rxs can cooperate, in Model 1, the sum per-user MG stays constant with the LLC per-user MG, and in Model 2, the sum per-user MG increases with the LLC per-user MG, and thus operating at large LLC per-user MG $\mathsf{S}^{(\mathsf{L})}$ does not penalize the achievable eMBB per-user MG $\mathsf{S}^{(\mathsf{e})}$. However, when only Rxs can cooperate, large LLC per-user MG $\mathsf{S}^{(\mathsf{L})}$ penalizes the achievable eMBB per-user MG $\mathsf{S}^{(\mathsf{e})}$ under both Model 1 and Model 2.

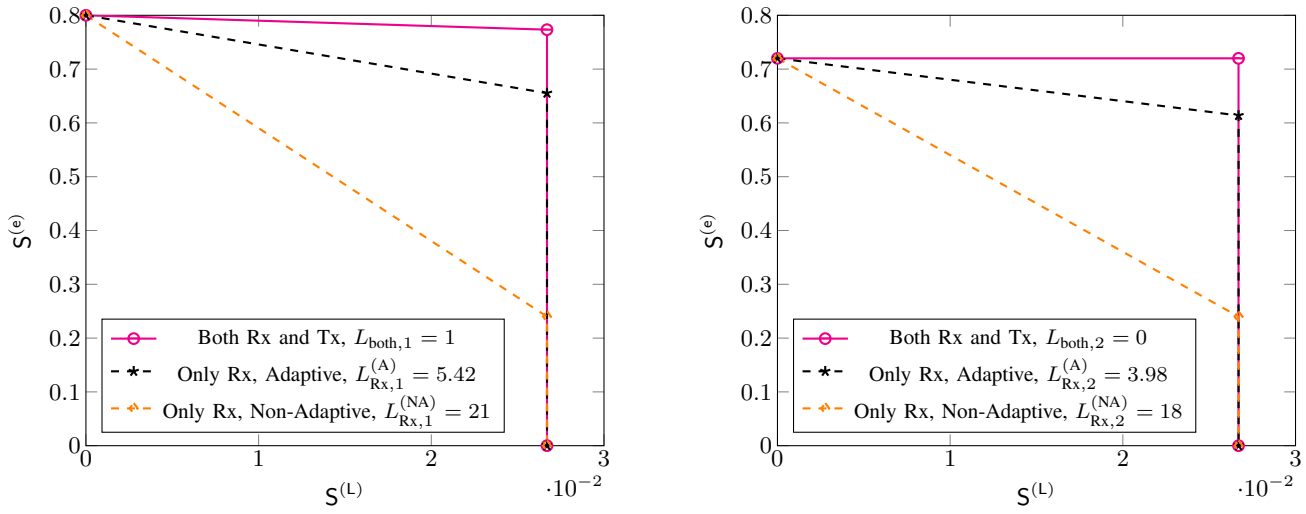

(a) Model 1

(b) Model 2

Fig. 15: Inner bounds on the fundamental per-user MG regions $\mathcal{S}_1^\star(\mathrm{D}=\infty,\rho,\rho_f)$ and $\mathcal{S}_2^\star(\mathrm{D}=\infty,\rho,\rho_f)$ under the two models for the hexagonal network with $\rho = 0.8$ and $\rho_f = 0.1$.

VII. Conclusions and Outlook

We have proposed and analyzed coding schemes to simultaneously transmit delay-sensitive and delay-tolerant traffic over interference networks with randomly activated users and random data arrivals in a setup with both Tx- and Rx-cooperation or with only Rx-cooperation. In both setups only delay-tolerant messages can benefit from Tx- or Rx-cooperation but not delay-sensitive messages. We further considered two user data arrival models. In Model 1 any active Tx has a delay-tolerant message to send and with probability ρ_f it has also a delay-sensitive message to send. In Model 2 a Tx only has a delay-tolerant message to send if it is active but has no delay-sensitive message to send.

We have derived inner and outer bounds on the per-user multiplexing gain (MG) region of the symmetric Wyner network for both setups and both models. Our bounds are tight in general and coincide in special cases. Moreover, they show that transmitting delay-sensitive data hardly penalizes the sum per-user MG (for Model 1) or the delay-tolerant per-user MG (for Model 2) as long as both Txs and Rxs can cooperate. This should in particular be considered in view of scheduling algorithms [48] where transmission of delay-sensitive data inherently causes a penalty on the sum-MG that is linear in the delay-sensitive and the sum per-user MG. We further observe that the influence of the number of cooperation rounds D vanishes with decreasing probability for a Tx to have a delay-tolerant message. In other words, for small ρ (under Model 1) or small $\rho(1-\rho_f)$ (under Model 2) a small number of cooperation rounds D allows the system to achieve the same performance as a larger number of rounds.

When only Rxs can cooperate, then the delay-tolerant per-user MG and the sum per-user MG degrade significantly for large delay-sensitive per-user MGs compared to the setup with both Tx- and Rx-cooperation. The reason is that Tx-cooperation seems required to cancel interference of delay-tolerant transmissions on delay-sensitive transmissions, without which the performance degrades. Notice that an analogous result can also be proved when only Txs but not the Rxs can cooperate, in which case the performance degradation comes from the fact that interference of delay-sensitive transmissions cannot be canceled at delay-sensitive Rxs.

We further have derived inner bounds on the MG region of the hexagonal model for both cooperation setups (Tx- and Rx-cooperation or only Rx-cooperation) and under both Models 1 and 2. The results have shown that when both Txs and Rxs can cooperate, in Model 1, the sum per-user MG stays constant with increasing delay-sensitive per-user MG and in Model 2, the delay-tolerant per-user MG remains constant while the sum per-user MG increases with increasing delay-sensitive per-user MG. As for the Wyner symmetric network, we observe that in our inner bounds, when only Rxs can cooperate, a large delay-sensitive per-user MG penalizes the achievable delay-sensitive per-user MG under both Models 1 and 2.

Future interesting research directions include the sectorized model studied in [49], [50]. We conjecture that also for the sectorized hexagonal model, a combination of Tx- and Rx-cooperation allows to mitigate most of the interference and essentially eliminate any penalty caused by transmission of large delay-sensitive data rates. Excellent interference cancellation performance is also expected for multi-antenna setups and more general networks [51]. Another interesting line of future research is to investigate the fundamental limits of this setup under imperfect channel state-information at the transmitters and receivers [52].

APPENDIX A
USEFUL SUMMATION FORMULAS

We start with the well-known formula for geometric sums. For any $d > 0$,

$$\sum_{\ell=0}^{K} d^{\ell} = \frac{1-d^{K+1}}{1-d}, \tag{102}$$

$$\sum_{\ell=0}^{K} \ell d^{\ell} = \frac{d(Kd^{K+1} - (K+1)d^{K} + 1)}{(d-1)^2} \tag{103}$$

Moreover, for any $c \in (0,1)$,

$$\sum_{\ell=1}^{\infty} \ell c^{\ell} = \frac{c}{(1-c)^2}, \tag{104}$$

$$\sum_{\ell=1}^{\infty} \ell^2 c^{\ell} = \frac{c(c+1)}{(1-c)^3}. \tag{105}$$

Since both sums converge we have,

$$\lim_{K\to\infty} \frac{1}{K} \sum_{\ell=1}^{K} \ell c^{\ell} = 0 \tag{106}$$

$$\tag{107}$$

and

$$\lim_{K\to\infty} \frac{1}{K} \sum_{\ell=1}^{K} \ell^2 c^{\ell} = 0. \tag{108}$$

We next prove that for any positive integers A, B so that B divides A and any $c \in [0,1)$ and $d \in [0,1]$,

$$\sum_{\ell=1}^{\infty} c^{\ell} \left\lfloor \frac{\ell}{A} \right\rfloor d^{\lfloor \frac{\ell}{B} \rfloor} = \frac{c^A d^{A/B}}{(1-c^A d^{A/B})(1-c^B d)} \cdot \frac{1-c^B}{1-c} \tag{109}$$

and

$$\sum_{\ell=1}^{\infty} c^{\ell} \left\lfloor \frac{\ell+1}{A} \right\rfloor d^{\lfloor \frac{\ell}{B} \rfloor} - \sum_{\ell=1}^{\infty} c^{\ell} \left\lfloor \frac{\ell}{A} \right\rfloor d^{\lfloor \frac{\ell}{B} \rfloor} = c^{A-1} d^{A/B-1} \frac{1}{1-c^A d^{A/B}}. \tag{110}$$

In particular, by specializing (109) and (110) to $d = 1$, we have that for any positive integer A and $c \in [0,1)$:

$$\sum_{\ell=1}^{\infty} c^{\ell} \left\lfloor \frac{\ell}{A} \right\rfloor = \frac{c^A}{(1-c^A)(1-c)}, \tag{111}$$

and

$$\sum_{\ell=1}^{\infty} c^{\ell} \left\lfloor \frac{\ell+1}{A} \right\rfloor - \sum_{\ell=1}^{\infty} c^{\ell} \left\lfloor \frac{\ell}{A} \right\rfloor = \frac{c^{A-1}}{(1-c^A)}. \tag{112}$$

Also, for any $A > 2$ and $B \geq 2$ so that B divides A and any $c \in [0,1)$ and $d \in [0,1]$,

$$\sum_{\ell=1}^{\infty} c^{\ell} \left\lfloor \frac{\ell}{A} \right\rfloor d^{\lceil \frac{\ell}{B} \rceil} = \frac{c^A d^{A/B}}{(1-c^A d^{A/B})} \left(1 + \frac{cd}{(1-c^B d)} \cdot \frac{1-c^B}{1-c} \right) \tag{113}$$

and

$$\sum_{\ell=1}^{\infty} c^{\ell} \left\lfloor \frac{\ell+1}{A} \right\rfloor d^{\lceil \frac{\ell}{B} \rceil} - \sum_{\ell=1}^{\infty} c^{\ell} \left\lfloor \frac{\ell}{A} \right\rfloor d^{\lceil \frac{\ell}{B} \rceil} = c^{A-1} d^{A/B} \frac{1}{1-c^A d^{A/B}}. \tag{114}$$

Similarly, for $B \geq 2$ and $c \in [0,1)$ and $d \in [0,1]$,

$$\sum_{\ell=1}^{\infty} c^{\ell} \ell d^{\lceil \frac{\ell}{B} \rceil} = \tag{115}$$

To prove (109), represent the summation index as

$$\ell = \left\lfloor \frac{\ell}{A} \right\rfloor A + \left\lfloor \frac{i}{B} \right\rfloor B + k, \tag{116}$$

for $i = \ell \mod A$, which lies in $i \in \{0, 1, \ldots, A-1\}$, and $k = \ell \mod B$, which lies in $\{0, 1, \ldots, B-1\}$. We can then write

$$\sum_{\ell=1}^{\infty} c^{\ell} \left\lfloor \frac{\ell}{A} \right\rfloor d^{\lfloor \frac{\ell}{B} \rfloor} = \sum_{j=1}^{\infty} \sum_{f=0}^{\frac{A}{B}-1} \sum_{k=0}^{B-1} c^{jA+fB+k} \cdot j \cdot d^{jA/B+f} \tag{117}$$

$$= \sum_{j=1}^{\infty} j \left(c^A d^{A/B}\right)^j \cdot \sum_{f=0}^{\frac{A}{B}-1} \left(c^B d\right)^f \cdot \sum_{k=0}^{B-1} c^k \tag{118}$$

$$= \frac{c^A d^{A/B}}{(1-c^A d^{A/B})^2} \cdot \frac{1-c^A d^{A/B}}{1-c^B d} \cdot \frac{1-c^B}{1-c} \tag{119}$$

$$= \frac{c^A d^{A/B}}{(1-c^A d^{A/B})(1-c^B d)} \cdot \frac{1-c^B}{1-c}, \tag{120}$$

which proves (109).

To prove (110), we notice that the two sums in (110) only differ in the terms $\ell = A - 1 + iA$ for all indices $i = 0, 1, \ldots$. In fact, we have

$$\sum_{\ell=1}^{\infty} c^{\ell} \left\lfloor \frac{\ell+1}{A} \right\rfloor d^{\lfloor \frac{\ell}{B} \rfloor} - \sum_{\ell=1}^{\infty} c^{\ell} \left\lfloor \frac{\ell}{A} \right\rfloor d^{\lfloor \frac{\ell}{B} \rfloor} = \sum_{\substack{\ell = A-1+iA \\ i \in \{0,1,\ldots\}}} c^{\ell} d^{\lfloor \frac{\ell}{B} \rfloor} \tag{121}$$

$$= \sum_{i=0}^{\infty} c^{A-1} \left(c^A\right)^i d^{\frac{A}{B}-1} \left(d^{A/B}\right)^i \tag{122}$$

$$= c^{A-1} d^{\frac{A}{B}-1} \sum_{i=0}^{\infty} \left(c^A d^{A/B}\right)^i \tag{123}$$

$$= \frac{c^{A-1} d^{\frac{A}{B}-1}}{1-c^A d^{A/B}}. \tag{124}$$

To prove (113), we use the fact that $\lceil \frac{\ell}{B} \rceil = \lfloor \frac{\ell-1}{B} \rfloor + 1$ which results in

$$\sum_{\ell=1}^{\infty} c^{\ell} \left\lfloor \frac{\ell}{A} \right\rfloor d^{\lceil \frac{\ell}{B} \rceil} = d \sum_{\ell=1}^{\infty} c^{\ell} \left\lfloor \frac{\ell}{A} \right\rfloor d^{\lfloor \frac{\ell-1}{B} \rfloor} \tag{125}$$

$$\overset{(i)}{=} d \sum_{\ell'=0}^{\infty} c^{\ell'+1} \left\lfloor \frac{\ell'+1}{A} \right\rfloor d^{\lfloor \frac{\ell'}{B} \rfloor} \tag{126}$$

$$\overset{(ii)}{=} dc \sum_{\ell'=1}^{\infty} c^{\ell'} \left\lfloor \frac{\ell'+1}{A} \right\rfloor d^{\lfloor \frac{\ell'}{B} \rfloor} \tag{127}$$

$$\overset{(iii)}{=} \frac{c^A d^{A/B}}{(1-c^A d^{A/B})} \left(1 + \frac{cd}{(1-c^B d)} \cdot \frac{1-c^B}{1-c}\right) \tag{128}$$

where (i) is obtained by setting $\ell' = \ell - 1$; step (ii) holds because $\left\lfloor \frac{\ell'+1}{A} \right\rfloor = 0$ when $A > 2$; and step (iii) holds by (109) and (110).

$$\sum_{\ell=1}^{\infty} c^{\ell} \left\lfloor \frac{\ell+1}{A} \right\rfloor d^{\lceil \frac{\ell}{B} \rceil} - \sum_{\ell=1}^{\infty} c^{\ell} \left\lfloor \frac{\ell}{A} \right\rfloor d^{\lceil \frac{\ell}{B} \rceil}$$

$$= \sum_{\ell=1}^{\infty} c^{\ell} \left\lfloor \frac{\ell+1}{A} \right\rfloor d^{\lfloor \frac{\ell-1}{B} \rfloor + 1} - \sum_{\ell=1}^{\infty} c^{\ell} \left\lfloor \frac{\ell}{A} \right\rfloor d^{\lfloor \frac{\ell-1}{B} \rfloor + 1} \tag{129}$$

$$= cd \left(\sum_{\ell'=1}^{\infty} c^{\ell'} \left\lfloor \frac{\ell'+2}{A} \right\rfloor d^{\lfloor \frac{\ell'}{B} \rfloor} - \sum_{\ell'=1}^{\infty} c^{\ell'} \left\lfloor \frac{\ell'+1}{A} \right\rfloor d^{\lfloor \frac{\ell'}{B} \rfloor} \right). \tag{130}$$

$$\tag{131}$$

Since the two sums in the above equation only differ in the terms $\ell' = A - 2 + iA$ for all indices $i = 0, 1, \ldots$, similarly to the proof of (110) we have

$$cd \left(\sum_{\ell'=1}^{\infty} c^{\ell'} \left\lfloor \frac{\ell'+2}{A} \right\rfloor d^{\lfloor \frac{\ell'}{B} \rfloor} - \sum_{\ell'=1}^{\infty} c^{\ell'} \left\lfloor \frac{\ell'+1}{A} \right\rfloor d^{\lfloor \frac{\ell'}{B} \rfloor} \right) = cd \sum_{\substack{\ell' = A-2+iA \\ i \in \{0,1,\ldots\}}} c^{\ell'} d^{\lfloor \frac{\ell'}{B} \rfloor} \tag{132}$$

$$= cd \sum_{i=0}^{\infty} c^{A-2} \left(c^A\right)^i d^{\frac{A}{B}-1} \left(d^{A/B}\right)^i \tag{133}$$

$$= c^{A-1} d^{\frac{A}{B}} \sum_{i=0}^{\infty} \left(c^A d^{A/B}\right)^i \tag{134}$$

$$= \frac{c^{A-1} d^{\frac{A}{B}}}{1 - c^A d^{A/B}}, \tag{135}$$

which proves (114).

Notice next that for any positive B and any $c \in [0,1)$ and $d \in [0,1]$,

$$\sum_{\ell=1}^{\infty} c^\ell \ell d^{\lfloor \frac{\ell}{B} \rfloor} = \frac{Bc^B d}{(1-c^B d)^2} \cdot \frac{1-c^B}{1-c} + \frac{(B-1)c^{B+1} - Bc^B + c}{(1-c^B d)(c-1)^2}, \tag{136}$$

which is proved as follows. Represent the summation index as

$$\ell = \left\lfloor \frac{\ell}{B} \right\rfloor B + k \tag{137}$$

for $k = \ell \mod B$, which lies in $\{0, 1, \ldots, B-1\}$. We then write

$$\sum_{\ell=1}^{\infty} c^\ell \ell d^{\lfloor \frac{\ell}{B} \rfloor} = \sum_{j=1}^{\infty} \sum_{k=0}^{B-1} c^{jB+k} \cdot (jB+k) \cdot d^j \tag{138}$$

$$= B \sum_{j=1}^{\infty} \sum_{k=0}^{B-1} c^{jB+k} \cdot j \cdot d^j + \sum_{j=1}^{\infty} \sum_{k=0}^{B-1} k \cdot c^{jB+k} \cdot d^j \tag{139}$$

$$= B \sum_{j=1}^{\infty} j (c^B d)^j \sum_{k=0}^{B-1} c^k + \sum_{j=1}^{\infty} (c^B d)^j \sum_{k=0}^{B-1} k \cdot c^k \tag{140}$$

$$= \frac{Bc^B d}{(1-c^B d)^2} \cdot \frac{1-c^B}{1-c} + \frac{(B-1)c^{B+1} - Bc^B + c}{(1-c^B d)(c-1)^2} \tag{141}$$

which proves (136).

We conclude this appendix with a few summation formulas that can be proved similarly to the above proofs. Notice that:

$$\sum_{\ell=1}^{\infty} c^\ell \left\lfloor \frac{\ell}{A} \right\rfloor d^{\lfloor \frac{\ell}{B} \rfloor} \mathbb{1}\{\ell \text{ is even }\} = \frac{c^A d^{A/B}}{(1-c^A d^{A/B})(1-c^B d)} \cdot \frac{1-c^B}{1-c^2}, \tag{142}$$

$$\sum_{\ell=1}^{\infty} c^\ell \ell d^{\lfloor \frac{\ell}{B} \rfloor} \mathbb{1}\{\ell \text{ is even }\} = \frac{Bc^B d}{(1-c^B d)^2} \cdot \frac{1-c^B}{1-c^2} + \frac{(B-2)c^{B+2} - Bc^B + 2c^2}{2(1-c^B d)(c^2-1)^2}. \tag{143}$$

For even values of A and B an integer divisor of A, we further have

$$\sum_{\ell=1}^{\infty} c^\ell \left\lfloor \frac{\ell+1}{A} \right\rfloor d^{\lfloor \frac{\ell}{B} \rfloor} \mathbb{1}\{\ell \text{ is even }\} - \sum_{\ell=1}^{\infty} c^\ell \left\lfloor \frac{\ell}{A} \right\rfloor d^{\lfloor \frac{\ell}{B} \rfloor} \mathbb{1}\{\ell \text{ is even }\} = 0. \tag{144}$$

Finally, notice that $\lceil \frac{\ell}{2} \rceil + \lfloor \frac{\ell}{2} \rfloor = \ell$ and $d^{\lceil \frac{\ell}{2} \rceil} = d^\ell \cdot \frac{1}{d}^{\lfloor \frac{\ell}{2} \rfloor}$. Replacing in (109), (110), and (136), the parameter c by cd, the parameter d by d^{-1}, and B by 2, we obtain that for any even A

$$\sum_{\ell=1}^{\infty} c^\ell \left\lfloor \frac{\ell}{A} \right\rfloor d^{\lceil \frac{\ell}{2} \rceil} = \frac{c^A d^{A/2}(1+cd)}{(1-c^A d^{A/2})(1-c^2 d)}, \tag{145}$$

$$\sum_{\ell=1}^{\infty} c^\ell \ell d^{\lceil \frac{\ell}{2} \rceil} = \frac{cd(2c + c^2 d + 1)}{(1-c^2 d)^2}, \tag{146}$$

$$\sum_{\ell=1}^{\infty} c^\ell \left\lfloor \frac{\ell+1}{A} \right\rfloor d^{\lceil \frac{\ell}{2} \rceil} - \sum_{\ell=1}^{\infty} c^\ell \left\lfloor \frac{\ell}{A} \right\rfloor d^{\lceil \frac{\ell}{2} \rceil} = c^{A-1} d^{A/2} \frac{1}{1-c^A d^{A/2}}. \tag{147}$$

APPENDIX B
PROOFS OF THEOREMS 1 AND 2

A. MG results with chosen message assignments

In this subsection, we characterize total MG pairs that are achievable over Wyner's symmetric network for *chosen* message assignments. These results will be used in the next-following sections to derive achievable per-user MG pairs under the *random* message-arrival models 1 and 2. For ease of readability of future sections, we denote the number of users in a subnet by ℓ.

In all our schemes LLC messages are only sent by non-consecutive Txs. We thus will make this assumption without further mentioning it in the titles of the sections.

1) Sending eMBB messages at Txs $2, D, D+4, 2D+2, 2D+6, 3D+4, \ldots$: We will start with an example of the message assignment. Choose $\mathcal{T}_{\text{LLC}}$ as the set of odd integers

$$\mathcal{T}_{\text{LLC}} \subseteq \{1, 3, 5, \ldots\}, \tag{148}$$

and silence Tx/Rx pairs

$$\mathcal{T}_{\text{silent}} \triangleq \big\{c(\mathrm{D}+2)\big\}_{c=0}^{\lfloor \frac{\ell}{\mathrm{D}+2} \rfloor}. \tag{149}$$

Choose the set of eMBB Txs as

$$\mathcal{T}_{\text{eMBB}} = \mathcal{K} \backslash \left(\mathcal{T}_{\text{silent}} \cup \mathcal{T}_{\text{LLC}}\right). \tag{150}$$

It can be verified that with this selection no adjacent Txs send LLC messages and the network is split into subnets, so that in each subnet there is a master Rx (namely Rx $(c+\frac{1}{2})\mathrm{D}$ for some integer $c \in \{0, 1, \ldots, \lceil \frac{\ell}{\mathrm{D}+2} \rceil - 1\}$) that can be reached by any other eMBB Rx in the same subnet in $\mathrm{D}/2 - 1$ cooperation hops. Our assignment (148)–(150) thus satisfies conditions C1 and C2 in Subsection III-A. By (25), the proposed message assignment thus allows to achieve a total sum MG of

$$\mathsf{M}_{\text{sum,full}}(\ell) \triangleq \ell - \left\lfloor \frac{\ell}{\mathrm{D}+2} \right\rfloor. \tag{151}$$

Since every second Tx sends a LLC message, the total LLC MG is

$$\mathsf{M}_{\text{LLC}}(\ell) = \left\lceil \frac{\ell}{2} \right\rceil. \tag{152}$$

Remark 3: The proposed scheme can easily be adapted to any other LLC Tx-set $\mathcal{T}_{\text{LLC}}$ that contains no two successive indices and that for any $c = 0, \ldots, \lfloor \frac{\ell}{\mathrm{D}+2} \rfloor$ satisfies[2]

$$c(\mathrm{D}+2)+2, c(\mathrm{D}+2)+\mathrm{D} \notin \mathcal{T}_{\text{LLC}}, \tag{153}$$

while the definitions in (149) and (150) are mantained. The scheme in Subsection III-A only needs to be adapted in the sense that in any subnet c the Txs $c(\mathrm{D}+2)+1, c(\mathrm{D}+2)+\mathrm{D}+1$ should act as LLC Txs even in case they are transmitting eMBB messages. This is possible by our assumption (153) that the neighbors of these Txs have eMBB messages to send. The same total sum MG is attained as before, i.e., (151). The total LLC MG is simply

$$\mathsf{M}_{\text{LLC,set}}(\ell) \triangleq |\mathcal{T}_{\text{LLC}}|. \tag{154}$$

2) Sending an eMBB message at Tx 2 or at Tx $D-1$ on a subnet of size $\ell \leq D$: In this case, no Tx has to be silenced, i.e., we choose

$$\mathcal{T}_{\text{silent}} \triangleq \emptyset, \tag{155}$$

and we can achieve a total sum-MG of $\mathsf{M}_{\text{sum,full}}(\ell) = \ell$.

Moreover, by assumption there are no consecutive LLC Txs. The key idea is to treat either Tx 1 or Tx D as a LLC Tx, irrespective of whether they have LLC or eMBB messages to transmit. Specifically, if $2 \in \mathcal{T}_{\text{eMBB}}$ we treat Tx 1 as if it was sending a LLC message and if $\mathrm{D}-1 \in \mathcal{T}_{\text{eMBB}}$ we treat Tx D as if it were sending a LLC message. We can then run the scheme in Subsection III-A because conditions C1 and C2 are satisfied. In particular, if $2 \in \mathcal{T}_{\text{eMBB}}$, then Rx $\frac{\mathrm{D}}{2}+1$ can act as a master Rx that jointly decodes all eMBB messages of Txs $2, \ldots, \ell$. (Recall that in this case Tx 1 acts as a LLC Tx even it has an eMBB message to send). If $\ell < \mathrm{D}$ or $\mathrm{D}-1 \in \mathcal{T}_{\text{eMBB}}$, then Rx $\frac{\mathrm{D}}{2}$ can act as a master Rx that jointly decodes all eMBB messages of Txs $1, \ldots, \min\{\ell, \mathrm{D}-1\}$. (Recall that in this case if Tx D exists, it acts as a LLC Tx, even if it has an eMBB message to send.)

[2]If Condition (153) is violated, then the scheme in Subsection III-A does require an extra cooperation round, thus violating the condition on D. For this reason, we propose a second scheme for a different message assignment in the next Subsection B-A2.

B. Achievability Result for $\mathsf{S}^{(\mathsf{L})} = 0$ under Model 1

In Wyner's symmetric network, the random user activity cuts the network into smaller non-interfering subnets. The total eMBB MG of the network is then simply the sum of the eMBB MGs achieved in the various subnets. Moreover, since in each subnet we send only eMBB messages, we are in the situation of Subsection B-A1, and the total eMBB MG is given by (151). We can then compute the expected per-user eMBB MG over the entire network as

$$\mathsf{S}^{(\mathsf{e})} = \varlimsup_{K\to\infty} \frac{1}{K} \sum_{k=1}^{K} \sum_{\ell=1}^{K-k+1} P_{\ell,k} \cdot \mathsf{M}_{\text{sum,full}}(\ell) \tag{156}$$

$$= \varlimsup_{K\to\infty} \frac{1}{K} \sum_{\ell=1}^{K} \sum_{k=1}^{K-\ell+1} P_{\ell,k} \cdot \mathsf{M}_{\text{sum,full}}(\ell), \tag{157}$$

where $P_{\ell,k}$ denotes the probability that a new subnet starts at user k and is of size ℓ, which equals

$$P_{\ell,k} = \begin{cases} \rho^{\ell}(1-\rho)^2 & \ell < K-k+1,\ k \geq 2 \\ \rho^{\ell}(1-\rho) & (\ell = K-k+1,\ k \geq 2) \\ & \text{or } (\ell < K-k+1,\ k=1) \\ \rho^{K} & k=1,\ \ell = K \end{cases}. \tag{158}$$

Plugging (158) into (157), we obtain

$$\mathsf{S}^{(\mathsf{e})} = \varlimsup_{K\to\infty} \left[\frac{1}{K} \sum_{\ell=1}^{K-1} \rho^{\ell}(1-\rho) \left((K-\ell-1)(1-\rho)+2 \right) \mathsf{M}_{\text{sum,full}}(\ell) + \frac{\rho^K}{K} \cdot \mathsf{M}_{\text{sum,full}}(K) \right]. \tag{159}$$

In the remainder of this subsection, we analyze the asymptotic behavior of the expression in (159), where recall that $\rho \in (0,1)$.

We observe the trivial bound

$$\mathsf{M}_{\text{sum,full}}(\ell) \leq \ell, \tag{160}$$

and thus since $\rho^K \to 0$ as $K \to \infty$ when $\rho \in (0,1)$, the last term in (159) vanishes as $K \to \infty$, i.e.,

$$\lim_{K\to\infty} \frac{\rho^K}{K} \cdot \left(K - \left\lfloor \frac{K}{\mathrm{D}+2} \right\rfloor \right) = 0. \tag{161}$$

The trivial bound in (160) also implies

$$0 \leq \sum_{\ell=1}^{K-1} \rho^{\ell}(1-\rho)^2(\ell+1)\mathsf{M}_{\text{sum,full}}(\ell) \leq \sum_{\ell=1}^{K-1} \rho^{\ell}(1-\rho)^2(\ell^2+\ell) \tag{162a}$$

$$0 \leq \sum_{\ell=1}^{K-1} 2\rho^{\ell}(1-\rho)\mathsf{M}_{\text{sum,full}}(\ell) \leq \sum_{\ell=1}^{K-1} 2\rho^{\ell}(1-\rho)\ell, \tag{162b}$$

and since the sums on the right-hand sides of (162) converge, see (106) and (108), the following limit holds:

$$\lim_{K\to\infty} \frac{1}{K} \sum_{\ell=1}^{K-1} \rho^{\ell}(1-\rho) \left((-\ell-1)(1-\rho)+2 \right) \cdot \mathsf{M}_{\text{sum,full}}(\ell) = 0. \tag{163}$$

Plugging Limits (161) and (163) into (159), we obtain an eMBB per-user MG of

$$\mathsf{S}^{(\mathsf{e})} = \varlimsup_{K\to\infty} \frac{1}{K} \sum_{\ell=1}^{K-1} K\rho^{\ell}(1-\rho)^2 \mathsf{M}_{\text{sum,full}}(\ell) = \sum_{\ell=1}^{\infty} \rho^{\ell}(1-\rho)^2 \left(\ell - \left\lfloor \frac{\ell}{\mathrm{D}+2} \right\rfloor \right) \tag{164}$$

$$= \rho - \frac{(1-\rho)\rho^{\mathrm{D}+2}}{1-\rho^{\mathrm{D}+2}}, \tag{165}$$

where the last equation holds by (105) and (111).

C. Converse Bound under Model 1

The steps described in the previous section can also be used to derive a converse bound on $\mathsf{S}^{(\mathsf{L})}+\mathsf{S}^{(\mathsf{e})}$ that holds for all achievable MG pairs. In fact, $\mathsf{M}_{\text{Sum,full}}$ also represents an upper bound on the total MG of any subnet of length ℓ. Following the same arguments as above but where we replace $\mathsf{S}^{(\mathsf{e})}$ by $\mathsf{S}^{(\mathsf{L})}+\mathsf{S}^{(\mathsf{e})}$, we obtain the upper bound

$$\mathsf{S}^{(\mathsf{L})}+\mathsf{S}^{(\mathsf{e})} \leq \rho - \frac{(1-\rho)\rho^{\mathrm{D}+2}}{1-\rho^{\mathrm{D}+2}}. \tag{166}$$

Combined with the trivial bound

$$\mathsf{S}^{(\mathsf{L})} \leq \frac{\rho\rho_f}{2}, \tag{167}$$

this proves Theorem 2 for $\rho \in (0,1)$.

For $\rho = 1$ the sum-rate bound follows from the findings in [47], which assumes that all Txs are eMBB.

D. Achievability Result for Large $\mathsf{S}^{(\mathsf{L})}$ under Model 1

As before, the user activity pattern $\mathbf{A}$ splits the network into multiple disjoint subnets. To ensure that each LLC message can be transmitted at same rate, we split the blocklength into two equally-long phases and time-share two schemes over the two phases. In Phase 1 we only send LLC messages on odd Txs and in Phase 2 only from even Txs.

Setting

$$\mathcal{K}_1 \triangleq \{1,3,\ldots,K-1\}, \tag{168}$$

$$\mathcal{K}_2 \triangleq \{2,4,\ldots,K\}, \tag{169}$$

in Phase 1 we choose

$$\mathcal{T}_{\text{LLC},1} \triangleq \mathcal{K}_1 \cap \mathcal{K}_{\text{LLC}} \tag{170}$$

and in Phase 2

$$\mathcal{T}_{\text{LLC},2} \triangleq \mathcal{K}_2 \cap \mathcal{K}_{\text{LLC}}. \tag{171}$$

The LLC message assignments in both phases satisfy the condition that no two consecutive Txs send LLC messages and are thus valid. In each of the phases, and for each of the subnets created by deactivated users, we can use one of the two schemes in Subsections B-A1 or B-A2, depending on the phase and the LLC user activity pattern in the subnet. In particular, for a subnet that starts at user k and is of length ℓ, in Phase $i \in \{1,2\}$ we use:

- If $k \in \mathcal{K}_i$ or if $k+(c-1)(\mathrm{D}+2)+1, k+c(\mathrm{D}+2)-3 \in \mathcal{K}_{\text{eMBB}}$ for all $c = 1,\ldots,\left\lceil \frac{\ell}{\mathrm{D}+2} \right\rceil$, then we use the scheme in Subsection B-A1 and achieve a total sum-MG of $\mathsf{M}_{\text{sum,full}}(\ell)$.
- Else if $\ell \leq \mathrm{D}$, we use the scheme described in Subsection B-A2 to transmit. Notice that the way that we defined the LLC Tx-sets $\mathcal{T}_{\text{LLC},i}$ in (170) and (171) and since $k \notin \mathcal{K}_i$ and D even, Tx $k+\mathrm{D}-2$ (if $\ell \geq \mathrm{D}-1$) sends an eMBB message and we satisfy the condition of Subsection B-A2. In this case, we again achieve a total sum-MG of $\mathsf{M}_{\text{sum,full}}(\ell)$ over the entire network.
- Else, we desactivate user $k+\mathrm{D}$, use the scheme in Subsection B-A2 to transmit on the subnet consisting of the first D Tx-Rx pairs $k, k+1, \ldots, k+\mathrm{D}-1$ and the scheme in Subsection B-A1 to transmit on the subnet consisting of the Tx-Rx pairs $k+\mathrm{D}+1,\ldots,k+\ell-1$ (where we notice that for this latter subnet Condition (153) is satisfied in Phase i because $k \notin \mathcal{K}_i$ and therefore also $k+c(\mathrm{D}+2), k+c(\mathrm{D}+2)+\mathrm{D} \notin \mathcal{T}_{\text{LLC},i}$ for all positive integers c). In this case, since we silenced Tx $k+\mathrm{D}$ (instead of $k+\mathrm{D}+1$), our scheme achieves at total sum-MG of

$$\mathsf{M}_{\text{sum,red}}(\ell) \triangleq \ell - \left\lfloor \frac{\ell+1}{\mathrm{D}+2} \right\rfloor. \tag{172}$$

As previously, the overall scheme achieves a per-user LLC MG of

$$\mathsf{S}^{(\mathsf{L})} = \frac{\rho\rho_f}{2}. \tag{173}$$

Moreover, by above considerations, in any subnet that starts at Tx k and is of size $\ell > \mathrm{D}$, the following expected sum MG is achievable over the two phases:

$$\bar{\mathsf{M}}_{\text{sum}}(\ell) \triangleq \frac{1}{2}\mathsf{M}_{\text{sum,full}}(\ell) + \frac{1}{2}\mathsf{M}_{\text{sum,full}}(\ell) \cdot \prod_{j\in\mathcal{L}} \mathbb{P}[B_j=1] + \frac{1}{2}\mathsf{M}_{\text{sum,red}}(\ell) \cdot \left(1 - \prod_{j\in\mathcal{L}_k} \mathbb{P}[B_j=1]\right) \tag{174}$$

$$= \left(\ell - \left\lfloor \frac{\ell}{\mathrm{D}+2} \right\rfloor\right) \left(\frac{1}{2} + \frac{(1-\rho_f)^L}{2}\right) + \left(\ell - \left\lfloor \frac{\ell+1}{\mathrm{D}+2} \right\rfloor\right) \left(\frac{1}{2} - \frac{(1-\rho_f)^L}{2}\right). \tag{175}$$

where

$$\mathcal{L}_k \triangleq \{k + (c-1)(\mathrm{D}+2) + 1, k + c(\mathrm{D}+2) - 3\}_{c=1}^{\lceil \frac{\ell}{\mathrm{D}+2} \rceil} \cap \{k, k+1, \ldots, k+L-1\} \tag{176a}$$

and

$$L \triangleq |\mathcal{L}_k| = \begin{cases} 2\left\lceil \frac{\ell}{\mathrm{D}+2} \right\rceil & \text{if } \ell \mod \mathrm{D}+2 \in \{0, \mathrm{D}, \mathrm{D}+1\} \\ 2\left\lfloor \frac{\ell}{\mathrm{D}+2} \right\rfloor & \text{if } \ell \mod \mathrm{D}+2 = 1 \\ 2\left\lfloor \frac{\ell}{\mathrm{D}+2} \right\rfloor + 1 & \text{otherwise.} \end{cases} \tag{176b}$$

If the subnet is of size $\ell \leq \mathrm{D}$ then the total sum MG $\bar{\mathsf{M}}_{\text{sum}}(\ell) = \ell$ is achievable. So (174) is achievable also for $\ell \leq \mathrm{D}$.

Similarly to (156)–(159) we then obtain

$$\mathsf{S}^{(\mathsf{e})} + \mathsf{S}^{(\mathsf{L})} = \overline{\lim_{K\to\infty}} \frac{1}{K} \sum_{k=1}^{K} \sum_{\ell=1}^{K-k+1} P_{\ell,k} \cdot \bar{\mathsf{M}}_{\text{sum}}(\ell) \tag{177}$$

$$= \overline{\lim_{K\to\infty}} \frac{1}{K} \sum_{\ell=1}^{K} \sum_{k=1}^{K-\ell+1} P_{\ell,k} \cdot \bar{\mathsf{M}}_{\text{sum}}(\ell) \tag{178}$$

$$= \overline{\lim_{K\to\infty}} \left[\frac{1}{K} \sum_{\ell=1}^{K-1} \rho^\ell (1-\rho) \left((K-\ell-1)(1-\rho)+2\right) \bar{\mathsf{M}}_{\text{sum}}(\ell) + \frac{\rho^K}{K} \cdot \bar{\mathsf{M}}_{\text{sum}}(K) \right]. \tag{179}$$

We continue to analyze the asymptotic expression in (179), where recall that we assume $\rho \in (0,1)$. Since $\bar{\mathsf{M}}_{\text{sum}}(\ell) \leq \ell$, following similar steps as in (160)–(165), we can conclude that

$$\mathsf{S}^{(\mathsf{e})} + \mathsf{S}^{(\mathsf{L})} = \sum_{\ell=1}^{\infty} \rho^\ell (1-\rho)^2 \bar{\mathsf{M}}_{\text{sum}}(\ell) \tag{180}$$

$$\overset{(i)}{\geq} (1-\rho)^2 \sum_{\ell=1}^{\infty} \rho^\ell \ell - \frac{(1-\rho)^2}{2} \sum_{\ell=1}^{\infty} \rho^\ell \left\lfloor \frac{\ell}{\mathrm{D}+2} \right\rfloor \left(1 + (1-\rho_f)^{2\lceil \frac{\ell}{\mathrm{D}+2} \rceil}\right)$$
$$- \frac{(1-\rho)^2}{2} \sum_{\ell=1}^{\infty} \rho^\ell \left\lfloor \frac{\ell+1}{\mathrm{D}+2} \right\rfloor \left(1 - (1-\rho_f)^{2\lceil \frac{\ell}{\mathrm{D}+2} \rceil}\right) \tag{181}$$

$$= (1-\rho)^2 \sum_{\ell=1}^{\infty} \rho^\ell \ell - \frac{(1-\rho)^2}{2} \sum_{\ell=1}^{\infty} \rho^\ell \left\lfloor \frac{\ell}{\mathrm{D}+2} \right\rfloor$$
$$- \frac{(1-\rho)^2}{2} \sum_{\ell=1}^{\infty} \rho^\ell \left(\left\lfloor \frac{\ell+1}{\mathrm{D}+2} \right\rfloor - \left\lfloor \frac{\ell}{\mathrm{D}+2} \right\rfloor \right) \left(1 - (1-\rho_f)^{2\lceil \frac{\ell}{\mathrm{D}+2} \rceil}\right) \tag{182}$$

$$\overset{(ii)}{=} (1-\rho)^2 \sum_{\ell=1}^{\infty} \rho^\ell \ell - (1-\rho)^2 \sum_{\ell=1}^{\infty} \rho^\ell \left\lfloor \frac{\ell}{\mathrm{D}+2} \right\rfloor - \frac{(1-\rho)^2}{2} \cdot \frac{\rho^{\mathrm{D}+1}}{1-\rho^{\mathrm{D}+2}}$$
$$+ \frac{(1-\rho)^2}{2} \frac{\rho^{\mathrm{D}+2-1}(1-\rho_f)^{2\frac{\mathrm{D}+2}{\mathrm{D}+2}}}{1-\rho^{\mathrm{D}+2}(1-\rho_f)^{2\frac{\mathrm{D}+2}{\mathrm{D}+2}}} \tag{183}$$

$$\overset{(iii)}{=} \rho - \frac{\rho^{\mathrm{D}+2}(1-\rho)}{1-\rho^{\mathrm{D}+2}} - \frac{(1-\rho)^2}{2} \cdot \frac{\rho^{\mathrm{D}+1}}{1-\rho^{\mathrm{D}+2}} + \frac{(1-\rho)^2}{2} \frac{\rho^{\mathrm{D}+1}(1-\rho_f)^2}{1-\rho^{\mathrm{D}+2}(1-\rho_f)^2} \tag{184}$$

$$\overset{(iv)}{=} \rho - \frac{\rho^{\mathrm{D}+1}(1-\rho^2)}{2(1-\rho^{\mathrm{D}+2})} + \frac{(1-\rho)^2}{2} \frac{\rho^{\mathrm{D}+1}(1-\rho_f)^2}{1-\rho^{\mathrm{D}+2}(1-\rho_f)^2}, \tag{185}$$

where in (i) we use that $\bar{\mathsf{M}}_{\text{sum,full}}(\ell)$ is decreasing in L and we can upper bound L by $2\left\lceil \frac{\ell}{\mathrm{D}+2} \right\rceil$; in (ii) the third term is the result of using the limiting expression (112) for $c = \rho$ and $A = \mathrm{D}+2$, and the fourth term is the result of using the limiting expression (114) for $c = \rho$, $A = \mathrm{D}+2$ and $B = \mathrm{D}+2$; in step (iii) we used the limits (104) and Limit (111); and in step (iv) we combined the second and third term into a single expression. Using (173), we finally obtain

$$\mathsf{S}^{(\mathsf{e})} = \rho - \frac{\rho\rho_f}{2} - \frac{(1-\rho^2)\rho^{\mathrm{D}+1}}{2(1-\rho^{\mathrm{D}+2})} + \frac{(1-\rho)^2\rho^{\mathrm{D}+1}(1-\rho_f)^2}{2\left(1-\rho^{\mathrm{D}+2}(1-\rho_f)^2\right)}. \tag{186}$$

APPENDIX C
PROOFS OF THEOREMS 3 AND 4

A. Achievability for $\mathsf{S}^{(\mathsf{L})}=0$ under Model 2:

We now consider Model 2, where each user either has an eMBB or a LLC message to transmit but never both. For $\mathsf{S}^{(\mathsf{L})}=0$, this is equivalent to considering LLC Txs as inactive. In this case, the probability that a subnet starts at Tx k and is of size ℓ now equals

$$P_{\ell,k}^{(2)}=\begin{cases}\rho^{\ell}(1-\rho_f)^{\ell}(1-\rho(1-\rho_f))^2 & \ell<K-k+1,\ k\geq 2\\ \rho^{\ell}(1-\rho_f)^{\ell}(1-\rho(1-\rho_f)) & (\ell=K-k+1,\ k\geq 2)\\ & \text{or }\ (\ell<K-k+1,\ k=1)\\ \rho^{K}(1-\rho_f)^{K} & k=1,\ \ell=K\end{cases}. \tag{187}$$

In each subnet we can employ the coding scheme in Subsection B-A1 (but without LLC messages) and thus achieve a total eMBB MG of $\mathsf{M}_{\text{sum,full}}(\ell)$, when ℓ denotes the length of the subnet. Therefore (similarly to (156)) we have

$$\mathsf{S}^{(\mathsf{e})}=\varlimsup_{K\to\infty}\frac{1}{K}\sum_{k=1}^{K}\sum_{\ell=1}^{K-k+1}P_{\ell,k}^{(2)}\cdot\mathsf{M}_{\text{sum,full}}(\ell) \tag{188}$$

$$=\varlimsup_{K\to\infty}\frac{1}{K}\sum_{\ell=1}^{K}\sum_{k=1}^{K-\ell+1}P_{\ell,k}^{(2)}\cdot\mathsf{M}_{\text{sum,full}}(\ell) \tag{189}$$

$$=\varlimsup_{K\to\infty}\Bigg[\frac{1}{K}\sum_{\ell=1}^{K-1}\rho^{\ell}(1-\rho_f)^{\ell}(1-\rho(1-\rho_f))\left((K-\ell-1)(1-\rho(1-\rho_f))+2\right)\mathsf{M}_{\text{sum,full}}(\ell)$$
$$+\frac{\rho^{K}(1-\rho_f)^{K}}{K}\cdot\mathsf{M}_{\text{sum,full}}(K)\Bigg]. \tag{190}$$

For $\rho_f=1$, obviously $\mathsf{S}^{(\mathsf{e})}=0$, which can also be verified on (190). In the following we assume that $\rho_f\in[0,1)$. Recall also that $\rho\in(0,1)$.

To analyze the limiting expression (190) we start by noticing that $\mathsf{M}_{\text{sum,full}}(\ell)\leq\ell$ implies

$$\varlimsup_{K\to\infty}\frac{\rho^{K}(1-\rho_f)^{K}}{K}\cdot\mathsf{M}_{\text{sum,full}}(K)=0, \tag{191}$$

$$\lim_{K\to\infty}\frac{1}{K}\sum_{\ell=1}^{K-1}\rho^{\ell}(1-\rho_f)^{\ell}(1-\rho(1-\rho_f))\left((-\ell-1)(1-\rho(1-\rho_f))+2\right)\cdot\mathsf{M}_{\text{sum,full}}(\ell)=0, \tag{192}$$

where the second limit (192) holds by the same arguments that we used to prove (163). Substituting (191) and (192) into (190), we then obtain

$$\mathsf{S}^{(\mathsf{e})}=\sum_{\ell=1}^{\infty}\rho^{\ell}(1-\rho_f)^{\ell}(1-\rho(1-\rho_f))^2\mathsf{M}_{\text{sum,full}}(\ell) \tag{193}$$

$$=\rho(1-\rho_f)-\frac{(1-\rho(1-\rho_f))\rho^{\mathrm{D}+2}(1-\rho_f)^{\mathrm{D}+2}}{1-\rho^{\mathrm{D}+2}(1-\rho_f)^{\mathrm{D}+2}}, \tag{194}$$

where the last equality holds by (104) and (111).

B. Converse Bound under Model 2

The steps described in the previous section can also be used to derive a converse bound on $\mathsf{S}^{(\mathsf{e})}$ that holds for all achievable eMBB MGs. In fact, $\mathsf{M}_{\text{Sum,full}}(\ell)$ also represents an upper bound on the total eMBB MG of any subnet of length ℓ. Following the same arguments as above we obtain the upper bound

$$\mathsf{S}^{(\mathsf{e})}\leq\rho(1-\rho_f)-\frac{(1-\rho(1-\rho_f))\rho^{\mathrm{D}+2}(1-\rho_f)^{\mathrm{D}+2}}{1-\rho^{\mathrm{D}+2}(1-\rho_f)^{\mathrm{D}+2}}. \tag{195}$$

Combined with the trivial bound

$$\mathsf{S}^{(\mathsf{L})}\leq\frac{\rho\rho_f}{2}, \tag{196}$$

this proves Theorem 4.

C. Achievability for Large $\mathsf{S}^{(\mathsf{L})}$ under Model 2:

As in Subsection B-D, to ensure that each LLC message can be transmitted at the same rate, we split the blocklength into two equally-long phases and time-share two schemes over the two phases. In Phase 1 we only send LLC messages from odd Txs and in Phase 2 only from even Txs. We thus reconsider the two LLC Tx sets $\mathcal{T}_{\mathrm{LLC},1}$ and $\mathcal{T}_{\mathrm{LLC},2}$ defined in (170) and (171). Though we use the same LLC Tx-sets as in Subsection B-D, now under Model 2 the network is split into smaller subnets, because not only deactivated users decompose the network but also LLC users that are not contained in the LLC Tx set $\mathcal{T}_{\mathrm{LLC},i}$ of the respective Phase i. (Under Model 1 these Txs still participated in the communication because besides their LLC message they also had an eMBB message to send.) We thus have different subnets in the two phases, even though the user activity pattern is the same.

In particular, in Phase $i \in \{1,2\}$ and for $k \in \mathcal{K}_i$ a subnet starts at Tx k and is of length ℓ,

1) for ℓ even, if Tx $k-1$ is LLC or deactivated; Txs $k, k+2, \ldots, k+\ell-2$ are active; Txs $k+1, k+3, \ldots, k+\ell-1$ are eMBB and active; and Tx $k+\ell$ is deactivated;
2) for ℓ odd, if Tx $k-1$ is LLC or deactivated; Txs $k, k+2, \ldots, k+\ell-1$ are active; Txs $k+1, k+3, \ldots, k+\ell-2$ are eMBB and active; and Tx $k+\ell$ is LLC or deactivated.

Similarly, for $k \notin \mathcal{K}_i$ a subnet starts at Tx k and is of length ℓ,

3) for ℓ even, if Tx $k-1$ is deactivated; Txs $k, k+2, \ldots, k+\ell-2$ are eMBB and active; Txs $k+1, k+3, \ldots, k+\ell-1$ are active; and Tx $k+\ell$ is LLC or deactivated;
4) for ℓ odd, if Tx $k-1$ is deactivated; Txs $k, k+2, \ldots, k+\ell-1$ are eMBB and active; Txs $k+1, k+3, \ldots, k+\ell-2$ are active; and Tx $k+\ell$ is deactivated.

The probability that in Phase i a subnet starts at Tx k and is of length ℓ is thus given by

$$\mathsf{P}^{(2)}_{\ell,k,i} = \begin{cases} \rho^\ell (1-\rho_f)^{\lfloor \frac{\ell}{2} \rfloor} \cdot a_{k,\ell}, & \text{if } k \in \mathcal{K}_i \\ \rho^\ell (1-\rho_f)^{\lceil \frac{\ell}{2} \rceil} \cdot b_{k,\ell}, & \text{if } k \notin \mathcal{K}_i \end{cases}, \qquad \ell = 1, 2, \ldots, \tag{197}$$

with

$$a_{k,\ell} \triangleq \begin{cases} (1-\rho(1-\rho_f))^2, & \ell < K-k+1,\ k \geq 2,\ \ell \text{ odd} \\ (1-\rho(1-\rho_f))(1-\rho), & \ell < K-k+1,\ k \geq 2,\ \ell \text{ even} \\ 1-\rho(1-\rho_f), & (\ell = K-k+1,\ k \geq 2) \\ & \text{or } (\ell < K-k+1,\ k=1,\ \ell \text{ odd}) \\ 1-\rho, & \ell < K,\ k=1,\ \ell \text{ even} \\ 1, & k=1,\ \ell = K \end{cases} \tag{198}$$

and

$$b_{k,\ell} \triangleq \begin{cases} (1-\rho)^2, & \ell < K-k+1,\ k \geq 2,\ \ell \text{ odd} \\ (1-\rho(1-\rho_f))(1-\rho), & \ell < K-k+1,\ k \geq 2,\ \ell \text{ even} \\ 1-\rho, & (\ell = K-k+1,\ k \geq 2) \\ & \text{or } (\ell < K-k+1,\ k=1,\ \ell \text{ odd}) \\ 1-\rho(1-\rho_f), & \ell < K,\ k=1,\ \ell \text{ even} \\ 1, & k=1,\ \ell = K. \end{cases} \tag{199}$$

In subnets of the form 1)–2), the scheme in Subsection B-A1 can be applied and a total sum-MG of $\mathsf{M}_{\text{sum,full}}(\ell)$ achieved. The same holds in subnets of the form 3)–4) if $\ell \leq \mathrm{D}$ or if in a subnet starting at Tx k all Txs in the set $\mathcal{L}_k$ as defined in (176) send eMBB messages. Otherwise, Tx $k+\mathrm{D}$ can be deactivated (notice that by our assumptions in 3) and 4), Tx $k+\mathrm{D}-2$ is not in $\mathcal{T}_{\mathrm{LLC}}$) and the scheme in Subsection B-A2 can be applied to the first D Tx/Rx pairs in the subnet and the scheme in Subsection B-A1 to the remaining non-silenced Tx/Rx pairs in the subnet. In this case, a sum-MG of $\mathsf{M}_{\text{sum,red}}(\ell)$ is achieved. For the expected total per-user MG we thus obtain

$$\begin{aligned} &\mathsf{S}^{(\mathsf{e})} + \mathsf{S}^{(\mathsf{L})} \\ &\geq \varlimsup_{K\to\infty} \frac{1}{2} \sum_{i=1}^{2} \frac{1}{K} \Bigg[\sum_{k \in \mathcal{K}_i} \sum_{\ell=1}^{K-k+1} P^{(2)}_{\ell,k,i} \cdot \mathsf{M}_{\text{sum,full}}(\ell) \\ &\qquad + \sum_{k \notin \mathcal{K}_i} \sum_{\ell=1}^{K-k+1} P^{(2)}_{\ell,k,i} \cdot \left(\mathsf{M}_{\text{sum,full}}(\ell)(1-\rho_f)^{2\lceil \frac{\ell}{\mathrm{D}+2} \rceil} + \mathsf{M}_{\text{sum,red}}(\ell) \cdot \left(1 - (1-\rho_f)^{2\lceil \frac{\ell}{\mathrm{D}+2} \rceil} \right) \right) \Bigg] \qquad (200) \\ &= \varlimsup_{K\to\infty} \frac{1}{K} \sum_{k=1}^{K} \sum_{\ell=1}^{K-k+1} \bar{\mathsf{M}}_{\text{sum}}(\ell,k) \qquad (201) \end{aligned}$$

$$= \varlimsup_{K\to\infty} \frac{1}{K} \sum_{\ell=1}^{K} \sum_{k=1}^{K-\ell+1} \bar{\mathsf{M}}_{\text{sum}}(\ell,k) \tag{202}$$

$$= \varlimsup_{K\to\infty} \frac{1}{K} \left[\sum_{\ell=1}^{K-2} \sum_{k=2}^{K-\ell} \bar{\mathsf{M}}_{\text{sum}}(\ell,k) + \sum_{\ell=1}^{K-1} \left(\bar{\mathsf{M}}_{\text{sum}}(\ell,1) + \bar{\mathsf{M}}_{\text{sum}}(\ell,K-\ell+1) \right) + \bar{\mathsf{M}}_{\text{sum}}(1,K) \right] \tag{203}$$

where

$$\begin{aligned} \bar{\mathsf{M}}_{\text{sum}}(\ell,k) \triangleq\ & \frac{1}{2} P^{(2)}_{\ell,k,1+\mathbb{1}\{k \text{ even}\}} \cdot \mathsf{M}_{\text{sum,full}}(\ell) \\ & + \frac{1}{2} P^{(2)}_{\ell,k,1+\mathbb{1}\{k \text{ odd}\}} \left(\mathsf{M}_{\text{sum,full}}(\ell)(1-\rho_f)^{2\lceil \frac{\ell}{\mathrm{D}+2} \rceil} + \mathsf{M}_{\text{sum,red}}(\ell) \left(1 - (1-\rho_f)^{2\lceil \frac{\ell}{\mathrm{D}+2} \rceil} \right) \right) \end{aligned} \tag{204}$$

In the following we analyze above asymptotic limit.

If $\rho_f = 1$, then $\mathsf{P}^{(2)}_{\ell,k,i} = 0$ except for $\ell = 1$ and $k \in \mathcal{K}_i$. In this case, from (200) we have

$$\mathsf{S}^{(\mathsf{e})} + \mathsf{S}^{(\mathsf{L})} = \varlimsup_{K\to\infty} \frac{1}{2} \sum_{i=1}^{2} \frac{1}{K} \sum_{k\in\mathcal{K}_i} P^{(2)}_{1,k,i} \cdot \mathsf{M}_{\text{sum,full}}(1) \tag{205}$$

$$= \varlimsup_{K\to\infty} \frac{1}{2} \frac{1}{K} K\rho \cdot 1 \tag{206}$$

$$= \frac{\rho}{2}. \tag{207}$$

Since in the described scheme, we generally have

$$\mathsf{S}^{(\mathsf{L})} = \frac{\rho\rho_f}{2}, \tag{208}$$

trivially we obtain that for $\rho_f = 1$ $\mathsf{S}^{(\mathsf{e})} = 0$ and $\mathsf{S}^{(\mathsf{L})}$ as in (208) is achievable.

If $\rho_f = 0$, we are back to the case with only eMBB messages studied in Subsection C-A.

For the remainder of this section, we assume that both $\rho, \rho_f \in (0,1)$. We notice that $P_{\ell,k,i} \le \rho^\ell$ and $\mathsf{M}_{\text{sum,full}}(\ell) \le \ell$, which implies that $\bar{\mathsf{M}}_{\text{sum}}(\ell,k) \le \rho^\ell \ell$. Therefore, by (106)

$$\varlimsup_{K\to\infty} \frac{1}{K} \left[\sum_{\ell=1}^{K-1} \left(\bar{\mathsf{M}}_{\text{sum}}(\ell,1) + \bar{\mathsf{M}}_{\text{sum}}(\ell,K-\ell+1) \right) + \bar{\mathsf{M}}_{\text{sum}}(1,K) \right] = 0, \tag{209}$$

and thus

$$\mathsf{S}^{(\mathsf{e})} + \mathsf{S}^{(\mathsf{L})} = \varlimsup_{K\to\infty} \frac{1}{K} \sum_{\ell=1}^{K-2} \sum_{k=2}^{K-\ell} \bar{\mathsf{M}}_{\text{sum}}(\ell,k). \tag{210}$$

For $\ell \in \{1,\dots,K-2\}$ and $k \in \{2,\dots,K-\ell\}$

$$\begin{aligned} \bar{\mathsf{M}}_{\text{sum}}(\ell,k) = & \frac{1}{2} \rho^\ell (1-\rho_f)^{\lfloor \frac{\ell}{2} \rfloor} (1-\rho(1-\rho_f))(1-\rho+\mathbb{1}\{\ell \text{ odd}\}\rho\rho_f) \mathsf{M}_{\text{sum,full}}(\ell) \\ & + \frac{1}{2} \rho^\ell (1-\rho_f)^{\lceil \frac{\ell}{2} \rceil} (1-\rho+\mathbb{1}\{\ell \text{ even}\}\rho\rho_f)(1-\rho) \\ & \cdot \left(\mathsf{M}_{\text{sum,full}}(\ell)(1-\rho_f)^{2\lceil \frac{\ell}{\mathrm{D}+2} \rceil} + \mathsf{M}_{\text{sum,red}}(\ell) \left(1 - (1-\rho_f)^{2\lceil \frac{\ell}{\mathrm{D}+2} \rceil} \right) \right) \end{aligned} \tag{211}$$

which does not depend on the index k. We can thus simplify the expression in (210) to

$$\mathsf{S}^{(\mathsf{e})} + \mathsf{S}^{(\mathsf{L})} = \varlimsup_{K\to\infty} \sum_{\ell=1}^{K-2} \frac{K-\ell-1}{K} \bar{\mathsf{M}}_{\text{sum}}(\ell,2) \tag{212}$$

$$= \varlimsup_{K\to\infty} \sum_{\ell=1}^{K-2} \bar{\mathsf{M}}_{\text{sum}}(\ell,2) \tag{213}$$

where the second equality holds because $\bar{\mathsf{M}}_{\text{sum}}(\ell,2) \le \rho^\ell \ell$ and thus the sum $\sum_{\ell=1}^{K-2} \frac{\ell+1}{K} \bar{\mathsf{M}}_{\text{sum}}(\ell,2)$ vanishes as $K \to \infty$, see (106).

Substituting (211) into (213), we obtain

$$\mathsf{S}^{(\mathsf{e})} + \mathsf{S}^{(\mathsf{L})} = \sum_{\ell=1}^{\infty} \bar{\mathsf{M}}_{\text{sum}}(\ell,2) \tag{214}$$

$$= -\frac{1}{2} \sum_{\ell=1}^{\infty} \rho^\ell (1-\rho_f)^{\lfloor \frac{\ell}{2} \rfloor} \left(\ell - \left\lfloor \frac{\ell}{\mathrm{D}+2} \right\rfloor \right) (1-\rho(1-\rho_f)) \rho\rho_f \mathbb{1}\{\ell \text{ is even }\}$$

$$
\begin{aligned}
&+\frac{1}{2}\sum_{\ell=1}^{\infty}\rho^{\ell}(1-\rho_f)^{\lfloor\frac{\ell}{2}\rfloor}\left(\ell-\left\lfloor\frac{\ell}{\mathrm{D}+2}\right\rfloor\right)(1-\rho(1-\rho_f))^2\\
&+\frac{1}{2}\sum_{\ell=1}^{\infty}\rho^{\ell}(1-\rho_f)^{\lceil\frac{\ell}{2}\rceil}(1-\rho)\rho\rho_f\left(1-(1-\rho_f)^{2\lceil\frac{\ell}{\mathrm{D}+2}\rceil}\right)\left(\ell-\left\lfloor\frac{\ell+1}{\mathrm{D}+2}\right\rfloor\right)\mathbb{1}\{\ell \text{ is even }\}\\
&+\frac{1}{2}\sum_{\ell=1}^{\infty}\rho^{\ell}(1-\rho_f)^{\lceil\frac{\ell}{2}\rceil}(1-\rho)^2\left(1-(1-\rho_f)^{2\lceil\frac{\ell}{\mathrm{D}+2}\rceil}\right)\left(\ell-\left\lfloor\frac{\ell+1}{\mathrm{D}+2}\right\rfloor\right)\\
&+\frac{1}{2}\sum_{\ell=1}^{\infty}\rho^{\ell}(1-\rho_f)^{\lceil\frac{\ell}{2}\rceil}(1-\rho)\rho\rho_f(1-\rho_f)^{2\lceil\frac{\ell}{\mathrm{D}+2}\rceil}\left(\ell-\left\lfloor\frac{\ell}{\mathrm{D}+2}\right\rfloor\right)\mathbb{1}\{\ell \text{ is even }\}\\
&+\frac{1}{2}\sum_{\ell=1}^{\infty}\rho^{\ell}(1-\rho_f)^{\lceil\frac{\ell}{2}\rceil}(1-\rho)^2(1-\rho_f)^{2\lceil\frac{\ell}{\mathrm{D}+2}\rceil}\left(\ell-\left\lfloor\frac{\ell}{\mathrm{D}+2}\right\rfloor\right) \qquad (215)\\
&\overset{(i)}{=}-\frac{\rho^2\rho_f^2}{2(1-\rho^2(1-\rho_f))}\left(\frac{2\rho^2(1-\rho_f)}{1-\rho^2(1-\rho_f)}-\frac{(\rho^2(1-\rho_f))^{\frac{\mathrm{D}+2}{2}}}{1-(\rho^2(1-\rho_f))^{\frac{\mathrm{D}+2}{2}}}\right)\\
&+\frac{(1-\rho(1-\rho_f))^2}{2(1-\rho^2(1-\rho_f))}\left(\rho+\frac{2\rho(1-\rho_f)(1+\rho)}{1-\rho^2(1-\rho_f)}-\frac{(1+\rho)(\rho^2(1-\rho_f))^{\frac{\mathrm{D}+2}{2}}}{1-(\rho^2(1-\rho_f))^{\frac{\mathrm{D}+2}{2}}}\right)\\
&+\frac{(1-\rho)^2}{2(1-\rho^2(1-\rho_f))}\left(\rho(1-\rho_f)(2\rho+2\rho^2(1-\rho_f)+1)-\frac{\rho^{\mathrm{D}+1}(1-\rho_f)^{\frac{\mathrm{D}+2}{2}}(1+\rho)}{1-(\rho^2(1-\rho_f))^{\frac{\mathrm{D}+2}{2}}}\right)\\
&+\frac{(1-\rho)^2\rho^{\mathrm{D}+1}(1-\rho_f)^{\frac{\mathrm{D}+6}{2}}}{2(1-\rho^{\mathrm{D}+2}(1-\rho_f)^{\frac{\mathrm{D}+6}{2}})} \qquad (216)\\
&=\frac{\rho(1-\rho_f)}{(1-\rho^2(1-\rho_f))^2}\left((1+\rho)(1-\rho(1-\rho_f))^2-\rho^3\rho_f^2\right)\\
&+\frac{\rho\left((1-\rho(1-\rho_f))^2+(1-\rho)^2(1-\rho_f)(2\rho+2\rho^2(1-\rho_f)+1)\right)}{2(1-\rho^2(1-\rho_f))}\\
&-\frac{\rho^{\mathrm{D}+2}(1-\rho_f)^{\frac{\mathrm{D}+2}{2}}}{2(1-\rho^2(1-\rho_f))(1-\rho^{\mathrm{D}+2}(1-\rho_f)^{\frac{\mathrm{D}+2}{2}})}\left((1+\rho)\left((1-\rho(1-\rho_f))^2+\frac{(1-\rho)^2}{\rho}\right)\right)\\
&+\frac{(1-\rho)^2\rho^{\mathrm{D}+1}(1-\rho_f)^{\frac{\mathrm{D}+6}{2}}}{2(1-\rho^{\mathrm{D}+2}(1-\rho_f)^{\frac{\mathrm{D}+6}{2}})}, \qquad (217)
\end{aligned}
$$

where in step (i) the first summation term of (215) is calculated by (142) for $c=\rho, d=1-\rho_f, B=2$ and $A=\mathrm{D}+2$ and by (143) for $c=\rho, d=1-\rho_f$ and $B=2$; the second summation term of (215) is calculated by (109) for $c=\rho, d=1-\rho_f, B=2$ and $A=\mathrm{D}+2$ and by (136) for $c=\rho, d=1-\rho_f$ and $B=2$; the third and the fifth summation terms of (215) are first combined together using the fact that for even values of ℓ the terms $\lfloor\frac{\ell+1}{\mathrm{D}+2}\rfloor-\lfloor\frac{\ell}{\mathrm{D}+2}\rfloor=0$ and $\lceil\frac{\ell}{2}\rceil=\frac{\ell}{2}$ and the resulting term is calculated by (104) for $c=\rho\sqrt{1-\rho_f}$ and by (111) for $c=\rho\sqrt{1-\rho_f}$ and $A=\mathrm{D}+2$ under the assumption that ℓ is even; and the fourth and the sixth summation terms of (215) are first combined together and the resulting term is calculated by (145) and (146) for $c=\rho$, $d=1-\rho_f$, $A=\mathrm{D}+2$ and $B=2$ and following the proof of (114). Using (173), we finally obtain

$$
\begin{aligned}
\mathsf{S}^{(\mathsf{e})}=&\frac{\rho(1-\rho_f)}{(1-\rho^2(1-\rho_f))^2}\left((1+\rho)(1-\rho(1-\rho_f))^2-\rho^3\rho_f^2\right)\\
&+\frac{\rho\left((1-\rho(1-\rho_f))^2+(1-\rho)^2(1-\rho_f)(2\rho+2\rho^2(1-\rho_f)+1)\right)}{2(1-\rho^2(1-\rho_f))}\\
&-\frac{\rho^{\mathrm{D}+2}(1-\rho_f)^{\frac{\mathrm{D}+2}{2}}}{2(1-\rho^2(1-\rho_f))(1-\rho^{\mathrm{D}+2}(1-\rho_f)^{\frac{\mathrm{D}+2}{2}})}\left((1+\rho)\left((1-\rho(1-\rho_f))^2+\frac{(1-\rho)^2}{\rho}\right)\right)\\
&+\frac{(1-\rho)^2\rho^{\mathrm{D}+1}(1-\rho_f)^{\frac{\mathrm{D}+6}{2}}}{2(1-\rho^{\mathrm{D}+2}(1-\rho_f)^{\frac{\mathrm{D}+6}{2}})}-\frac{\rho\rho_f}{2}. \qquad (218)
\end{aligned}
$$

APPENDIX D
PROOFS OF THEOREMS 5 AND 7

A. Achievability Results for $\mathsf{S}^{(\mathsf{L})}=0$ Under Model 1

When $\mathsf{S}^{(\mathsf{L})}=0$ and only eMBB messages are transmitted, only Rx-Cooperation is as powerful as Tx-Cooperation. In particular, in any subnet of size ℓ one can achieve a total eMBB MG of $M_{\text{sum,full}}(\ell)$. Following the same steps as in

Appendix B-B, one can thus conclude achievability of the per-user MG pair $\mathsf{S}^{(\mathsf{L})}=0$ and $\mathsf{S}^{(\mathsf{e})}$ as in (165):

$$\mathsf{S}^{(\mathsf{e})}=\rho-\frac{(1-\rho)\rho^{\mathrm{D}+2}}{1-\rho^{\mathrm{D}+2}}. \tag{219}$$

B. Achievability Results for Large $\mathsf{S}^{(\mathsf{L})}$ *under Model* 1

Notice that, when only Rxs can cooperate, it is not possible to precancel the interference of eMBB transmissions on LLC Txs and thus eMBB Tx interfering LLC transmissions should be deactivated. To achieve $\mathsf{S}^{(\mathsf{L})}=\frac{\rho\rho_f}{2}$, we schedule each LLC Tx in $\mathcal{K}_{\text{LLC}}$ to send its LLC message over half of the blocklength, during which it is not interfered by any other communication. We thus split the blocklength in two equally-long phases, where in Phase 1 we only send LLC messages from odd Txs and in Phase 2 only LLC messages from even Txs. We thus reconsider the two LLC Tx sets $\mathcal{T}_{\text{LLC},1}$ and $\mathcal{T}_{\text{LLC},2}$ in (170) and (171) and in the scheme of Phase i we deactivate the users adjacent to $\mathcal{T}_{\text{LLC},i}$. This way we split the network into small *eMBB-subnets* over which we only send eMBB messages, and thus can achieve an eMBB total MG of $\mathsf{M}_{\text{sum,full}}$ as described in the previous Subsection D-A.

So in Phase $i\in\{1,2\}$ and for $k\in\mathcal{K}_i$, an eMBB-subnet of length ℓ starts at Tx k:

1) for ℓ even, if Tx $k-1$ is inactive or its left neighbor Tx $k-2$ is LLC ; Txs $k,k+2,\ldots,k+\ell-2$ are eMBB and active; Txs $k+1,k+3,\ldots,k+\ell-1$ are active; and Tx $k+\ell$ is inactive;
2) for ℓ odd, if Tx $k-1$ is inactive or Tx $k-2$ is LLC; Txs $k,k+2,\ldots,k+\ell-2$ are eMBB and active; Txs $k+1,k+3,\ldots,k+\ell-1$ are active; and Tx $k+\ell$ is inactive or its right neighbor Tx $k+\ell+1$ is LLC .

Similarly, for $k\notin\mathcal{K}_i$ an eMBB-subnet of length ℓ starts at Tx k:

3) for ℓ even, if Tx $k-1$ is inactive; Txs $k,k+2,\ldots,k+\ell-2$ are active; Txs $k+1,k+3,\ldots,k+\ell-1$ are eMBB and active; and Tx $k+\ell$ is inactive or its right neighbor Tx $k+\ell+1$ is LLC;
4) for ℓ odd, if Tx $k-1$ is inactive; Txs $k,k+2,\ldots,k+\ell-2$ are active; Txs $k+1,k+3,\ldots,k+\ell-1$ are eMBB and active; and Tx $k+\ell$ is inactive.

The probability that in Phase i an eMBB-subnet starts at Tx k and is of length $\ell\geq 2$ is thus given by

$$\tilde{\mathsf{P}}_{\ell,k,i}=\begin{cases}\rho^{\ell}(1-\rho_f)^{\lceil\frac{\ell}{2}\rceil}\cdot\tilde{a}_{k,\ell}, & \text{if } k\in\mathcal{K}_i\\ \rho^{\ell}(1-\rho_f)^{\lfloor\frac{\ell}{2}\rfloor}\cdot\tilde{b}_{k,\ell}, & \text{if } k\notin\mathcal{K}_i\end{cases},\qquad \ell=1,2,\ldots, \tag{220}$$

with

$$\tilde{a}_{k,\ell}\triangleq\begin{cases}(1-\rho(1-\rho_f))^2, & \ell<K-k+1,\ k\geq 2,\ \ell \text{ odd}\\ (1-\rho(1-\rho_f))(1-\rho), & \ell<K-k+1,\ k\geq 2,\ \ell \text{ even}\\ 1-\rho(1-\rho_f), & (\ell=K-k+1,\ k\geq 2)\\ & \text{or } (\ell<K-k+1,\ k=1,\ \ell \text{ odd})\\ 1-\rho, & \ell<K,\ k=1,\ \ell \text{ even}\\ 1, & k=1,\ \ell=K\end{cases} \tag{221}$$

and

$$\tilde{b}_{k,\ell}\triangleq\begin{cases}(1-\rho)^2, & \ell<K-k+1,\ k\geq 2,\ \ell \text{ odd}\\ (1-\rho(1-\rho_f))(1-\rho), & \ell<K-k+1,\ k\geq 2,\ \ell \text{ even}\\ 1-\rho, & (\ell=K-k+1,\ k\geq 2)\\ & \text{or } (\ell<K-k+1,\ k=1,\ \ell \text{ odd})\\ 1-\rho(1-\rho_f), & \ell<K,\ k=1,\ \ell \text{ even}\\ 1, & k=1,\ \ell=K.\end{cases} \tag{222}$$

Under this scheme, $\mathsf{S}^{(\mathsf{L})}=\frac{\rho\rho_f}{2}$ and

$$\mathsf{S}^{(\mathsf{e})}=\varlimsup_{K\to\infty}\frac{1}{K}\sum_{k=1}^{K}\sum_{\ell=1}^{K-k+1}\tilde{\mathsf{P}}_{\ell,k,i}\cdot\mathsf{M}_{\text{sum,full}}(\ell) \tag{223}$$

$$=\varlimsup_{K\to\infty}\frac{1}{K}\sum_{\ell=1}^{K}\sum_{k=1}^{K-\ell+1}\tilde{\mathsf{P}}_{\ell,k,i}\cdot\mathsf{M}_{\text{sum,full}}(\ell) \tag{224}$$

$$=\varlimsup_{K\to\infty}\frac{1}{K}\cdot\frac{1}{2}\sum_{i=1}^{2}\Bigg[\sum_{\ell=1}^{K-2}\sum_{k=2}^{K-\ell}\tilde{\mathsf{P}}_{\ell,k,i}\mathsf{M}_{\text{sum,full}}(\ell)$$

$$+\sum_{\ell=2}^{K-1}\mathsf{M}_{\text{sum,full}}(\ell)\left(\tilde{\mathsf{P}}_{\ell,1,i}+\tilde{\mathsf{P}}_{\ell,K-\ell+1,i}\right)+\tilde{\mathsf{P}}_{1,K,i}\cdot\mathsf{M}_{\text{sum,full}}(K)\Bigg]. \tag{225}$$

In the following we analyze above asymptotic limit.

If $\rho_f=0$, trivially $\mathsf{S}^{(\mathsf{L})}=0$ and we are back to Subsection D-D. If $\rho_f=1$, then $\tilde{\mathsf{P}}_{\ell,k,i}=0$ except for $\ell=1$ when $k\notin\mathcal{K}_i$. In this case, from (225) we have

$$\mathsf{S}^{(\mathsf{e})}=\varlimsup_{K\to\infty}\frac{1}{K}\frac{1}{2}\sum_{i=1}^{2}\sum_{k\notin\mathcal{K}_i}\tilde{\mathsf{P}}_{1,k,i}\cdot\mathsf{M}_{\text{sum,full}}(1) \tag{226}$$

$$=\varlimsup_{K\to\infty}\frac{1}{K}\frac{K}{2}\rho(1-\rho)^2\cdot 1 \tag{227}$$

$$=\frac{\rho(1-\rho)^2}{2}, \tag{228}$$

and

$$\mathsf{S}^{(\mathsf{L})}=\frac{\rho}{2}. \tag{229}$$

For the remainder of this section, we assume that $\rho\in(0,1)$ and $(1-\rho_f)\in(0,1)$. We notice that $\tilde{P}_{\ell,k,i}\le\rho^\ell$ and $\mathsf{M}_{\text{sum,full}}(\ell)\le\ell$, which implies that $\bar{\mathsf{M}}_{\text{sum}}(\ell,k)\le\rho^\ell\ell$. Therefore, by (106)

$$\varlimsup_{K\to\infty}\frac{1}{K}\cdot\frac{1}{2}\sum_{i=1}^{2}\left[\sum_{\ell=2}^{K-1}\mathsf{M}_{\text{sum,full}}(\ell)\left(\tilde{\mathsf{P}}_{\ell,1,i}+\tilde{\mathsf{P}}_{\ell,K-\ell+1,i}\right)+\tilde{\mathsf{P}}_{1,K,i}\cdot\mathsf{M}_{\text{sum,full}}(K)\right]=0, \tag{230}$$

and thus

$$\mathsf{S}^{(\mathsf{e})}=\varlimsup_{K\to\infty}\frac{1}{K}\cdot\frac{1}{2}\sum_{i=1}^{2}\left[\sum_{\ell=1}^{K-2}\sum_{k=2}^{K-\ell}\mathsf{P}_{\ell,k,i}\mathsf{M}_{\text{sum,full}}(\ell)\right]. \tag{231}$$

Following the same argument as in (211)–(213), we obtain

$$\begin{aligned}\mathsf{S}^{(\mathsf{e})}=&-\frac{1}{2}\sum_{\ell=1}^{\infty}\rho^\ell(1-\rho_f)^{\lceil\frac{\ell}{2}\rceil}\left(\ell-\left\lfloor\frac{\ell}{\mathrm{D}+2}\right\rfloor\right)(1-\rho(1-\rho_f))\rho\rho_f\mathbb{1}\{\ell\text{ is even }\}\\&+\frac{1}{2}\sum_{\ell=1}^{\infty}\rho^\ell(1-\rho_f)^{\lceil\frac{\ell}{2}\rceil}\left(\ell-\left\lfloor\frac{\ell}{\mathrm{D}+2}\right\rfloor\right)(1-\rho(1-\rho_f))^2\\&+\frac{1}{2}\sum_{\ell=1}^{\infty}\rho^\ell(1-\rho_f)^{\lfloor\frac{\ell}{2}\rfloor}(1-\rho)\rho\rho_f\left(\ell-\left\lfloor\frac{\ell}{\mathrm{D}+2}\right\rfloor\right)\mathbb{1}\{\ell\text{ is even }\}\\&+\frac{1}{2}\sum_{\ell=1}^{\infty}\rho^\ell(1-\rho_f)^{\lfloor\frac{\ell}{2}\rfloor}(1-\rho)^2\left(\ell-\left\lfloor\frac{\ell}{\mathrm{D}+2}\right\rfloor\right)\end{aligned} \tag{232}$$

$$\begin{aligned}=&-\frac{\rho^2\rho_f^2}{2}\sum_{\ell=1}^{\infty}\rho^\ell(1-\rho_f)^{\lfloor\frac{\ell}{2}\rfloor}\left(\ell-\left\lfloor\frac{\ell}{\mathrm{D}+2}\right\rfloor\right)\mathbb{1}\{\ell\text{ is even }\}\\&+\frac{1}{2}\sum_{\ell=1}^{\infty}\rho^\ell(1-\rho_f)^{\lceil\frac{\ell}{2}\rceil}\left(\ell-\left\lfloor\frac{\ell}{\mathrm{D}+2}\right\rfloor\right)(1-\rho(1-\rho_f))^2\\&+\frac{1}{2}\sum_{\ell=1}^{\infty}\rho^\ell(1-\rho_f)^{\lfloor\frac{\ell}{2}\rfloor}(1-\rho)^2\left(\ell-\left\lfloor\frac{\ell}{\mathrm{D}+2}\right\rfloor\right)\end{aligned} \tag{233}$$

$$\begin{aligned}\overset{(i)}{=}&-\frac{\rho^4\rho_f^2(1-\rho_f)}{2(1-\rho^2(1-\rho_f))}\left(\frac{2}{(1-\rho^2(1-\rho_f))}-\frac{\rho^{\mathrm{D}}(1-\rho_f)^{\frac{\mathrm{D}}{2}}}{1-\rho^{\mathrm{D}+2}(1-\rho_f)^{\frac{\mathrm{D}+2}{2}}}\right)\\&+\frac{\rho(1-\rho_f)(1-\rho(1-\rho_f))^2}{2(1-\rho^2(1-\rho_f))}\left(2\rho+2\rho^2(1-\rho_f)+1-\frac{\rho^{\mathrm{D}+1}(1-\rho_f)^{\frac{\mathrm{D}}{2}}(1+\rho(1-\rho_f))}{(1-\rho^{\mathrm{D}+2}(1-\rho_f)^{\frac{\mathrm{D}+2}{2}})}\right)\\&+\frac{\rho(1-\rho)^2}{2(1-\rho^2(1-\rho_f))}\left(\frac{2\rho(1-\rho_f)}{(1-\rho^2(1-\rho_f))}+1-\frac{\rho^{\mathrm{D}+1}(1-\rho_f)^{\frac{\mathrm{D}+2}{2}}(1+\rho)}{(1-\rho^{\mathrm{D}+2}(1-\rho_f)^{\frac{\mathrm{D}+2}{2}})}\right).\end{aligned} \tag{234}$$

C. Proof of the Converse Result under Model 1

Fix K and realizations of the sets $\mathcal{K}_{\text{active}}$, $\mathcal{K}_{\text{eMBB}}$, and $\mathcal{K}_{\text{LLC}}$. Following the steps in [46, Section V], we can prove that for each $k \in \mathcal{K}_{\text{active}}$,

$$\begin{aligned} R_k^{(\mathsf{L})} + R_k^{(\mathsf{e})} + R_{k+1}^{(\mathsf{L})} \\ \leq \frac{1}{2}\log(1+(|h_{k,k}|^2+|h_{k,k+1}|^2)\mathsf{P}) + \frac{1}{2}\log(|h_{k,k}|^2+|h_{k,k+1}|^2) \\ + \max\{-\log|h_{k,k+1}|, 0\} + \frac{\epsilon_n}{n}, \end{aligned} \tag{235}$$

where $R_k^{(\mathsf{L})}$ and $R_{k+1}^{(\mathsf{L})}$ denote the rates of the LLC message at Rxs k and $k+1$, respectively. Recall that in our setup a LLC rate $R_k^{(\mathsf{L})}$ is equal to 0 if $k \in \mathcal{K}_{\text{LLC}}$ (i.e., with probability $1-\rho\rho_f$) and it is equal to the global LLC rate $R^{(\mathsf{L})}$ if $k+1 \notin \mathcal{K}_{\text{LLC}}$ (i.e., with probability $\rho\rho_f$). Similarly for $R_{k+1}^{(\mathsf{L})}$.

Abbreviating the right hand-side of (235) by Δ, and summing up this bound for all values of $k \in \mathcal{K}_{\text{active}}$, we obtain

$$\sum_{k\in\mathcal{K}_{\text{active}}} \left(R_k^{(\mathsf{L})} + R_k^{(\mathsf{e})} + R_{k+1}^{(\mathsf{L})}\right) \leq |\mathcal{K}_{\text{active}}|\cdot\Delta. \tag{236}$$

Taking expectation over the random activity sets $\mathcal{K}_{\text{active}}$, $\mathcal{K}_{\text{eMBB}}$, and $\mathcal{K}_{\text{LLC}}$ of (235) and dividing by K, we further have

$$\mathbb{E}[\bar{R}^{(\mathsf{e})}] + R^{(\mathsf{L})}\left(\rho\rho_f + \rho^2\rho_f\right) \leq \rho\cdot\Delta, \tag{237}$$

because the expected number of indices $k \in \mathcal{K}_{\text{active}}$ for which $R_k^{(\mathsf{L})} = R^{(\mathsf{L})}$ equals $\rho\cdot\rho_f$ and the expected numbers of indices $k \in \mathcal{K}_{\text{active}}$ for which $R_{k+1}^{(\mathsf{L})} = R^{(\mathsf{L})}$ equals $\rho^2\cdot\rho_f$. (For this latter formula, observe that $R_{k+1}^{(\mathsf{L})} = R^{(\mathsf{L})}$ with probability $\rho\rho_f$, however it is counted only if $k \in \mathcal{K}_{\text{active}}$, which happens with probability ρ.)

Dividing by $\frac{1}{2}\log\mathsf{P}$ and letting $\mathsf{P}\to\infty$ proves Theorem 6.

D. Achievability Results for $\mathsf{S}^{(\mathsf{L})} = 0$ under Model 2

As mentioned, when we only wish to send eMBB messages, only Rx-cooperation suffices and we can achieve the same per-user MG pairs as with Tx and Rx cooperation. Thus $\mathsf{S}^{(\mathsf{e})} = \rho(1-\rho_f) - \frac{(1-\rho(1-\rho_f))\rho^{\mathrm{D}+2}(1-\rho_f)^{\mathrm{D}+2}}{1-\rho^{\mathrm{D}+2}(1-\rho_f)^{\mathrm{D}+2}}$ as in (195) is achievable.

E. Achievability Results for Large $\mathsf{S}^{(\mathsf{L})}$ Under Model 2

As before in Section D-B, we split the blocklength into two equally-long phases, where in Phase 1 we only send LLC messages from odd Txs in $\mathcal{T}_{\text{LLC},1}$ (see (170)) and in Phase 2 only from even Txs in $\mathcal{T}_{\text{LLC},2}$ ((171)). In Phase i we further deactivate the users adjacent to $\mathcal{T}_{\text{LLC},i}$ and send only eMBB messages over the remaining eMBB-subnets.

So in Phase $i \in \{1,2\}$ and for $k \in \mathcal{K}_i$ an eMBB-subnet starts at Tx k and is of length ℓ,

1) for ℓ even, if Tx $k-1$ is inactive or its left neighbor Tx $k-2$ is LLC ; Txs $k, k+1, \ldots, k+\ell-1$ are eMBB and active;
2) for ℓ odd, if Tx $k-1$ is inactive or Tx $k-2$ is LLC; Txs $k, k+1, \ldots, k+\ell-1$ are eMBB and active; and Tx $k+\ell$ is inactive or its right neighbor Tx $k+\ell+1$ is LLC .

Similarly, for $k \notin \mathcal{K}_i$ an eMBB-subnet starts at Tx k and is of length ℓ,

3) for ℓ even, if Tx $k-1$ is inactive; Txs $k, k+1, \ldots, k+\ell-1$ are eMBB and active; and Tx $k+\ell$ is inactive or its right neighbor Tx $k+\ell+1$ is LLC;
4) for ℓ odd, if Tx $k-1$ is inactive; Txs $k, k+1, \ldots, k+\ell-1$ are eMBB and active; and Tx $k+\ell$ is inactive.

The probability that in Phase i an eMBB-subnet starts at Tx k and is of length $\ell \geq 2$ is thus given by

$$\tilde{\mathsf{P}}^{(2)}_{\ell,k,i} = \begin{cases} \rho^\ell(1-\rho_f)^\ell\cdot\tilde{a}_{k,\ell}, & \text{if } k\in\mathcal{K}_i \\ \rho^\ell(1-\rho_f)^\ell\cdot\tilde{b}_{k,\ell}, & \text{if } k\notin\mathcal{K}_i \end{cases}, \qquad \ell = 1,2,\ldots, \tag{238}$$

with $\tilde{a}_{k,\ell}$ and $\tilde{b}_{k,\ell}$ are defined (221) and (222).

Under this scheme, $\mathsf{S}^{(\mathsf{L})} = \frac{\rho\rho_f}{2}$ and

$$\mathsf{S}^{(\mathsf{e})} = \varlimsup_{K\to\infty}\frac{1}{K}\sum_{k=1}^{K}\sum_{\ell=1}^{K-k+1}\tilde{\mathsf{P}}^{(2)}_{\ell,k,i}\cdot\mathsf{M}_{\text{sum,full}}(\ell) \tag{239}$$

$$= \varlimsup_{K\to\infty}\frac{1}{K}\sum_{\ell=1}^{K}\sum_{k=1}^{K-\ell+1}\tilde{\mathsf{P}}_{\ell,k,i}\cdot\mathsf{M}_{\text{sum,full}}(\ell) \tag{240}$$

$$= \varlimsup_{K\to\infty}\frac{1}{K}\cdot\frac{1}{2}\sum_{i=1}^{2}\Bigg[\sum_{\ell=1}^{K-2}\sum_{k=2}^{K-\ell}\tilde{\mathsf{P}}^{(2)}_{\ell,k,i}\mathsf{M}_{\text{sum,full}}(\ell)$$

$$+\sum_{\ell=2}^{K-1}\mathsf{M}_{\text{sum,full}}(\ell)\left(\tilde{\mathsf{P}}^{(2)}_{\ell,1,i}+\tilde{\mathsf{P}}^{(2)}_{\ell,K-\ell+1,i}\right)+\tilde{\mathsf{P}}^{(2)}_{1,K,i}\mathsf{M}_{\text{sum,full}}(K)\Bigg]. \tag{241}$$

In the following we analyze the above asymptotic limit.

If $\rho_f=0$, trivially $\mathsf{S}^{(\mathsf{L})}=0$ and we are back to Subsection D-D. If $\rho_f=1$ then $\mathsf{S}^{(\mathsf{e})}=0$.

For the remainder of this section, we assume that $\rho,\rho_f\in(0,1)$. We notice that $\tilde{\mathsf{P}}^{(2)}_{\ell,k,i}\le\rho^\ell$ and $\mathsf{M}_{\text{sum,full}}(\ell)\le\ell$, which implies that $\bar{\mathsf{M}}_{\text{sum}}(\ell,k)\le\rho^\ell\ell$. Therefore, by (106)

$$\overline{\lim_{K\to\infty}}\frac{1}{K}\cdot\frac{1}{2}\sum_{i=1}^{2}\left[\sum_{\ell=1}^{K-1}\mathsf{M}_{\text{sum,full}}(\ell)\left(\tilde{\mathsf{P}}^{(2)}_{\ell,1,i}+\tilde{\mathsf{P}}^{(2)}_{\ell,K-\ell+1,i}\right)+\tilde{\mathsf{P}}^{(2)}_{1,K,i}\cdot\mathsf{M}_{\text{sum,full}}(K)\right]=0, \tag{242}$$

and thus

$$\mathsf{S}^{(\mathsf{e})}=\overline{\lim_{K\to\infty}}\frac{1}{K}\cdot\frac{1}{2}\sum_{i=1}^{2}\sum_{\ell=1}^{K-2}\sum_{k=2}^{K-\ell}\tilde{\mathsf{P}}^{(2)}_{\ell,k,i}\cdot\mathsf{M}_{\text{sum,full}}(\ell). \tag{243}$$

Following the same arguments as in (211)–(213), we obtain

$$\begin{aligned}\mathsf{S}^{(\mathsf{e})}=&-\frac{1}{2}\sum_{\ell=1}^{\infty}\rho^\ell(1-\rho_f)^\ell\left(\ell-\left\lfloor\frac{\ell}{\mathrm{D}+2}\right\rfloor\right)(1-\rho(1-\rho_f))\rho\rho_f\mathbb{1}\{\ell\text{ is even }\}\\&+\frac{1}{2}\sum_{\ell=1}^{\infty}\rho^\ell(1-\rho_f)^\ell\left(\ell-\left\lfloor\frac{\ell}{\mathrm{D}+2}\right\rfloor\right)(1-\rho(1-\rho_f))^2\\&+\frac{1}{2}\sum_{\ell=1}^{\infty}\rho^\ell(1-\rho_f)^\ell(1-\rho)\rho\rho_f\left(\ell-\left\lfloor\frac{\ell}{\mathrm{D}+2}\right\rfloor\right)\mathbb{1}\{\ell\text{ is even }\}\\&+\frac{1}{2}\sum_{\ell=1}^{\infty}\rho^\ell(1-\rho_f)^\ell(1-\rho)^2\left(\ell-\left\lfloor\frac{\ell}{\mathrm{D}+2}\right\rfloor\right)\end{aligned} \tag{244}$$

$$\begin{aligned}=&-\frac{\rho^2\rho_f^2}{2}\sum_{\ell=1}^{\infty}\rho^\ell(1-\rho_f)^\ell\left(\ell-\left\lfloor\frac{\ell}{\mathrm{D}+2}\right\rfloor\right)\mathbb{1}\{\ell\text{ is even }\}\\&+\frac{(1-\rho(1-\rho_f))^2+(1-\rho)^2}{2}\sum_{\ell=1}^{\infty}\rho^\ell(1-\rho_f)^\ell\left(\ell-\left\lfloor\frac{\ell}{\mathrm{D}+2}\right\rfloor\right)\end{aligned} \tag{245}$$

$$\begin{aligned}=&-\frac{\rho^4\rho_f^2(1-\rho_f)^2}{2(1-\rho^2(1-\rho_f)^2)}\left(\frac{2}{1-\rho^2(1-\rho_f)^2}-\frac{\rho^{\mathrm{D}}(1-\rho_f)^{\mathrm{D}}}{1-\rho^{\mathrm{D}+2}(1-\rho_f)^{\mathrm{D}+2}}\right)\\&+\frac{\rho(1-\rho_f)\left((1-\rho(1-\rho_f))^2+(1-\rho)^2\right)}{2(1-\rho(1-\rho_f))}\left(\frac{1}{1-\rho(1-\rho_f)}-\frac{\rho^{\mathrm{D}+1}(1-\rho_f)^{\mathrm{D}+1}}{1-\rho^{\mathrm{D}+2}(1-\rho_f)^{\mathrm{D}+2}}\right).\end{aligned} \tag{246}$$

F. Proof of the Converse Results under Model 2

Fix K and realizations of the sets $\mathcal{K}_{\text{eMBB}}$ and $\mathcal{K}_{\text{LLC}}$. Following the steps in [46, Section V], we can prove that for each $k\in\mathcal{K}_{\text{eMBB}}$,

$$\begin{aligned}R_k^{(\mathsf{e})}+R_{k+1}^{(\mathsf{L})}\le&\frac{1}{2}\log(1+(|h_{k,k}|^2+|h_{k,k+1}|^2)\mathsf{P})+\frac{\epsilon_n}{n}\\&+\frac{1}{2}\log(|h_{k,k}|^2+|h_{k,k+1}|^2)+\max\{-\log|h_{k,k+1}|,0\},\end{aligned} \tag{247}$$

where $R_{k+1}^{(\mathsf{L})}$ is the rate of the LLC messages at Rx $k+1$, which is either 0 (when $k\notin\mathcal{K}_{\text{LLC}}$, i.e., with probability $1-\rho\rho_f$) or equal to the global LLC rate $R^{(\mathsf{L})}$ (when $k\in\mathcal{K}_{\text{LLC}}$, i.e., with probability $\rho\rho_f$).

Abbreviating the right-hand side of (247) by $\tilde{\Delta}$, and summing up this bound for all values of $k\in\mathcal{K}_{\text{eMBB}}$, we obtain

$$\sum_{k\in\mathcal{K}_{\text{eMBB}}}\left(R_k^{(\mathsf{e})}+R_{k+1}^{(\mathsf{L})}\right)\le|\mathcal{K}_{\text{eMBB}}|\cdot\tilde{\Delta}, \tag{248}$$

or equivalently

$$K\bar{R}^{(\mathsf{e})}+\sum_{\substack{k\in\mathcal{K}_{\text{eMBB}}\\k+1\in\mathcal{K}_{\text{LLC}}}}R^{(\mathsf{L})}\le|\mathcal{K}_{\text{eMBB}}|\cdot\tilde{\Delta}. \tag{249}$$

Dividing both sides of (249) by K and taking expectation over the random user activity sets $\mathcal{K}_{\text{eMBB}}$ and $\mathcal{K}_{\text{LLC}}$, we obtain:

$$\mathbb{E}[\bar{R}^{(\mathsf{e})}]+R^{(\mathsf{L})}\left(\rho^2\rho_f(1-\rho_f)\right)\le\rho(1-\rho_f)\cdot\tilde{\Delta}. \tag{250}$$

Dividing by $\frac{1}{2}\log\mathsf{P}$ and letting $\mathsf{P}\to\infty$ and $K\to\infty$, then proves Theorem 8.

APPENDIX E
HEXAGONAL NETWORK WITH RX-COOPERATION ONLY: PROOF OF THEOREMS 9 AND 10

A. Achievability Result for $\mathsf{S}^{(\mathsf{L})} = 0$ under Model 1

Substituting $\mathcal{T}'_{\text{eMBB}} = \mathcal{K}$ and $\alpha = 0$ into (40) establishes achievability of the eMBB per-user MG $\mathsf{S}^{(\mathsf{e})} = \rho$.

B. Achievability Result for Large $\mathsf{S}^{(\mathsf{L})}$ under Model 1

Reconsider the partition $\mathcal{K}_1, \mathcal{K}_2, \mathcal{K}_3 \subseteq \mathcal{K}$ given in Fig. 13b, for which each of the three sets $\mathcal{K}_i$ only contains non-interfering cells:

$$k' \notin \mathcal{I}_{\text{Rx},k''} \quad \text{and} \quad k'' \notin \mathcal{I}_{\text{Rx},k'}, \quad \forall k', k'' \in \mathcal{K}_i. \tag{251}$$

Notice that the three sets $\mathcal{K}_1, \mathcal{K}_2, \mathcal{K}_3$ are of equal size.

We time-share three schemes, where in each scheme $i \in \{1, 2, 3\}$ only Txs in subset $\mathcal{T}_i$ are scheduled to send LLC messages if they have any. So in scheme i, we set

$$\mathcal{T}_{\text{LLC},i} := \mathcal{K}_i \cap \mathcal{K}_{\text{LLC}}. \tag{252a}$$

Then we silence all Tx/Rx pairs that interfere at Rxs in $\mathcal{T}_{\text{LLC},i}$:

$$\mathcal{T}_{\text{silent},i} := \{\tilde{k} \in \mathcal{K} \colon \exists k' \in \mathcal{T}_{\text{LLC},i} \text{ so that } k \in \mathcal{I}_{k'}\}, \tag{252b}$$

and schedule the remaining Txs to send eMBB messages if they are active

$$\mathcal{T}_{\text{eMBB},i} := \mathcal{K}_{\text{active}} \backslash (\mathcal{T}_{\text{LLC},i} \cup \mathcal{T}_{\text{silent},i}). \tag{252c}$$

Since we can use an unlimited number of cooperation rounds, each scheduled eMBB Tx can send at full MG. The probability of a user k to be scheduled as an eMBB user in scheme i is:

- If $k \in \mathcal{K}_i$ it is $\rho(1-\rho_f)$. (This is the probability that Tx k has an eMBB but no LLC message to send.)
- If $k \notin \mathcal{K}_i$ it is $\rho(1-\rho\rho_f)^3$. (This is the probability that none of the 3 adjacent Txs in $\mathcal{K}_i$ has a LLC message to send and Tx k is active.)

By above considerations, the scheme thus achieves the per-user MG pair

$$\mathsf{S}^{(\mathsf{L})} = \frac{\rho\rho_f}{3} \tag{253}$$

$$\mathsf{S}^{(\mathsf{e})} = \frac{2\rho(1-\rho\rho_f)^3}{3} + \frac{\rho(1-\rho_f)}{3}. \tag{254}$$

Time-sharing the described scheme with the scheme in Appendix E-A proves Theorem 9.

C. Achievability Results for $\mathsf{S}^{(\mathsf{L})} = 0$ Under Model 2

Substituting $\mathcal{T}'_{\text{eMBB}} = \mathcal{K}$ and $\alpha = 0$ into (41) establishes achievability of the eMBB per-user MG $\mathsf{S}^{(\mathsf{e})} = \rho$.

D. Achievability Results for Large $\mathsf{S}^{(\mathsf{L})}$ Under Model 2

We again time-share three schemes, where in scheme i, we again choose

$$\mathcal{T}_{\text{LLC},i} := \mathcal{K}_i \cap \mathcal{K}_{\text{LLC}} \tag{255a}$$

and

$$\mathcal{T}_{\text{silent},i} := \{\tilde{k} \in \mathcal{K} \colon \exists k' \in \mathcal{T}_{\text{LLC},i} \text{ so that } k \in \mathcal{I}_{k'}\}. \tag{255b}$$

Under Model 2 however we can only schedule users that have eMBB messages to send:

$$\mathcal{T}_{\text{eMBB},i} := \mathcal{K}_{\text{eMBB}} \backslash (\mathcal{T}_{\text{LLC},i} \cup \mathcal{T}_{\text{silent},i}). \tag{255c}$$

Since we can use an unlimited number of cooperation rounds, each scheduled eMBB Tx can send at full MG. The probability that a user k will be scheduled as an eMBB user in scheme i is:

- If $k \in \mathcal{K}_i$ it is $\rho(1-\rho_f)$. (This is the probability that Tx k has an eMBB but no LLC message to send.)
- If $k \notin \mathcal{K}_i$ it is $\rho(1-\rho_f)(1-\rho\rho_f)^3$. (This is the probability that none of the 3 adjacent Txs in $\mathcal{K}_i$ has a LLC message to send and Tx k has an eMBB message to send.)

By above considerations, the scheme thus achieves the per-user MG pair

$$\mathsf{S}^{(\mathsf{L})} = \frac{\rho\rho_f}{3} \tag{256}$$

$$\mathsf{S}^{(\mathsf{e})} = \rho(1-\rho_f)\frac{2(1-\rho\rho_f)^3}{3} + \frac{\rho(1-\rho_f)^2}{3}. \tag{257}$$

Time-sharing this scheme with the scheme in Appendix E-A proves Theorem 9.

REFERENCES

[1] H. Nikbakht, M. Wigger and S. Shamai (Shitz), "Random user activity with mixed delay traffic," in *Proceedings of the IEEE Information Theory Workshop*, Riva del Garda, Italy, Apr. 11–14, 2021.

[2] H. Nikbakht, M. Wigger, S. S. Shitz, and J-M. Gorce, "Cooperative encoding and decoding of mixed delay traffic under random-user activity," in *Proceedings of the IEEE Information Theory Workshop*, Kanazawa, Japan, pp. 1–6, Oct. 17 - 21, 2021.

[3] L. Chettri and R. Bera, "A comprehensive survey on Internet of Things (IoT) toward 5G wireless systems," *IEEE Internet of Things Journal*, vol. 7, no. 1, pp. 16–32, Jan. 2020.

[4] K. -H. Ngo, A. Lancho, G. Durisi, and A. Graell i. Amat, "Massive uncoordinated access with random user activity," in *Proceedings of the IEEE International Symposium on Information Theory*, Melbourne, Australia, pp. 3014–3019, July 12–20, 2021.

[5] A. Sankararaman and F. Baccelli, "Spatial birth-death wireless networks," in *Proceedings of the 54th Annual Allerton Conference on Communication, Control, and Computing*, Monticello, IL, USA, pp. 916–923, 2016.

[6] X. Wu et al., "FlashLinQ: A synchronous distributed scheduler for peer-to-peer Ad Hoc networks," *IEEE/ACM Transactions on Networking*, vol. 21, no. 4, pp. 1215–1228, Aug. 2013.

[7] B. S. Khan, S. Jangsher, A. Ahmed, and A. Al-Dweik, "URLLC and eMBB in 5G industrial IoT: A survey," *IEEE Open Journal of the Communications Society*, vol. 3, pp. 1134–1163, 2022.

[8] A. Anand, G. de Veciana, D. Malak, A. Elezabi, and A. Venkatakrishnan, "Opportunistic overlapping: Joint scheduling of uplink URLLC/eMBB traffic in NOMA based wireless systems," in *Proceedings of the 19th International Symposium on Modeling and Optimization in Mobile, Ad hoc, and Wireless Networks (WiOpt)*, Philadelphia, PA, USA, 2021, pp. 1–8.

[9] H. Nikbakht, M. Wigger, M. Egan, S. Shamai (Shitz), J-M. Gorce, and H. V. Poor, "An information-theoretic view of mixed-delay traffic in 5G and 6G," *Entropy*, vol. 24, no. 5, article 637, 2022.

[10] N. Chen, Z. Cheng, Y. Zhao, L. Huang, X. Du, and M. Guizani, "Joint dynamic spectrum allocation for URLLC and eMBB in 6 G networks," *IEEE Transactions on Network Science and Engineering (Early Access)*, pp. 1–14, 2023.

[11] X. Yang, Z. Zho, and B. Huang, "URLLC key technologies and standardization for 6G power internet of things," *IEEE Communications Standards Magazine*, vol. 5, no. 2, pp. 52–59, June 2021.

[12] N. H. Mahmood, I. Atzeni, E. A. Jorswieck, and O. L. A. López, "Ultra-reliable low-latency communications: Foundations, enablers, system design, and evolution towards 6G", *Foundations and Trends® in Communications and Information Theory*, vol. 20, no. 5-6, pp. 512–747, 2023.

[13] E. A. Jorswieck, "Next-generation multiple access: From basic principles to modern architectures," *Proceedings of the IEEE*, 2024.

[14] M. E. Haque, F. Tariq, M. R. A. Khandaker, K. -K. Wong, and Y. Zhang, "A survey of scheduling in 5G URLLC and outlook for emerging 6G systems," *IEEE Access*, vol. 11, pp. 34372–34396, 2023.

[15] H. Ren, C. Pan, Y. Deng, M. Elkashlan, and A. Nallanathan, "Resource allocation for secure URLLC in mission-critical IoT scenarios," *IEEE Transactions on Communications*, vol. 68, no. 9, pp. 5793–5807, Sept. 2020.

[16] R. Kassab, O. Simeone, P. Popovski, and T. Islam, "Non-orthogonal multiplexing of ultra-reliable and broadband services in fog-radio architectures," *IEEE Access*, vol. 7, pp. 13035–13049, 2019.

[17] M. Amjad, L. Musavian, and M. H. Rehmani, "Effective capacity in wireless networks: A comprehensive survey," *IEEE Communications Surveys & Tutorials*, vol. 21, no. 4, pp. 3007–3038, Fourthquarter 2019.

[18] A. Kumar Bairagi, Md. S. Munir, M. Alsenwi, N. H. Tran, and C. S. Hong. "A matching based coexistence mechanism between eMBB and uRLLC in 5G wireless networks," *Proceedings of the 34th ACM/SIGAPP Symposium on Applied Computing (SAC '19)*, New York, NY, USA, pp. 2377–2384.

[19] H. Zarini, N. Gholipoor, M. R. Mili, M. Rasti, H. Tabassum, and E. Hossain, "Resource management for multiplexing eMBB and URLLC services over RIS-aided THz communication," *IEEE Transactions on Communications*, vol. 71, no. 2, pp. 1207–1225, Feb. 2023.

[20] H. Yin, L. Zhang, and S. Roy, "Multiplexing URLLC traffic within eMBB services in 5G NR: fair scheduling," *IEEE Transactions on Communications*, vol. 69, no. 2, pp. 1080–1093, Feb. 2021.

[21] X. Song and M. Yuan, "Performance analysis of one-way highway vehicular networks with dynamic multiplexing of eMBB and URLLC traffics," *IEEE Access*, vol. 7, pp. 118020–118029, 2019.

[22] H. Nikbakht, E. Ruzomberka, M. Wigger, S. Shamai, and H. V. Poor, "Joint coding of eMBB and URLLC in vehicle-to-everything (V2X) communications," in *Proceedings of the IEEE Global Communications Conference*, Kuala Lumpur, Malaysia, Dec. 4–8, to appear, available on arXiv:2305.07769.

[23] Y. Zhao, X. Chi, L. Qian, Y. Zhu, and F. Hou, "Resource allocation and slicing puncture in cellular networks with eMBB and URLLC terminals coexistence," *IEEE Internet of Things Journal*, vol. 9, no. 19, pp. 18431–18444, Oct. 2022.

[24] R. Kassab, O. Simeone and P. Popovski, "Coexistence of URLLC and eMBB services in the C-RAN uplink: an information-theoretic study," in *Proc. IEEE GLOBECOM*, Abu Dhabi, United Arab Emirates, Dec. 9–13, 2018.

[25] H. Nikbakht, M. Wigger, W. Hachem, and S. Shamai (Shitz), " Mixed delay constraints on a fading C-RAN uplink," in *Proceedings of the IEEE Information Theory Workshop*, Visby, Sweden, Aug. 25–28, 2019.

[26] K. M. Cohen, A. Steiner, and S. Shamai (Shitz) "The broadcast approach under mixed delay constraints," in *Proceedings of the IEEE International Symposium on Information Theory*, Cambridge (MA), USA, pp. 209–213, July 1–6, 2012.

[27] H. Nikbakht, M. Egan, and J. -M. Gorce, "Dirty paper coding for consecutive messages with heterogeneous decoding deadlines in the finite blocklength regime," in *Proceedings of the IEEE International Symposium on Information Theory*, pp. 2100–2105, Espoo, Finland, 2022.

[28] P. -H. Lin, S. -C. Lin, P. -W. Chen, M. A. Mross, and E. A. Jorswieck, "Second order rate regions of Gaussian broadcast channels under heterogeneous blocklength constraints," *IEEE Transactions on Communications*, vol. 72, no. 2, pp. 801–814, Feb. 2024.

[29] M. A. Mross, P. -H. Lin, and E. A. Jorswieck, "Gaussian broadcast channels with heterogeneous finite blocklength constraints: Inner and outer bounds," *IEEE Transactions on Communications*, Jan. 2024.

[30] H. Nikbakht, M. Wigger, and S. Shamai Shitz, "Coordinated multi point transmission and reception for mixed-delay traffic," *IEEE Transactions on Communications,* vol. 69, no. 12, pp. 8116–8131, Dec. 2021.

[31] M. H. M. Costa, "Writing on dirty paper (Corresp.)," *IEEE Transactions on Information Theory*, vol. 29, no. 3, pp. 439–441, May 1983.

[32] J. Scarlett, "On the dispersions of the Gel'fand - Pinsker channel and dirty paper coding," *IEEE Transactions on Information Theory*, vol. 61, no. 9, pp. 4569–4586, Sept. 2015.

[33] V. S. Annapureddy, A. El Gamal and V. V. Veeravalli, "Degrees of freedom of interference channels with CoMP transmission and reception," *IEEE Transactions on Information Theory*, vol. 58, no. 9, pp. 5740-5760, Sept. 2012.

[34] N. Devroye, P. Mitran and V. Tarokh, "Achievable rates in cognitive radio channels," *IEEE Transactions on Information Theory,* vol. 52, no. 5, pp. 1813-1827, May 2006.

[35] N. Devroye and M. Sharif, "The multiplexing gain of MIMO X-channels with partial transmit side-information," *IEEE International Symposium on Information Theory*, Nice, France, pp. 111-115, 2007.

[36] M. Singhal, T. Seyfi, and A. E. Gamal, "Joint uplink-downlink cooperative interference management with flexible cell associations," *IEEE Transactions on Communications*, vol. 68, no. 9, pp. 5420–5434, Sept. 2020.

[37] H. Nikbakht, M. Wigger, and S. Shamai (Shitz), "Multiplexing gains under mixed-delay constraints on Wyner's soft-handoff model," *Entropy*, vol. 22, no. 2, pp. 182, 2020.

[38] L. Liu and W. Yu, "Massive connectivity with massive MIMO—part I: Device activity detection and channel estimation," *IEEE Transactions on Signal Processing*, vol. 66, no. 11, pp. 2933–2946, June, 2018.

[39] Z. Chen, F. Sohrabi, and W. Yu, "Sparse activity detection for massive connectivity," *IEEE Transactions on Signal Processing*, vol. 66, no. 7, pp. 1890-1904, April, 2018.

[40] Q. Wang, L. Liu, S. Zhang, and F. C. M. Lau, "On massive IoT connectivity with temporally-correlated user activity," in *Proceedings of the IEEE International Symposium on Information Theory*, Melbourne, Australia, July 12–20, 2021.

[41] O. Somekh, O. Simeone, H. V. Poor and S. Shamai (Shitz), "The two-tap input-earasure Gaussian channel and its application to cellular communications," in *Proceedings of the 46th Annual Allerton Conference on Communication, Control, and Computing*, Monticello, IL, USA, Sept. 23–26, 2008.

[42] N. Levy and S. Shamai (Shitz), "Information theoretic aspects of users' activity in a Wyner-like cellular model," *IEEE Transactions on Information Theory*, vol 56, pp. 2241–2248, Apr. 2010.

[43] O. Somekh, O. Simeone, H. V. Poor and S. Shamai (Shitz), "Throughput of cellular uplink with dynamic user activity and cooperative base-stations," in *Proceedings of the IEEE Information Theory Workshop*, Taormina, Italy, Oct. 11–16, 2009.

[44] P. Minero, M. Franceschetti, and D. N. C. Tse, "Random access: An information-theoretic perspective," *IEEE Transactions on Information Theory*, vol. 58, no. 2, pp. 909–930, Feb. 2012.

[45] G. Caire and S. Shamai, "On the achievable throughput of a multiantenna Gaussian broadcast channel," *IEEE Transactions on Information Theory*, vol. 49, no. 7, pp. 1691–1706, July 2003.

[46] H. Nikbakht, M. Wigger, and S. S. Shitz, "Mixed delay constraints in Wyner's soft-handoff network," in *Proceedings of the IEEE International Symposium on Information Theory*, Vail, CO, USA, pp. 1171-1175, 2018.

[47] M. Wigger, R. Timo and S. Shamai Shitz, "Conferencing in Wyner's asymmetric interference network: Effect of number of rounds," *IEEE Transactions on Information Theory*, vol. 63, no. 2, pp. 1199–1226, Feb. 2017.

[48] A. K. Bairagi et al., "Coexistence mechanism between eMBB and uRLLC in 5G wireless networks," *IEEE Transactions on Communications*, vol. 69, no. 3, pp. 1736–1749, Mar. 2021.

[49] H. Nikbakht, M. Wigger, and S. Shamai, "Multiplexing gain region of sectorized cellular networks with mixed delay constraints," in *Proceedings of the IEEE International Workshop on Signal Processing Advances in Wireless Communications*, Cannes, France, July 2–5, 2019.

[50] P. Promponas, T. Chen, and L. Tassiulas, "Optimizing sectorized wireless networks: Model, analysis, and algorithm," available online: arXiv:2308.10970v1, Aug. 2023.

[51] M. Franceschetti, M. D. Migliore, P. Minero, and F. Schettino, "The degrees of freedom of wireless networks via cut-set integrals," *IEEE Transactions on Information Theory,* vol. 57, no. 5, pp. 3067–3079, May 2011.

[52] J. Wang, S. A. Jafar, B. Yuan and L. Huang, "GDoF of interference channel with limited cooperation under finite precision CSIT," in *Proceedings of the IEEE Global Communications Conference*, Waikoloa, HI, USA, pp. 1–6, 2019.